

Application of Temperature-Responsive Polymers to Oil Sands Tailings Management

by

Ian Osborn

A thesis submitted in partial fulfillment of the requirements for the degree of

Master of Science

in

Chemical Engineering

Department of Chemical and Materials Engineering  
University of Alberta

© Ian Osborn, 2015

## **Abstract**

A multi-purpose settling column was designed to determine settling rate and sediment height allowing the in-situ measurement of yield stress and drainage without disturbing the sediment particle network. The settling column was applied to studying flocculation/densification of model oil sands tailings. A cationic temperature sensitive copolymer, poly[N-isopropylacrylamide-co-N-[3-(Dimethylamino)propyl]methacrylamide], known as CP05, containing 95 mol% NIPAM and 5 mol% DMAPMA was synthesized in-house. CP05 possess attributes of both NIPAM and DMAPMA polymers. NIPAM creates a temperature responsive feature of the copolymer exhibiting a sharp conformation transition at specific conditions (LCST), while DMAPMA provides a pH dependent cationic charge. Cycling temperatures around the CP05 LCST increased the solids mass fraction and yield stress of the sediment of model tailings flocculated by the synthesized copolymer. Polymer charge density, solubility, elasticity and conformation of CP05 were modified through the change of suspension pH and temperature, which were used to optimize flocculation efficiency and sediment rheology.

## **Acknowledgements**

First, I offer my sincerest gratitude to my supervisors, Dr. Jacob Masliyah, Dr. Zhenghe Xu, and Dr. David Harbottle who have provided excellent guidance and supported me with their patience and knowledge throughout the course of my research. It is great teachers like them who are responsible for making the new talent that will drive Canada's future.

This thesis would not have been completed without the help of the oil sands engineering research group's technicians, Mr. Jim Skwarok (our friendly ogre) and the lovely Ms. Jie Ru who provided laboratory support and kept everyone well-stocked in essential supplies. My gratitude also goes to Ms. Lisa Carreiro for being helpful and giving a friendly smile at each of the countless times I needed to meet with my supervisors. Lastly, I extend my sincere thanks to Dr. Sean Sanders and his research group for allowing me open access to their viscometer for my research needs.

I am grateful to the Natural Sciences and Engineering Research Council of Canada (NSERC) Industrial Research Chair in Oil Sands Engineering for funding my study. I would also like to thank the Department of Chemical and Materials Engineering for providing an excellent environment for graduate studies.

In the end, the acknowledgements on a thesis are only read by the researcher's closest friends and family. Therefore the following inside jokes and references are for you. My deepest gratitude goes to Ly, may her light shine on me forever. Lastly, thanks to all my friends, family, and companions in these years of science-ing.

## Table of Contents

Chapter 1 : Introduction .....	1
Chapter 2 : Literature Review .....	5
2.1 Particle Dynamics .....	5
2.1.1 Clays and their Behaviour in Suspension .....	5
2.1.2 Electrical Double Layer .....	7
2.1.3 DLVO Theory .....	9
2.2 Mechanisms of Coagulation and Flocculation .....	9
2.2.1 Double Layer Compression .....	9
2.2.2 Surface Charge Neutralization .....	10
2.2.3 Flocculation and Bridging Mechanism .....	11
2.2.4 Additional Effects on Flocculation .....	12
2.3 Previous Studies on Flocculation of Oil Sands Fine Tailings .....	13
2.4 Temperature Sensitive Polymers .....	15
2.4.1 Previous Research involving NIPAM as a Flocculant or Dispersant .....	16
2.5 Rheology .....	19
2.5.1 Newtonian and Bingham Fluids .....	19
2.5.2 Rheology Measurements and Vane Yield Stress .....	21
2.5.3 Previous Research on Rheology of Flocculated Suspensions .....	23
Chapter 3 : Materials and Experimental Procedures .....	26
3.1 Material Preparation and Chemical Synthesis .....	26
3.1.1 Particle Characterisation - Kaolinite .....	26
3.1.2 Preparation of Kaolinite Suspensions .....	27
3.1.3 Synthesis procedure for p[NIPAM-co-DMAPMA] .....	28
3.1.4 CP05 Polymer Solution Preparation .....	30

3.2 Instruments and Procedures .....	30
3.2.1 Settling Column .....	30
3.2.2 Suspension Agitation and Mixers .....	32
3.2.3 Settling Tests and Procedures .....	34
3.2.4 Shear Yield Stress Measurement Test Procedure .....	36
3.2.5 Quartz Crystal Microbalance with Dissipation Monitoring (QCM-D).....	37
Chapter 4 : Effect of p[NIPAM-co-DMAPMA] Temperature Response on Settling, Rheology, and Dewatering of Kaolinite Suspensions.....	40
4.1 Coil-Globule Transition Properties.....	40
4.2 Effect of Settling Procedure.....	42
4.3 Application of Temperature Responsive Polymer.....	44
4.3.1 Settling.....	44
4.3.2 Supernatant Turbidity .....	48
4.3.3 Yield Stress .....	50
4.3.4 Drainage of Sediments.....	52
4.3.5 Raking and Yield Stress.....	56
4.4 Conclusions.....	57
Chapter 5 : Studies of Isothermal Flocculation using CP05.....	58
5.1 Kaolinite Flocculation.....	58
5.1.1 Isothermal Settling.....	58
5.2 Studies of p[NIPAM-co-DMAPMA] Adsorption using QCM-D .....	59
5.2.1 Polymer Adsorption Kinetics.....	59
5.2.2 Temperature Ramp QCM-D Experiment.....	62
5.3 Polymer Elasticity and Floc Strength .....	66
5.4 pH Switch and Polymer Response .....	69

5.5 Sediment Dewatering and Filtration .....	71
5.4 Conclusions.....	73
Chapter 6 : Conclusions .....	74
6.1 Future Work .....	75
References.....	76
Appendix A : Dual Polymer Flocculation .....	83
A.1 Flocculation and Rheology of Dual Polymer Flocculation.....	83
A.2 Dual Polymer Flocculation Kinetics .....	87
Appendix B : Supplemental Data .....	91
Appendix C : Polymer Molecular Weight Determination .....	93

## List of Figures

Figure 1-1: Schematic flowchart of oil sands surface mining-bitumen extraction [2, 3] .....	2
Figure 2-1: Three dimensional structure of the clay layers making up kaolinite [11].....	5
Figure 2-2: Different structures of clay particles - stacking structure of a perfect crystal (left) and “house of cards” structure (right) [11].....	6
Figure 2-3: Electrical double layer according to Stern model and corresponding electrical potential profile [17] .....	8
Figure 2-4: Adsorption of polymers, and formation of loops and bridging mechanisms [28] .....	11
Figure 2-5: Two phase diagram for temperature sensitive polymers in solution [43].....	16
Figure 2-6: Flocculation mechanism by temperature sensitive polymers[3].....	17
Figure 2-7: Rheogram for Newton and Bingham fluid models .....	20
Figure 2-8: Bingham fluid model compared to actual viscoplastic fluid behaviour.....	21

Figure 2-9: Torque versus time curve from a vane viscosity measurement (right) and schematic diagram of a vane (left) [59] .....	22
Figure 3-1: The volume-based passing size of kaolinite particles[3] .....	26
Figure 3-2: Size distribution of kaolinite particles [3].....	27
Figure 3-3: Apparatus used for polymer synthesis [3].....	29
Figure 3-4: Disassembled and assembled two-part settling column.....	31
Figure 3-5: Disassembled drainage column and dimensions drawing.....	32
Figure 3-6: Set-up for suspension agitation and flocculant addition .....	33
Figure 4-1: Lower critical solutions temperatures (LCST) of CP05 at different pH measured by solution turbidity.....	41
Figure 4-2: Phase diagram of CP05 constructed using LCST, measured by turbidity at different pH.....	42
Figure 4-3: Initial settling rate of 5 wt% kaolinite suspensions dosed with CP05 at increasing concentration from 0 to 100 ppm. The mixing and settling temperatures are indicated in the legend [3] .....	43
Figure 4-4: Initial settling rate of 5 wt% kaolinite suspensions flocculated by the addition of CP05. Experimental variables: solution pH and temperature protocols. Settling column – 100 mL .....	44
Figure 4-5: Initial settling rate of 5 wt% kaolinite suspensions flocculated by the addition of CP05. Experimental variables: solution pH and temperature protocols. Settling column – 1 L. 45	
Figure 4-6: Zeta potential of kaolinite and silica particles. Experimental variables: solution pH and CP05 addition.....	47
Figure 4-7: Supernatant turbidity of 5 wt% kaolinite suspensions flocculated by the addition of CP05. Experimental variables: solution pH and temperature protocols. Settling column – 1 L..	48

Figure 4-8: Shear yield stress of settled kaolinite suspensions with 100 ppm CP05. Experimental variables: suspension pH and temperature protocol .....	50
Figure 4-9: Dewatering of settled kaolinite suspensions flocculated with 100 ppm CP05 at pH 8.5 over 35 minutes. Experimental variable: suspension heating procedures .....	53
Figure 4-10: Initial drainage rates of settled kaolinite suspensions flocculated with 100 ppm CP05 at pH 8.5. Experimental variable: suspension heating procedures .....	54
Figure 4-11: Shear yield stress of dewatered settled kaolinite suspensions flocculated with 100 ppm CP05 at pH 8.5. Experimental variable: suspension heating procedures .....	55
Figure 4-12: Shear yield stress and solids content of dewatered kaolinite suspensions flocculated with 100 ppm CP05 at pH 8.5 using RMRS procedure, varying dewatering times .....	55
Figure 4-13: Solids content of dewatered settled kaolinite suspensions flocculated with 100 ppm CP05 at pH 8.5 using RMRS procedure, illustrating the influence of raking samples.....	56
Figure 4-14: Shear yield stress of dewatered settled kaolinite suspensions with 100 ppm CP05 at pH 8.5 using RMRS procedure, illustrating the influence of raking samples .....	57
Figure 5-1: Initial settling rates as a function of suspension temperature for 5 wt% kaolinite at pH 8.5, flocculated with 100 ppm CP05.....	58
Figure 5-2: CP05 polymer adsorption on silica sensor surface as a function of temperature at pH 8.5 using 10 ppm CP05.....	60
Figure 5-3: Polymer adsorption rate and suspension initial settling rate as a function of temperature. Flocculation performed with 5 wt% kaolinite at pH 8.5 with 100 ppm CP05. Polymer adsorption onto silica QCM-D sensor, using 10 ppm CP05 at pH 8.5 .....	61
Figure 5-4: CP05 polymer adsorption onto silica as a function of temperature. Frequency and dissipation responses of the QCM-D silica sensor using 10ppm CP05 at 8.5 pH.....	62
Figure 5-5: Frequency and dissipation response of QCM-D sensors as a function of solution temperature. Symbols: Milli-Q water at pH 8.5 (solid line), CP05 polymer (square symbols).	



CP05 (500 ppm) first adsorbed at 20°C and subsequently washed with 10 mM KCl water at pH 8.5 to form a stable film.....	63
Figure 5-6: Frequency shift of deionized water versus temperature ramp for silica QCM-D crystal. Solid line was the response predicted by Kanazawa model, symbols represent different experimental runs.....	64
Figure 5-7: Frequency and dissipation shifts caused by temperature ramp on QCM-D silica sensor, isolating the response of the adsorbed CP05 polymer layer.....	65
Figure 5-8: Mean floc size of 5 wt% kaolinite suspensions flocculated with 100 ppm of CP05, comparison of different settling procedures .....	67
Figure 5-9: Comparison of floc strength indexes of 5 wt% kaolinite suspensions flocculated with 100 ppm CP05, using different settling procedures.....	68
Figure 5-10: Initial settling rate of 5 wt% kaolinite suspensions, demonstrating the application of coil-globule transition by pH Switch. Experimental variables: pH and temperature protocols. Settling column – 100 mL.....	70
Figure 5-11: Shear yield stress of flocculated kaolinite suspensions with 100 ppm CP05, demonstrating the application of coil-globule transition by pH Switch. Experimental variables: suspension pH and temperature protocol. Settling column – 1 L.....	71
Figure 5-12: Dewatering of settled kaolinite suspensions flocculated with 100 ppm CP05 at pH 8.5. Experimental variables: settling procedure. Settling column – 1 L.....	71
Figure 5-13: Initial drainage rates of settled kaolinite suspensions flocculated with 100 ppm CP05 at pH 8.5. Experimental variables: settling procedure. Settling column – 1 L.....	72
Figure 5-14: Shear yield stress and solids content of dewatered kaolinite suspensions flocculated with 100 ppm CP05 at pH 8.5. Experimental variables: settling procedure. Settling column – 1 L .....	73

Figure A-1: Initial settling rate of 5 wt% kaolinite suspensions. Experimental variables: single and dual polymer settling systems, and solution pH. Settling column – 1 L.....	84
Figure A-2: Shear yield stress of settled kaolinite suspensions flocculated with 100 ppm CP05 and 12 ppm AF246. Experimental variables: suspension heating procedures and solution pH. Settling column – 1 L.....	85
Figure A-3: Dewatering of flocculated kaolinite suspensions at pH 8.5. Experimental variables: single and dual polymer settling systems. Settling column – 1 L.....	86
Figure A-4: Shear yield stress of dewatered flocculated kaolinite suspensions at pH 8.5, comparison of dual and single polymer settling procedures.....	87
Figure A-5: Initial settling rate of 5 wt% kaolinite suspensions at 8.5 pH, treated with varying dosages of CP05 cationic polymer and HyChem AF246 anionic polymer .....	88
Figure A-6: Shear yield stress of settled kaolinite suspensions at 8.5 pH, flocculated with varying dosages of CP05 cationic polymer and HyChem AF246 anionic polymer .....	89
Figure B-1: Initial settling rate of 5 wt% kaolinite suspensions with 100 ppm CP05. Experimental variables: pH and settling procedures, RMRS and 50M50S (HMHS). Settling column – 1 L.....	91
Figure B-2: Yield stress of settled kaolinite suspensions with 100 ppm CP05. Experimental variables: pH and settling procedures, RMRS and 50M50S (HMHS). Settling column – 1 L ....	91
Figure B-3: Solids content of settled kaolinite suspensions flocculated with 100 ppm CP05. Experimental variables: temperature protocols and solution pH. Settling column – 1 L.....	92
Figure C-1: Dual Huggins-Kraemer plot for CP05.....	94

## List of Tables

Table 2-1: Polymer research on oil sands tailings management.....	19
Table 3-1: Mixing vessel sizing and geometric scale comparison .....	33

Table A-1: Mean floc size of 5 wt% kaolinite suspensions at pH 8.5 flocculated with 100 ppm of CP05 and 12 ppm AF 246..... 90

## Nomenclature

MFT: Mature Fine Tailings

LCST: Lower Critical Solution Temperature

AER: Alberta Energy Regulator

NIPAM: N-isopropylacrylamide

DMAPMA: *N*-[3-(Dimethylamino)propyl]methacrylamide

$f_v$ : Yield Stress

$D_v$ : Vane Diameter

$H_v$ : Vane Height

$\tau_v$ : Vane Torque (N\*m)

$\zeta$ : Zeta Potential (mV)

$M_n$ : Average Molecular Weight

$\eta$ : Viscosity (Pa\*s)

QCM-D: Quartz Crystal Microbalance with Dissipation Monitoring

$\Delta F$ : Quartz Crystal Frequency Shift (Hz)

$\Delta D$ : Quartz Crystal Dissipation Shift ( $*10^6$ )

ISR: Initial Settling Rate (m/hr)

FBRM: Focused Beam Reflectance Measurement

RMRS: Room Temperature Mixing, Room Temperature Settling

RMHS: Room Temperature Mixing, High Temperature Settling

EMES: Elevated Temperature Mixing, Elevated Temperature Settling

## **Chapter 1 : Introduction**

Oil sands are naturally occurring mixtures of water, sand, clay, and bitumen. Deposits similar to Alberta's oil sands exist in several locations around the globe, including Venezuela, the United States, and Russia. The main deposits of oil sands in Alberta are located in the regions of Peace River, Cold Lake and Athabasca. The proven remaining reserves of the oil sands, in terms of crude oil, are estimated to be 27.5 billion cubic meters (173 billion barrels) [1]. This puts Canada the third globally in terms of oil reserves, behind only Saudi Arabia and Venezuela [1].

The oil sands deposits are composed primarily of 8 to 14 percent bitumen, which is a heavy and extremely viscous oil that must be treated or upgraded before being used in refineries to produce conventional fuels [2]. The primary means of bitumen recovery are surface mining-extraction and in-situ thermal production. In-situ recovery techniques, such as Steam Assisted Gravity Drainage (SAGD) and Cyclic Steam Stimulation (CSS), are used in areas where the overburden (the materials situated above the bitumen deposit) has a thickness greater than 75-100 meters [2]. These deposits account for about 85% of the oil sands resource and are the reason why the majority of future projects will be utilizing in-situ methods. These methods are similar in that both involve the injection of steam into the formation for the purpose of decreasing the viscosity of the bitumen. The heated bitumen is recovered from the production well with a minimal amount of fine solids due to the placement of mesh screens. The lack of fine particles eliminates the use of large tailings ponds to contain fines and process water as encountered in mineable oil sands operations [2].

Bitumen recovery by surface mining-extraction is limited to the few areas where the deposits are located at a depth of less than 65 meters. In this case a minimal amount of overburden removal makes open-pit mining economically feasible. Figure 1-1 is a simplified flowchart of bitumen extraction and upgrading from a surface mine.

Oil sands are mined and crushed into smaller pieces. They are then mixed with warm water and chemical additives to make a slurry that is transported by a hydrotransport pipeline. In this pipeline the slurry is subjected to heat and mechanical shear under which the bitumen is liberated from the sands. After aeration (bubble attachment to bitumen droplets) the liberated bitumen is separated by flotation in a separation vessel to produce bitumen froth. Flotation cells are used to

further aerate the remaining bitumen in the middlings so that it can be separated from the remaining slurry phases. Water and solids in the bitumen froth are removed by froth treatment and the bitumen is upgraded into synthetic crude oil. The separation process outlined above, known as Clark Hot Water Extraction process, produces a barrel of upgraded bitumen from approximately two tonnes of oil sands [2].

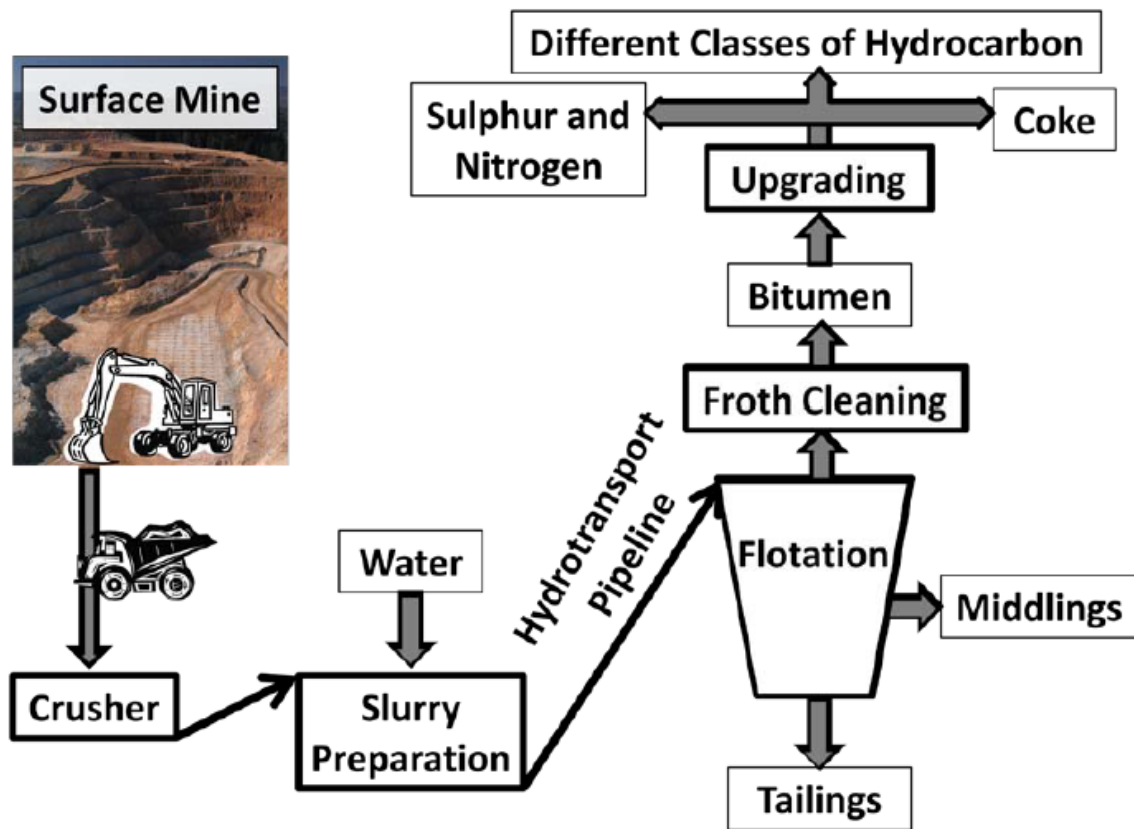


**Figure 1-1: Schematic flowchart of oil sands surface mining-bitumen extraction [2, 3]**

Oil sands tailings are the inevitable by-product of the extraction process. The tailings consist of large amounts of water and solids (sand, silt, and clays) as well as residual bitumen. All tailings from both the primary and secondary separation vessels, as well as from the froth treatment plant, are discharged into a tailings pond for storage and dewatering [2]. The coarse sands rapidly settle out and are used to construct dykes to hold the remaining slurry [2].

The fine-grained silts and clays, as well as the residual bitumen, sink slowly in the pond to form a layer known as fine tails. The fine tails accumulate in the tailings ponds under a layer of expelled water and slowly consolidate under gravity. It takes several years for the slurry to form

a fine solids suspension, termed as mature fine tails (MFT), that stabilizes at around 30 wt% solids. The MFT will remain in a fluid state for decades because of its negligible consolidation rate and water release characteristics [4].

There are several key issues related to the disposal of fine tailings that pose challenges to the oil sands industry, with the most pertinent being the accumulation of large volumes of MFT. Neither the tailings solids nor the released water can be discharged into the environment as part of the operating license agreements between the Alberta Provincial Government and oil sands operators [5]. It is estimated that about 0.25 m<sup>3</sup> of MFT is produced per barrel of bitumen production [6]. The high production rate of MFT coupled with the slow settling of the fine solids in the tailings ponds creates an ever increasing size of tailings facilities covering large areas of land. At present in Alberta there are more than 170 km<sup>2</sup> of tailings ponds [7].

The demand for raw water in bitumen production is increasing due to the growing production of existing oil sands operations and the development of new open pit mining plants in the Fort McMurray area of Alberta. To produce a barrel of Syncrude Sweet Blend, 16.5 barrels of water are required, thus requiring an efficient recovery and recycling plan for the process water [2]. The main loss of water in the fine tailings is to the voids and pores of the fine tailings. The fresh water required for makeup is small in comparison with the water which is recycled through the process. In general 15% of the needed water in the oil sands industry is withdrawn from raw water sources and the remainder is from the pond's recycle water [7]. This means, on average, 3 barrels of fresh water is consumed to produce one barrel of bitumen [6]. The intake of fresh water is limited by strict regulations, making it necessary to develop processes to maximize water recycling and ensure efficient use of water [7].

In addition to these challenges, mature fine tailings pose a potential environmental concern. MFT contain naphthenic acids, residual bitumen and hydrocarbons that are toxic for the environment. These toxic chemicals cause adverse chronic effects on aquatic organisms and wildlife in areas surrounding the MFT storage site. Research indicates that MFT in tailings ponds continue to release elevated concentrations of metals and other elements to surface and groundwater for many years [5].

In response to the challenge of fluid fine tailings management, various attempts have been made by the oil sands operators, government and research institutions to identify and develop suitable

technologies, aiming at reducing both the total MFT inventory and the MFT produced per barrel of bitumen. The settling characteristics of the fine tailings must be improved in an economic and environmentally acceptable manner. Such practices have the benefit of increasing the recovery rate of water and decreasing the overall volume of MFT. New provincial government directives call for the rapid reclamation of tailings sediments to produce trafficable solids (Directive 74) [8]. This directive provides the impetus for research into new tailings management technologies. Major physical treatments that have emerged include centrifugation, filtration, electrophoresis, electro-coagulation, and freeze-thaw cycles [2]. There are also chemical methods for the treatment of MFT involving the addition of chemicals such as sodium silicate, organic flocculants, inorganic coagulants, oxidizing and reducing agents, and most recently carbon dioxide [2, 9]. Further investigating the feasibility of a particular temperature responsive polymer flocculant, a copolymer of N-isopropylacrylamide (NIPAM) with 5% mole of *N*-[3-(Dimethylamino) propyl]methacrylamide (DMAPMA) to enhance fine solids settling and consolidation, is the focus of this study.

### **Organization of Thesis**

The body of this thesis consists of 6 chapters. Chapter 1 provides background information on Canada's oil sands, bitumen extraction processes and tailings management. Chapter 2 presents an overview of the fundamentals of colloidal forces and surface chemistry, and reviews the relevant literature of the present work. Chapter 3 describes experimental procedures, including the set-up and procedures for the settling and rheology tests, polymer preparation, and QCM-D measurements. Chapter 4, as one of the core chapters of this thesis, presents the results and discussion on the performance and functionality of the temperature-responsive polymer known as CP05. The settling and rheological behaviour of flocculated kaolinite suspensions are reported. Chapter 5, the other core chapter, presents the results and discussions on the functionality of CP05 flocculation when operating near the polymer's critical transformation conditions (LCST). The results are interpreted using measurements of CP05's adsorption kinetics, conformation, and polymer elasticity. In chapter 6 conclusions are given and recommendations for further study are suggested.

## Chapter 2 : Literature Review

### 2.1 Particle Dynamics

Colloids are defined as a dispersion of small particles that range in size from 1 nanometer to 10 micrometers. These particles are heavily influenced by Brownian motion and form a homogeneously dispersed mixture in aqueous fluids [2]. Oil sands investigations show that it is the dispersing nature of the oil sands tails that results in its poor settling and high water-holding capacity. As discussed in Section 1, the tailings in the Athabasca oil sands tailings ponds settle into layers of stable suspensions. The bottom layer is a dispersion of fine clay particles, sand, water, and bitumen [10]. This chapter will begin with information on clay mineralogy and its influence on stability of colloidal dispersions.

#### 2.1.1 Clays and their Behaviour in Suspension

Clay particles are composed of sheets of silicon-oxygen tetrahedrons (T) and sheets of aluminum or magnesium-oxygen octahedrons (O) as illustrated in Figure 2-1. Different types of clays have different arrangements of these sheets as their unit layer. Illite is a tightly bound three-layer structure, composed of an aluminum-oxygen-hydroxyl octahedron layer sandwiched between two silicon oxide tetrahedron layers. Kaolinite is an example of a two-layered clay particle, having a unit layer of one tetrahedral silicon-oxygen sheet attached to one octahedral aluminum-oxygen-hydroxyl sheet.

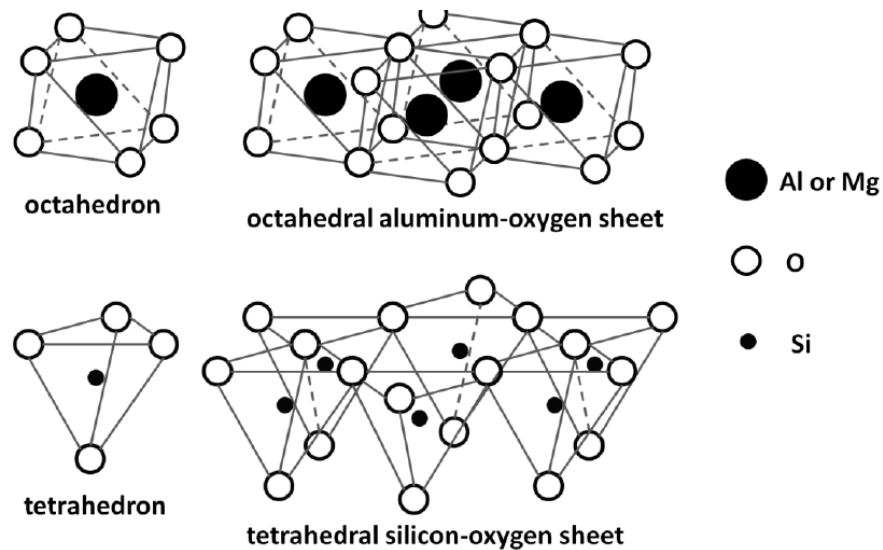
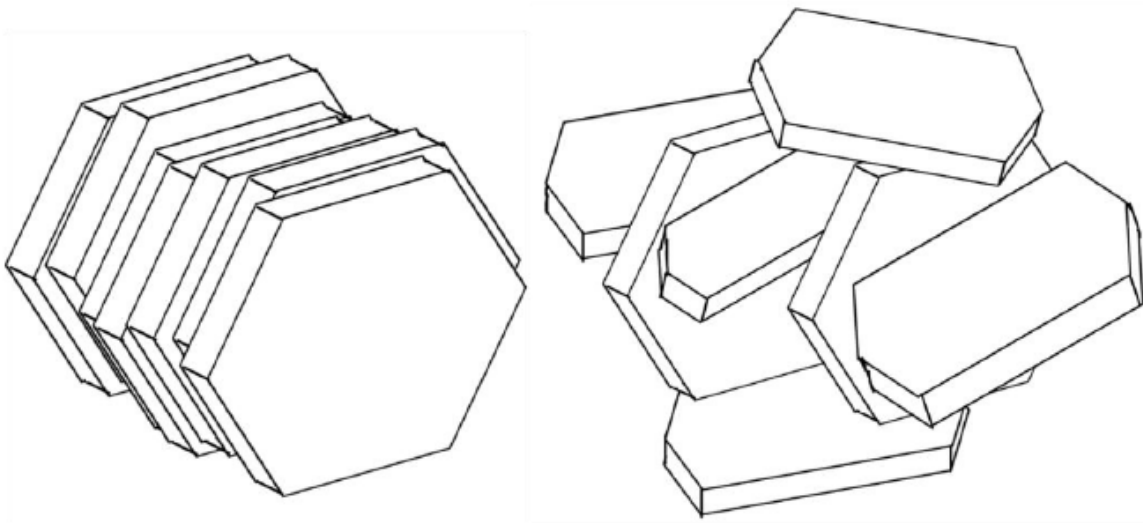


Figure 2-1: Three dimensional structure of the clay layers making up kaolinite [11]



Years of research has established that kaolinite particles are of plate-like shape and comprised of two distinct basal planes (or faces) [12-14]. The typical structure of clays is hexagonal sheets with length to thickness ratio of 10:1. Within clay particles, charge imbalances are created by the process of isomorphic substitution, where high valence cations in the layers of the clay are substituted by cations of lower valency. For example, a negative charge is created on the structure when a tetravalent silicon ion is replaced by a trivalent aluminum ion because of the similar morphology (size) of the ions [2]. The charges on the T-basal plane are considered to be permanent and independent of pH. The primary alumina and silica bonds are broken on the edge of the plate and become protonated in water, leading to a pH dependent charge [15].

The edge of the kaolinite is positively charged in acidic conditions and negatively charged in alkaline conditions. Therefore, based on the ionic species and their strength in water, these particles can remain dispersed or associate with each other in different ways. In an acidic suspension, the positively charged edges may attach to the negatively charged basal plane. These edge-to-face and edge-to-edge modes of association, shown in Figure 2-2 (right), create a space-filling “house of cards” structure. An example of a perfect clay crystal built by stacking unit layers on top of another is also shown (left). The “house of cards” [14] can trap large amounts of water within the associations and lead to the long lasting structure of the MFT slurry discussed earlier.



**Figure 2-2: Different structures of clay particles - stacking structure of a perfect crystal (left) and “house of cards” structure (right) [11]**

Michaels and Bolger (1962) described fine particle interactions of kaolinite in detail [16]. There are two major forces with opposing influences: repulsive electrostatic double layer force and attractive van der Waals forces. Due to the high surface to mass ratio of fine particles, the effects of electrostatic double layer and van der Waals forces outweigh any influence of hydrodynamic and gravitational forces. These forces control the rheology of the suspension and which colloidal force dominates depends on surface charge of the particle, pH, ionic strength and ionic species in water [16]. To understand the effective treatment and flocculation of these systems, it is necessary to understand how clay particles interact with each other and with polymer flocculants. The following section describes the forces of attraction and repulsion in a colloid suspension, and the mechanisms for flocculation relevant to solid-liquid separation.

### **2.1.2 Electrical Double Layer**

Due to the small size of colloidal particles, the stability of these systems is dependent on surface properties of the particles and their interparticle interactions. Fine particles in colloidal systems tend to have charged surfaces [16]. Because this surface charge is from similar type particles and are of same charge, adjacent particles repel each other, which leads to stabilization of the suspension as observed in MFT slurry. The electrostatic interaction between charged particles and ions in an electrolyte solution is explained by both Gouy-Chapman and Stern double layer models [17].

In colloidal systems a charged surface attracts oppositely charged ions in solution (counter-ions), while the ions of similar charge to the surface (co-ions) are repelled. The electric double layer is formed when the charged surface of the particles is surrounded by an excess of counter-ions. Stern models are used to illustrate the profile of electrical potential distribution near the charged surface. A positively charged particle surface and its surrounding electrolyte solution are shown in a sample Stern model in the top half of Figure 2-3 (top) with the corresponding electric profile shown in the lower part of this figure [17, 18].

The Stern layer is the region between the particle surface and the location in solution where solvent and ions can move and diffuse freely. The Stern layer potential is at its maximum on the surface and decreases linearly from this point to the Stern layer due to the presence of immobilized counter-ions [18]. The potential at the Stern plane is called the Stern potential, beyond which the potential decreases exponentially. The Shear plane is considered to be the no-

slip boundary around the surface. The potential at the point between this no-slip layer and the ion diffuse layer is known as zeta potential ( $\zeta$ ). The zeta potential is the measurable potential difference between the charged surface and the surrounding bulk phase. The zeta potential can be measured experimentally and is used to predict the stability of fine particle suspensions. The potential within the double layer region, including the zeta potential, depends on the type of electrolytes and their concentrations. Therefore, the manipulation of these factors is critical to controlling the attractive and repulsive forces between particles and managing the stability of the suspension.

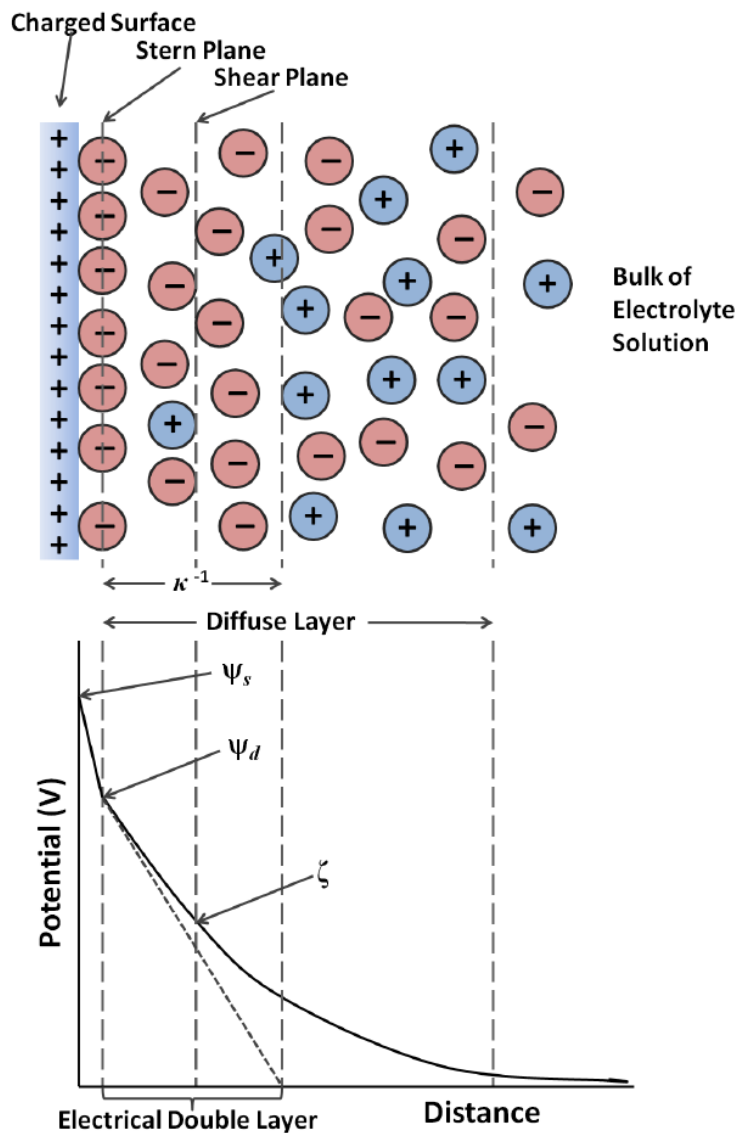


**Figure 2-3: Electrical double layer according to Stern model and corresponding electrical potential profile [17]**

### **2.1.3 DLVO Theory**

The DLVO theory is named for the research of Derjaguin and Landau in 1941 and Verwey and Overbeek in 1948 [2, 17, 19, 20]. It describes the forces between particles in a suspension and is used for the prediction of colloidal stability. The DLVO theory takes into account two balancing forces: attractive van der Waals and the repulsive electrostatic double layer forces. Other forces, such as hydrodynamic forces, are ignored in this theory. The stability of the system or the tendency of ideal spherical particles to remain stable or coagulate depends on the net interaction resulting from the attraction and repulsion between the particles [17].

If the repulsive electrostatic double layer forces exceed van der Waals forces, the net interaction between the particles is repulsive and particle aggregation is prevented. In a dispersed suspension there is an energy barrier that prevents the aggregation of particles. Otherwise, the particles will attract to each other and form aggregates. The size of the aggregates depends on the balance of forces acting on them. An aggregate can thus be viewed as a basic unit which is formed due to strong attraction among its constituent particles [21].

## **2.2 Mechanisms of Coagulation and Flocculation**

To enact the aggregation of colloidal particles in a stable suspension the system must have the energy necessary to overcome the activation energy. This can be accomplished in a brute force method by physical means like centrifugation, or by increasing the temperature of the suspension to increase the kinetic energy of particles. There are alternative methods of destabilizing a suspension that involve changing the magnitude of the energy barrier itself. The energy barrier for particle aggregation can be lowered or removed to make the net interaction attractive. This can be achieved by many different mechanisms, which can be classified as either coagulation or flocculation. Flocculation involves the use of an organic polymer to destabilize colloidal particles and allow them to combine into a larger sized aggregate, known as flocs. The large flocs settle quickly under gravity. Coagulation generally refers to the process of changing the forces that are acting to keep the particles apart from each other. This is accomplished by the addition of inorganic chemical, known as coagulants that reduce the particle's repulsive forces.

### **2.2.1 Double Layer Compression**

Double layer compression involves increasing the electrolyte concentration in the suspensions. The addition of a salt such as KCl which is indifferently attracted to the colloidal surfaces will

have a minimal effect on pH. Increasing ionic strength of the electrolyte forces the counter-ions of the stern plane closer to the particle surface. In essence, more ions of opposite charge diffuse to the particle and compress the electric double layer. The distance at which the colloidal particles are influenced by the repulsive electrostatic double layer decreases with increasing ionic strength of the electrolyte [17]. Hence, two particles are able to get closer and aggregate because they can fall into the range where the van der Waals attractive forces dominate.

### **2.2.2 Surface Charge Neutralization**

The charge neutralization of a particle surface occurs when the charged counter-ions have a specific affinity for the surface of the colloid. This affinity goes beyond the electrostatic attraction for double layer compression. This type of ion have a strong tendency to adsorb onto the particle surface and reduce the primary charge of the colloid to the point where the zeta-potential is neutralized or reversed. The addition of multivalent ions such as  $Al^{3+}$  and  $Ca^{2+}$  is more effective for this purpose. Therefore reagents such as lime, alumina, and gypsum are widely used in water treatment industries [22].

Oil sands producers utilize this mechanism in new technologies for the reduction of their MFT buildup. One widely used technology is the composite tailings (CT) process in which a mixture of gypsum and coarse sands are mixed into the MFT. The  $Ca^{2+}$  ions of gypsum compress the double layer of the fine particles, resulting in improved aggregation [9]. In composite tailings operations hydrocyclones use centripetal force produce to compressed solid sediments. Within 30 days a consolidated sediment of 82% solids is produced [9]. A similar method to produce non-segregated tailings has been attempted with sulphuric acid [23].

The primary risk of these processes is the effect on ionic content and pH of the recovered tailings water. The recycled water fails to meet the criteria for the oil sands extraction process, due to the high salt concentration and the presence of  $Ca^{2+}$  ions [23]. These divalent cations are detrimental to bitumen liberation. They are responsible for the compression of the electric double layer of the fine clay particles. The compression of the electrostatic double layer decreases the detachment efficiency of bitumen from solids and increases the fines content of the froth [24]. These issues can be addressed with an alternate technology of particle aggregation known as paste technology which employs a "bridging" polymer flocculant as the chemical additive.

### 2.2.3 Flocculation and Bridging Mechanism

The first research to define flocculation by bridging was carried out by Ruehrwein and Ward in 1952 [25]. A long chain polymer comes into contact with a particle, and some of its functional groups will adsorb and bind to the surface. The other end of the polymer extends into the solution and will potentially adsorb onto several other particles, with the polymers acting as a “bridge” to create a larger aggregate [25]. Large molecular weight polymers can attach to a particle several times in a series of loops that also extend outwards into the solution.

Long chain polymers must be added in small doses since there is an optimal polymer concentration for any suspension, beyond which addition of more polymer is detrimental to flocculation [26]. The “bridging” mechanism is compromised if the available particle surface is limited by an overdose of polymer, hence there is an optimal coverage of the particle surface by adsorbed polymers [26].

There are many factors and trade-offs regarding the performance of polymers as flocculants. Too low polymer dosage results in insufficient bridging links and small flocs. Excess polymer dosage leads to a restablization of the suspension, known as steric stabilization [27]. Bridging flocculation has an optimal flocculant dosage when only half of the particle surface area is covered by adsorbed polymers. Exceeding this polymer dosage is detrimental to flocculation kinetics and leads to smaller floc size.

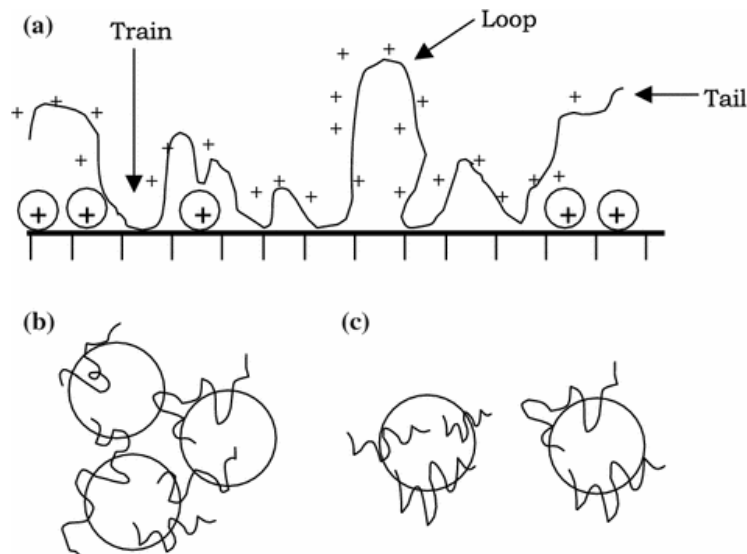


Figure 2-4: Adsorption of polymers, and formation of loops and bridging mechanisms [28]

#### **2.2.4 Additional Effects on Flocculation**

For bridging flocculation, the polymer molecule must be capable of spanning the gap between the particles. Adsorbed polymers of higher molecular weight extend further away from the particle surface and are slower to reach equilibrium. Therefore, the higher the molecular weight of a polymer the larger the floc size [29]. There is an economic trade-off if the end-user prefers water recovery over rapid flocculation. The lower molecular weight polymers usually produce small tight flocs with small amounts of entrained water. The larger flocs are also more likely to be broken up when subjected to the shear stress in a pump or pipeline. Moss and Dymond (1978) reported that average polymer molecular weight is not the only criterion for effective flocculation. They observed several factors affecting flocculation, including effect of polymer dosage, particle size, effect of shear and agitation, particle concentration, and the polymer molecular weight distribution [30]. The slurry conditions and polymer conformation have an influence on flocculation performance, and will be discussed briefly in this section.

Excessive agitation of a flocculating suspension causes breakage of flocs. This has an adverse effect on flocculation efficiency, as the smaller flocs formed have a lower settling rate. Floc breakage leads to exposure of fresh particle surfaces to polymer adsorption, thereby resulting in increased adsorption capacity of the flocculant. The flocs do not reform efficiently as the excess adsorbed polymer causes repulsion. The trade-off for slurry agitation is a balance between sufficient turbulence for the efficient mixing of the polymer and particle collision balanced against floc breakage, with larger flocs being less resistant to breakage from the shear. The optimum dosage for a polymer only holds at a particular degree of agitation, since the floc size increases with polymer dosage until the point of system overdose [3, 31].

Mpofu (2004) examined a temperature-sensitive non-ionic polyethylene oxide (PEO) [32]. The polymer has two configurations: a relaxed hydrophilic configuration at room temperature, and a collapsed configuration at temperature  $>45^{\circ}\text{C}$ . In this respect it is similar to the CP05 copolymer, the focus of this thesis. PEO has been used to flocculate a kaolinite suspension, demonstrating that flocculation kinetics and settling rates were strongly influenced by the polymer conformation. At low temperatures the polymer extends out into the solution with many loops and tails. This phenomenon creates effective bridging between particles, leading to larger flocs and a high settling rate. At higher temperatures the polymer collapses and clings in a tight

configuration to any surface it encounters. The lack of loops and tails extending into the solution results in poor bridging and flocculation [32].

An observation of special interest in this research is the flocculation behaviour when the PEO is still in its relaxed configuration, from 20°C to 40°C. The settling rate increases with temperature right up to the point where the configuration transition occurred [32]. This phenomenon might be explained by the polymer adsorption kinetics. The investigations carried out by McFarlane (2007) and Hogg (1999) are the most useful ones in explaining this phenomenon [33, 34]. It has been noted that the adsorption of polymers onto fines is extremely rapid, lasting for only a few seconds when there is sufficient agitation. This leads to issues such as local overdoses of the solutions when the polymer preferentially adsorbs onto larger particles [33]. MacFarlane compared the adsorption rate of different polymers against the settling rate, and noticed an inverse correlation [34]. Despite the simultaneous adsorption of the polymer and the growth of flocs observed by Hogg (1999), the slowest adsorbing polymer results in the highest settling rates and largest flocs. This observation holds true in circumstances where adsorption rates are modified, such as by temperature changes. Increasing the temperature of flocculation decreases the adsorption rates and increases the floc settling rates, in agreement with the results reported by Mpofu et al. [32, 34].

### **2.3 Previous Studies on Flocculation of Oil Sands Fine Tailings**

As mentioned in Section 1.0, the buildup of mature fine tails is an issue for commercial oil sands mining operations. The process of flocculation has been reported in the literature as an effective method for increasing the efficiency of the fine tails consolidation process. Baillie and Malmberg experimented with many different inorganic electrolytes and organic polymers as potential coagulation and flocculation reagents for the fine tailings [31, 35]. Their experiments showed poor performance of flocculants at the normal pH of the tailings slurry (~ 8.5). The MFT has to be destabilized for good flocculation by adjusting the pH to either below 7.5 or above 9.5 [31]. The downside of this approach is a build-up of undesirable ions in the recycle water, similar to what was discussed in the CT process [24].

Cymerman et al. (1999) showed that high molecular weight, medium charge anionic copolymers of acrylamide and acrylates, such as Magnafloc 1011 (also known as Percol 727), induced flocculation of the fine tailings at the normal pH of the tailings slurry with relatively low dosages



[36]. Their results showed that Magnafloc 1011 produced fast settling flocs and a turbid supernatant water layer containing about 1.5 % solids by weight [36].

Building on this breakthrough Sworska et al. (2000) studied the effect of Magnafloc 1011 dosage, pH and divalent cation concentration on settling rate and turbidity of Syncrude fine tailings [37, 38]. Different dosages of Magnafloc led to different optimal pH ranges, possibly due to contamination of the mineral surface with polar organic matter. Further studies conducted by Sworska (2000) on Syncrude fine tailings showed that flocculation performance has a strong dependency on mixing conditions. Their investigation shows proof that turbulent hydrodynamic conditions improve the polymer distribution in the flocculating suspension and results in a smaller polymer dosage required to achieve good flocculation [39].

A flocculant screening investigation carried out by Xu et al. (2003) on Syncrude extraction tailings produced similar results [40]. They concluded that only anionic polymers with a narrow range of charge densities can efficiently flocculate the fine tails at a process water pH of 8.5 [40]. The high molecular weight flocculants can form large flocs, resulting in increased settling rates. In these cases the large anionic polymers Percol LT27A and Percol 727 caused rapid settling of tailings at optimal dosages, but were susceptible to overdosing and restabilizing the suspension. Xu et al. were unable to obtain a clear supernatant even at optimal dosage using a single polymer additive [40]. The goal of this study was to meet key requirements of oil sands tailings processing, faster aggregate settling to recycle warm supernatant water of low turbidity and divalent ion concentration. The latter two points were accomplished by utilizing a low molecular weight, highly charged cationic polymer called Percol 368 to the supernatant. The use of a polymer flocculant replaces the divalent ions that are unsuitable for recycling of process water.

It seems counterintuitive that an anionic polymer like Magnafloc 1011 is the most effective at flocculating MFT, a mostly anionic colloidal dispersion. The prevailing theory proposes that there is polymer molecule expansion due to charge repulsion between the mineral surface and polymer. The flocculation kinetics of Magnafloc 1011 facilitates increased bridging of hydrogen-bonding functional groups due to increased polymer length and long adsorption time. Using QCM-D to track adsorption conformation, Alagha et al. (2013) suggested that Magnafloc preferably adsorbs onto the alumina ('O' basal plane) surface of the kaolinite through weak electrostatic attraction and hydrogen bonding. The repulsive forces acting on this high-molecular

weight polymer led to a low degree of compaction of the polymer on the surface, which is beneficial to the degree of bridging between particles [41].

The issue with many of these polymer treatments is that while the initial settling rates and clarity of the supernatant can be drastically improved at optimum dosages, the addition of polymers by themselves (such as Magnafloc 1011) does not significantly improve consolidation (compressibility) of the settled suspension. The solids content of the final sediment is a key consideration of tailings disposal. The requirement of tailings managements is to make a trafficable deposit with a high shear yield stress [8]. Mechanical forces are also often pursued with schemes involving thickeners or filtration [40, 42]. A recent advance is the research of Alamgir et al. (2012) who used a two-step flocculation and filtration process to produce trafficable MFT sediments. A cationic organic–inorganic hybrid polymer called Al-PAM was mixed in diluted MFT. The large fluffy flocs were created with low solids content supernatant. These products are ideal for a thickener-filtration set-up. These studies demonstrate that there are still many novel approaches in paste technology that can be pursued.

## **2.4 Temperature Sensitive Polymers**

Temperature sensitive polymers exhibit drastic step changes in properties with temperature. In most cases this refers to polymers that are soluble in water at low temperatures, but are not soluble once the temperature exceeds an intrinsic transition point of the polymer [43]. The polymer has gaps in its miscibility range in a temperature-composition phase diagram for a particular solvent system. The polymer can rapidly dissolve into or separate out of the solution at critical temperatures. The Flory-Huggins solution theory is used to explain the role of temperature in the phase changes of non-crystallizing temperature-sensitive polymers [43].

The Flory-Huggins theory proposes that all polymer-solvent systems should have a phase diagram showing the upper critical solution temperature (UCST) and the lower critical solution temperature (LCST), see Figure 2-5 [43]. The UCST is the temperature above which the polymer and the solvent are miscible in all compositions, while the LCST is the temperature below which the polymer and the solvent are miscible for all concentrations [43].

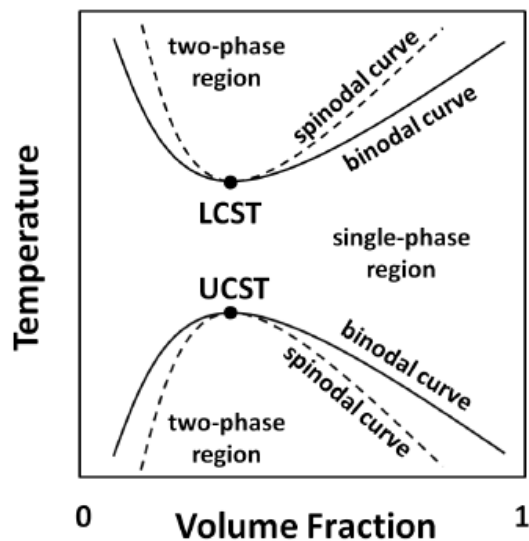


**Figure 2-5: Two phase diagram for temperature sensitive polymers in solution [43]**

The LCST behaviour occurs in temperature sensitive polymers which exhibit a coil-globule transition. A coil-globule transition is a reversible process in which polymer molecules collapse from expanded hydrophilic coils to shrunk hydrophobic globules as the temperature of the solution increases above the LCST, and vice versa when temperature drops below the LCST [44, 45]. Poly(N-isopropylacrylamide) (pNIPAM) is one such temperature-sensitive polymer which has a coil-globule transition in aqueous systems at 32°C. NIPAM is hydrophilic and soluble in water at temperatures below its LCST of 32°C. Above this temperature the hydrogen bonds between water molecules and polymer chains are disrupted in favor of intramolecular and intermolecular hydrogen bonds. The formation of such bonds causes the molecule to coil up and aggregate, forming precipitates. The hydrophilic sites on the polymer are used up, resulting in a hydrophobic polymer that is insoluble in water [44, 45].

#### **2.4.1 Previous Research involving NIPAM as a Flocculant or Dispersant**

The method of NIPAM synthesis and its potential as a flocculation agent of suspensions was first described in a patent by Guillet et al. in 1985 [46]. His method employed cationic temperature-sensitive polymers prepared by copolymerizing NIPAM with cationic monomers. The patent claims that below the transition temperature cationic NIPAM is an effective flocculant of suspensions containing negatively charged colloids such as aqueous mixture of titanium oxide (TiO<sub>2</sub>), clay and paper fibres. This is the result of the polymeric bridging mechanism described earlier. At temperatures above the LCST of NIPAM cationic copolymers the flocculation

efficiency is significantly reduced. The work of Deng et al. (1995) suggests that the cationic temperature sensitive polymer can still induce the flocculation of TiO<sub>2</sub> suspension above the transition temperature [47]. The cationic copolymer is transformed into cationic colloidal particles above the LCST, and still holds the ability to induce aggregation.

The research of Frank et al. over the past decade has demonstrated that as a flocculant, the cationic NIPAM stands on equal footing to similar cationic PAM polymers [48]. Unlike conventional PAM polymers that have no response to stimuli, the temperature-sensitive polymers have manipulatable interparticle forces that can disperse or flocculate particles. Franks et al. (2009) investigated the use of NIPAM for multiple functions in mineral processing by cycling between its hydrophobic and hydrophilic states [48]. The coil-globule transition is the attribute of interest in NIPAM for developing flocculants. In recent years different research groups have exploited it. Li et al. [49] and Franks et al. [29] showed that pNIPAM produced flocs of significantly higher settling rates when the polymer is added at temperatures below the LCST, and the suspension settled at a temperature above the LCST. The proposed mechanism for this phenomenon is that coil-globule transition of the pNIPAM inside a floc pulls the clay colloids tighter together, as illustrated in Figure 2-6.

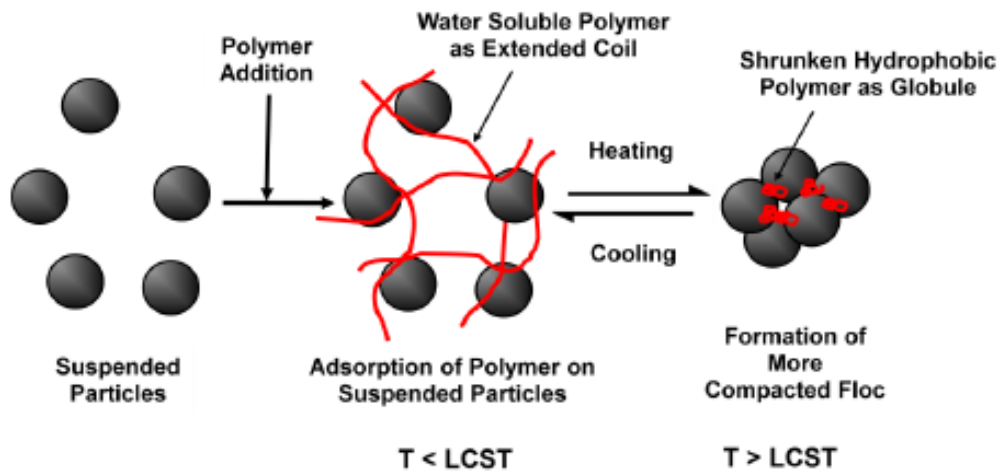


**Figure 2-6: Flocculation mechanism by temperature sensitive polymers[3]**

The mechanism of temperature-cycling is also useful after the polymer-clay suspension has settled. Secondary consolidation in the sediment occurs when the LCST is exceeded, decreasing the final moisture content. Increasing the average molecular weight of the pNIPAM (from 0.7 to

3.6 MDa) is a key factor in improving the flocculation efficiency of the pNIPAM [50, 51] and an important consideration in the synthesis of CP05.

Franks et al. [48] and Forbes et al. [52] pushed this concept of temperature-cycling even further to utilize responsive polymers as multi-function flotation aids. The transition of the pNIPAM at high temperature to a hydrophobic state, and the presence of the polymer on the aggregate surface significantly increases the probability of attachment between particle and air bubbles [48]. The cycle of temperatures above and below the LCST can, with a charged pNIPAM copolymer, be used to selectively collect specific charged particles from a suspension [52]. It should be noted that Franks et al. utilizes non-ionic pNIPAM, and the hydrophobic force is the primary means for causing aggregation.

Sakohara and Nishikawa (2007) used a copolymer of N,N-dimethylaminopropylacrylamide (DMPAA) and NIPAM as a flocculant of TiO<sub>2</sub> suspensions [53]. Their investigation showed that the coil-globule transition of the flocculant is affected by pH, temperature, and the DMPAA content. p(NIPAM-co-DMPAA) is similar in function and property to the synthesized CP05 copolymer of this thesis. In subsequent investigations Sakohara et al. focused on the dewatering and compaction of different suspensions using oppositely charged pNIPAM copolymers [54, 55]. The coil-globule transition during sedimentation produced a large reduction in sediment volume. The method of using oppositely charged polymers demonstrates how temperature sensitive polymers can match the performance of commercial flocculants [54]. Fujishige et al. established that the coil-globule transition of pNIPAM in water is independent of molecular weight [45]. The different copolymers of pNIPAM and the transition temperature in all these different studies will depend on the composition of the copolymer and the suspension pH [53]. The following table summarizes the research and polymer properties of relevant researchers mentioned thus far.

Previous researchers in oil sands tailings treatment are developing incrementally more effective flocculants and techniques for settling of MFT. Researchers who investigated pNIPAM demonstrated small improvements of suspension settling and dewatering utilizing the polymer's temperature response. This body of work aims to investigate how the switchable characteristics of pNIPAM polymers can influence sediment rheology, particularly yield stress and drainage.

**Table 2-1: Polymer research on oil sands tailings management**

<b>Polymer Name</b>	<b>Researchers</b>	<b>Object of Research</b>	<b>Polymer Characteristics</b>
Al – PAM	Lana Algaha [41]	Rapid settling and Polymer adsorption	Cationic colloid core with multiple polymer branches
Magnafloc 1011	Sworska et al. [38] and Xu et al. [36, 40]	Settling of MFT	Anionic with high avg. molecular weight
pNIPAM, with no copolymers	Franks, O’Shea and Burdukova [29, 48, 51]	Targeted reactant for floatation and settling	Neutral switchable pNIPAM
pNIPAM-co-acrylic acid and pNIPAM-co-DMAEA quaternary chloride	O’Shea (2011) [56]	Polymer switchability during settling and influence on sediment height	Anionic and Cationic switchable pNIPAM copolymers
NIPAM-co-DMAPAA	Sakohara and Nishikawa [53]	Activated sludge dewatering and compaction	Cationic switchable polymer
NIPAM-co-DMAPMA	Zhenghe Xu [3]	Polymer switchability during and after settling. Effect on suspension settling and sediment rheology/dewatering	Cationic switchable polymer

## 2.5 Rheology

### 2.5.1 Newtonian and Bingham Fluids

Rheology is defined as the study of deformation and flow. The knowledge of these key properties is essential to engineering applications. The understanding of these properties and how they relate to particle suspensions is necessary for the design and creation of dewatering systems. There are a number of different models describing the rheological behaviour of different fluids and liquids. The simplest and most well-known model is Newton’s law of viscosity. For Newtonian fluid, the relation between shear stress and shear rate is linear, with a shear-independent proportionality constant, known as viscosity. However, there are many fluids and mixtures that do not obey Newton’s law of viscosity. A Newtonian fluid requires only one parameter, viscosity, to characterize its rheological behavior. The study of rheology tends to

focus on non-Newtonian fluids that require more than one parameter to define their rheological properties.

This study utilizes chemical additives to flocculate fine particles in suspension. When the flocs are at rest, in the form of sediments, the interactions among the aggregates create a continuous structure throughout the sediment [16]. The sediment is a non-Newtonian fluid and does not flow until a critical stress is reached, known as yield stress. The applied shear stress must be greater than the yield stress that is applied to force the fluid to flow. Therefore the yield stress is a measure of resistance of the particle network to applied force.

If the fluid flow exhibits a linear relationship between shear stress and shear rate, and the fluid starts to flow when the applied stress exceeds the yield stress, the fluid is known as Bingham fluid. The Bingham fluid model contains a yield stress term and a linear viscosity term, and is sufficient for approximating the behavior of most sediments containing flocculated fine particles within a certain shear rate range. Many researchers have made similar assumptions when modeling the flow behaviour of aggregated particles. Michaels and Bolger (1962) and Litzenger (2004) found the Bingham plastic model suitable for describing the rheological behaviour of mixtures similar to the kaolinite suspension used in this investigation [16, 21]. A typical rheogram for Bingham plastic model is shown in Figure 2-7.

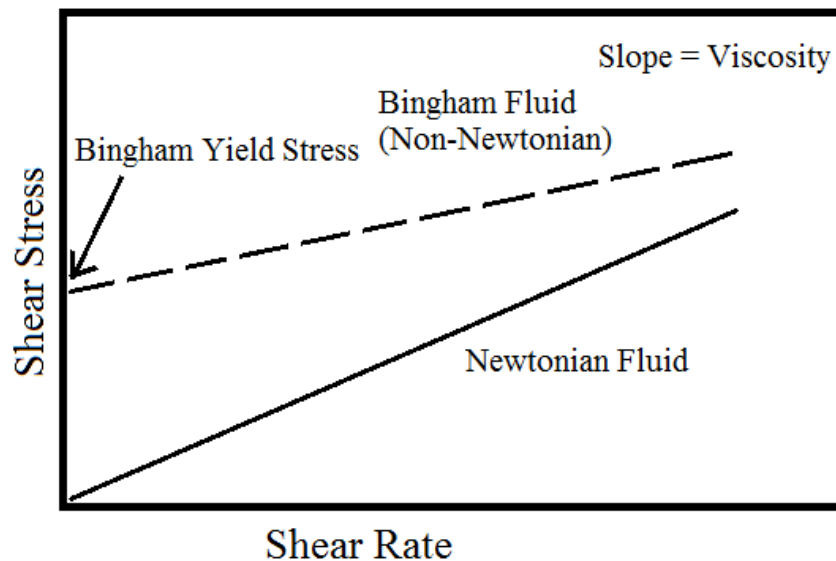


**Figure 2-7: Rheogram for Newton and Bingham fluid models**

### 2.5.2 Rheology Measurements and Vane Yield Stress

The rheological behaviour of the tailings sediments is crucial to the management of the oil sands fine tailings. There are rheological properties that the AER (Alberta Energy Regulator) requires operators of the treated fine solids deposit tailings to achieve within a certain timeframe for both land reclamation and water recovery. It is therefore necessary to be able to model and verify experimentally the behaviour of the treated fine tails suspensions. In Figure 2-7, the Bingham yield stress was the minimum shear stress required to initiate flow. Bingham yield stress can be obtained indirectly by drawing a best-fit straight line through a set of torque versus spindle speed data from rheological measurement. Extrapolating that line backward to zero shear rate where it intersects the y-axis gives the yield stress.

The inherent drawback of the Bingham plastic model is that the extrapolation does not recognize the curvature of the rheogram at very low spindle speeds. Suspensions behave in an elastic manner at very low shear rates. These are known as viscoelastic materials. As a result, the calculated Bingham yield stress of a mixture is typically not the true yield stress. An example of this extrapolation and a comparison of the Bingham and true yield stresses are shown in Figure 2-8.

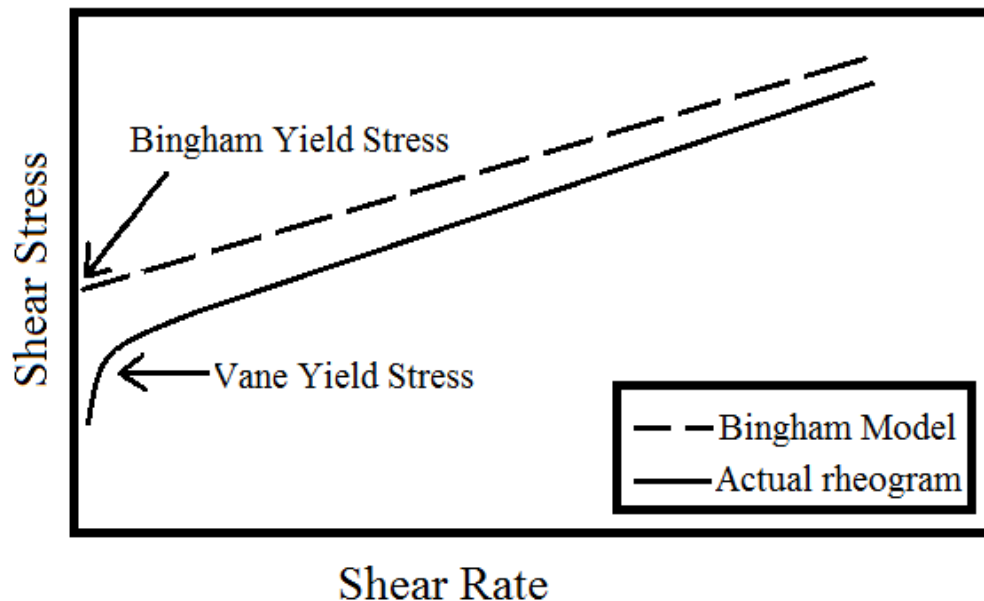


**Figure 2-8: Bingham fluid model compared to actual viscoplastic fluid behaviour**



Nguyen and Boger et al. proposed a yield stress measurement technique using a Vane and spindle [57, 58]. Due to the consolidation of aggregates a rotating vane experiences resistance from the suspension, measured as torque. As shown in Figure 2-9, the torque applied to the vane is determined as a function of time, which exhibits a maximum torque when the vane is rotated at a very low and constant speed. The maximum torque is then converted to the stress based on the geometry of the vane. Vane yield stress is a true material property which is independent of any fluid model for its determination, while Bingham yield stress is a fitted parameter from the model.

A vane consists of thin blades of identical length and width, all connected to a cylindrical shaft at equal angles, as shown in Figure 2-9. According to Nguyen and Boger (1983), this geometrical shape has several advantages. It minimizes the disturbance of aggregate networks or gel during the insertion of the vane and eliminates the effect of wall slip in the measurements [57].

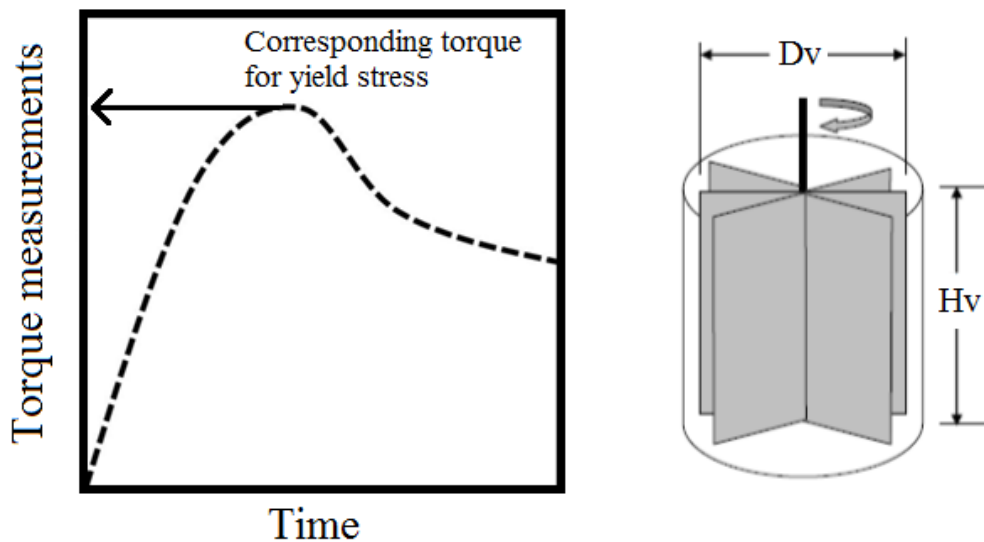


**Figure 2-9: Torque versus time curve from a vane viscosity measurement (right) and schematic diagram of a vane (left) [59]**

The vane must be fully immersed into the sample to obtain an accurate reading, and several conditions must be met in order to minimize any effect caused by the rigid boundaries of the vessel holding the sample:

- 1) Mixture depth =  $2 \times$  Vane height ( $H_v$ )

2) Vessel diameter = 2 × Vane diameter ( $D_v$ )

The relation developed by Nguyen and Boger (1983) uses the maximum recorded torque (see Figure 2-9) to calculate the Vane yield stress ( $f_v$ ) [57, 58].

$$f_v = \frac{(\tau_v)_{max}}{\frac{\pi D_v^3}{2} \left[ \frac{H_v}{D_v} + \frac{1}{3} \right]} \quad (2.2)$$

where  $\tau_v$  is the maximum torque;  $f_v$  is yield stress;  $H_v$  is vane height; and  $D_v$  is the vane diameter.

### 2.5.3 Previous Research on Rheology of Flocculated Suspensions

This literature review aims to argue that a settled suspension will resist flow based on the strength of the particle network. There are many forces and factors in a suspension that determine the rheology. This is not limited to the relative magnitudes of occasionally opposing forces and parameters such as particle size, concentration, and volume fraction. The strength of inter-particle forces of the particles, enhanced by the polymer, will depend on the suspension conditions such as the pH and salt concentration. It will also be dependent on conditions such as polymer type, charge, and concentration. To generalize these factors, the strength and number of bonds between particles that need to be broken have a direct relationship with the strength of the attractive particle network [60]. This section summarizes a portion of the wide ranging research performed on flocculated sediments.

The yield stress increases sharply with increasing solid loading. A power-law equation for correlating yield stress with volume fraction showed an exponent of four [61]. Zhou et al. (1999) and Leong et al. (1995) concluded that the yield stress of sediment is inversely proportional to the square of the average diameter of fine particles [61, 62]. This dependence occurs because the diameter of a particle is directly related to the available surface area for inter-particle bonds. In summary, the larger the water release in flocculation, the higher the yield strength of the resulting sediment.

Litzenberger et al. (2004) suggested that the relative magnitude of opposing forces, such as electrostatic repulsive and van der Waals attractive forces, in a suspension will control the rheology [21]. This investigation compared the opposing effects of a flocculant and a dispersant on yield stress [21]. The addition of a flocculant helped the van der Waals attractive forces to

exert more influence over the electrostatic repulsive forces, increasing the yield stress of the mixture. Conversely, with a high dose of dispersant the formation of flocs and aggregates is halted. The increase in electrostatic repulsive forces decreases the yield stress of the suspension.

Nasser et al. summarized many competing effects that polymer charge, type, and molecular weight will have on rheology [63, 64]. Cationic polymers adsorb quickly onto negatively charged kaolin, accomplishing this by electrostatic attraction and hydrogen bonds to create a strong network of flocs. Intuitively, the higher molecular weight cationic polymers produce sediments of higher yield strength since the polymer acts as a longer and more effective bridge between multiple particles [64]. The polymer charge is an equally important factor for determining the yield stress of the flocculated suspensions. An increase in polymer charge does produce a stronger particle network, however, it has the additional effect of reducing the average floc size. Since the particle is strongly attracted through electrostatic force, it adsorbs more rapidly onto fewer particle surfaces, which limits the bridging mechanism for creating large flocs [63]. For polymers with low charge density, the yield stress can be improved by increasing salt concentration or pH. This approach is consistent with the prediction by DLVO theory. This relationship is not seen in polymers of high charge density.

The flocculation performance of cationic polymers on kaolinite suspensions can be contrasted with the flocculation performance of an anionic PAM based polymer. The polymer is not completely repelled by electrostatic forces and can still form strong bonds with particles due to hydrogen bonding. The anionic polymer adsorbs slowly onto the particle surfaces. The slow adsorption gives the polymer time to relax and stretch its structure, creating loops and tails which lead to the formation of large, open-structure flocs [63]. The cationic polymers naturally have the stronger bonds, reflected in the high resistance to shear (yield stress) and compression (compressive yield stress) [63]. The particle network produced by anionic polymers is comparably weaker, but this weak network may be useful for tailings management. The low compressive yield stress of the flocculated clay makes the solid sediments easier to compact in certain mechanical processes, such as in a high-speed centrifugation [63]. The flocculated paste by anionic polymers will consolidate to a greater extent and release more water than higher yield stress sediments produced by cationic polymers.

In 2009 Zhou et al. came to a similar conclusion when examining the relationship of yield stress and polymer charge. Floccs and particle networks are created through different means using differently charged polymers [65]. The most important are the charge neutralization and the patch and bridging mechanism. Which mechanism is dominant in a particle network of polymer-clay suspension has a critical influence on yield stress, and bed drainage.

In 2011 Margo Chan aimed to encapsulate the research areas of temperature-responsive polymers and flocculation [3]. Her research tied together the influence of polymer transition during settling with the strength and filterability of the flocculated clay suspensions. Adding a cationic temperature sensitive polymer in a batch settling test of a clay suspension below its LCST produced relatively large porous floccs. The settling rates and filterability of the particle network are improved when the suspension temperature is raised above the LCST, densifying the attached temperature sensitive polymers and hence the floccs. Optimizing this flocculation system in terms of pH and temperature, as well as utilizing the polymer transition to control settled clay rheology and drainage are the focus of this investigation.

## Chapter 3 : Materials and Experimental Procedures

The primary objective of this study is to understand the behaviour of kaolinite suspensions flocculated with a temperature responsive copolymer. The rheological and drainage behaviour of settled suspensions are tested “in place” using a custom-designed novel experimental set-up. With this set-up, the particle network created through flocculation and deposition is not destroyed by avoiding the transfer of the sediment.

### 3.1 Material Preparation and Chemical Synthesis

#### 3.1.1 Particle Characterisation - Kaolinite

Kaolin clay, known also as kaolinite, is a hydrous alumina silicate comprised of a tetrahedral silica sheet bonded to an octahedral alumina sheet through the sharing of oxygen atoms between silicon and aluminum atoms in adjacent sheets. The general chemical composition of kaolinite is  $\text{Al}_2\text{O}_3 \cdot 2\text{SiO}_2 \cdot 2\text{H}_2\text{O}$ . In the current study, acid washed kaolin (K2-500, Fisher Scientific), with less than 2% acid-soluble substances and less than 0.001% lead was used. The particle size distribution of the kaolin was measured using a Mastersizer 2000 (Malvern Instruments, UK). A kaolin suspension prepared to 5 wt% and pH adjusted to 8.5 was used. As shown in Figure 3-1, the particle size distribution shows the  $d_{10}$ ,  $d_{50}$ , and  $d_{90}$  of 0.17  $\mu\text{m}$ , 3.8  $\mu\text{m}$ , and 15.6  $\mu\text{m}$ , respectively.

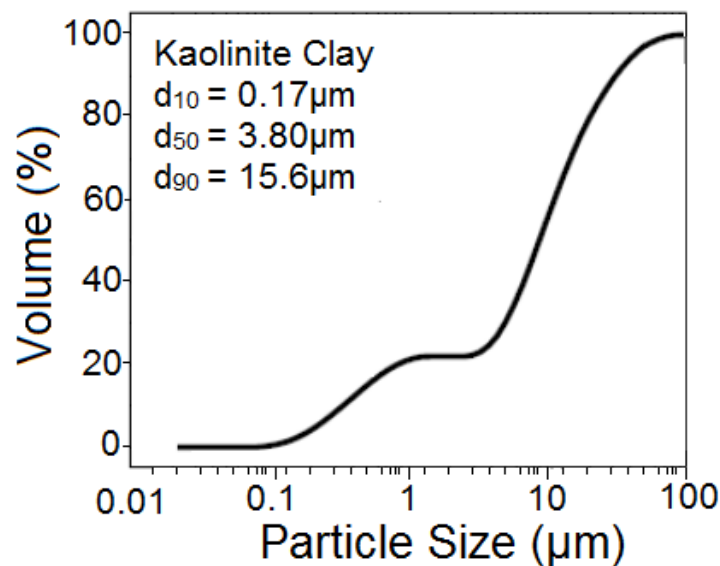
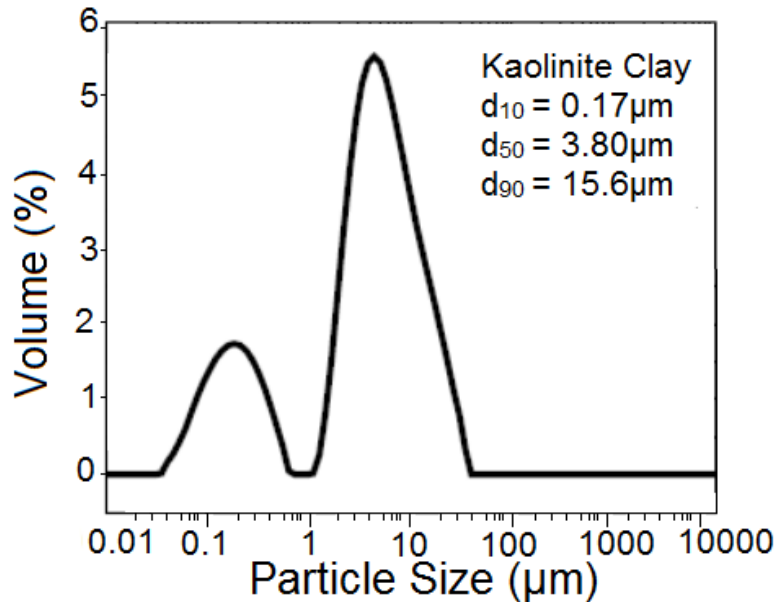


Figure 3-1: The volume-based passing size of kaolinite particles[3]

The uniformity coefficient,  $d_{90}/d_{10}$ , refers to the sharpness of the particle size distribution. The  $d_{90}/d_{10}$  was calculated to be 31.5 for the kaolinite clay used. The large uniformity coefficient implies a wide range of particle sizes. As shown in Figure 3-2, the kaolinite clay particles exhibited significant polydispersity with two distinct fractions with a  $d_{50}$  at 0.16  $\mu\text{m}$  and 4.4  $\mu\text{m}$ , i.e. ultra-fines and fines, respectively. The existence of ultra-fines represents a better model for real fine tails slurry by the suspensions used in flocculation research [3, 66].



**Figure 3-2: Size distribution of kaolinite particles [3]**

Even though kaolinite is an anisotropic particle, the overall surface potential is negative in slightly acidic and basic solutions. A negative charge can occur when  $\text{Al}^{3+}$  replaces  $\text{Si}^{4+}$  in the tetrahedral sheet (silica basal plane) of the clay surface. This charging mechanism is known as isomorphic substitution. The iso-electric point of kaolinite is dependent on pH, ion concentration and the cation valency [67].

### 3.1.2 Preparation of Kaolinite Suspensions

A model tailings system was used in all the experiments of this study. Approximately 400mL of 5 wt% kaolinite clay suspension (kaolinite K2-500, Fisher Scientific) was dispersed in model tailings water and stirred at 500 rpm for a minimum of 12 hrs. Model tailings water was prepared as a 10 mM KCl solution using deionized water with resistivity of 18.2  $\Omega$ . Using a background electrolyte ensured that the ionic concentration was consistent at different pHs between pH 5.5 and 10.5.

### 3.1.3 Synthesis procedure for p[NIPAM-co-DMAPMA]

The primary flocculant used in this study was a copolymer of (N-isopropylacrylamide) (NIPAM), and *N*-[3-(Dimethylamino)propyl]methacrylamide (DMAPMA). The copolymer, CP05, synthesized in house contained 5 mole% of DMAPMA. The copolymer was synthesized by free radical polymerization, following procedures described by Guillet and Heskins [46]. This monomer ratio was targeted such that CP05 would have an LCST below the industrial tailings process temperature of 45°C. The synthesis, purification, and characterization of this class of temperature-sensitive and NIPAM-based polymers have been discussed in detail by Hongjun Li (2007) [49], and is briefly described in following paragraphs.

The monomers *N*-[3-(Dimethylamino)propyl]methacrylamide (DMAPMA, 99wt% Sigma-Aldrich) and N-isopropylacrylamide (NIPAM, 99 wt%, Fisher Scientific) were stabilized with 500 ppm MEHQ. The initiator and accelerators of this polymerization reaction were ammonium persulfate (APS) (>98 wt%) and *N, N, N', N'*-tetramethylethylenediamine (>99 wt%), respectively. *N, N, N', N'*-tetramethylethylenediamine (>99 wt%, GC, Sigma-Aldrich) contained less than 0.02 wt% water as an impurity. Ammonium persulfate (>98 wt% APS, ACS reagent, Sigma-Aldrich) had total impurities of less than 0.005 wt% insolubles and less than 0.04 meq/g acid as determined by the titration test. The APS also contained trace amounts of anions Cl<sup>-</sup> and ClO<sub>4</sub><sup>-</sup> of less than 0.001 wt%, trace amount of cations (<0.001 wt% Fe, <0.5 ppm Mn), and <0.005 wt% heavy metals such as Pb.

The mixture was stirred by a magnetic stir bar (octagonal, 5/16" in diameter, 1" in length) at 250 rpm. Nitrogen gas (grade 5.0) was sparged into the mixture vigorously through a stainless steel needle or plastic tube under the liquid surface. One of the necks of the flask should be open during this period to allow the purging gases to exit. The total weight of NIPAM and DMAPMA for synthesis was set at approximately 5 g, although, reactions with up to 10 grams of monomers were acceptable. In either case both monomers were dissolved in Milli-Q water in a 100 mL 3-necked glass flask. The monomers were added to the solution in a well-ventilated area to counter the noxious fumes of the DMAPMA. 45µL of *N, N, N', N'*- tetramethylethylenediamine was added as an accelerator of the polymerization reaction. The reactor flask was wrapped with aluminum foils to prevent the exposure of the reactants to light sources. A schematic diagram of the synthesis setup is shown in Figure 3-3.

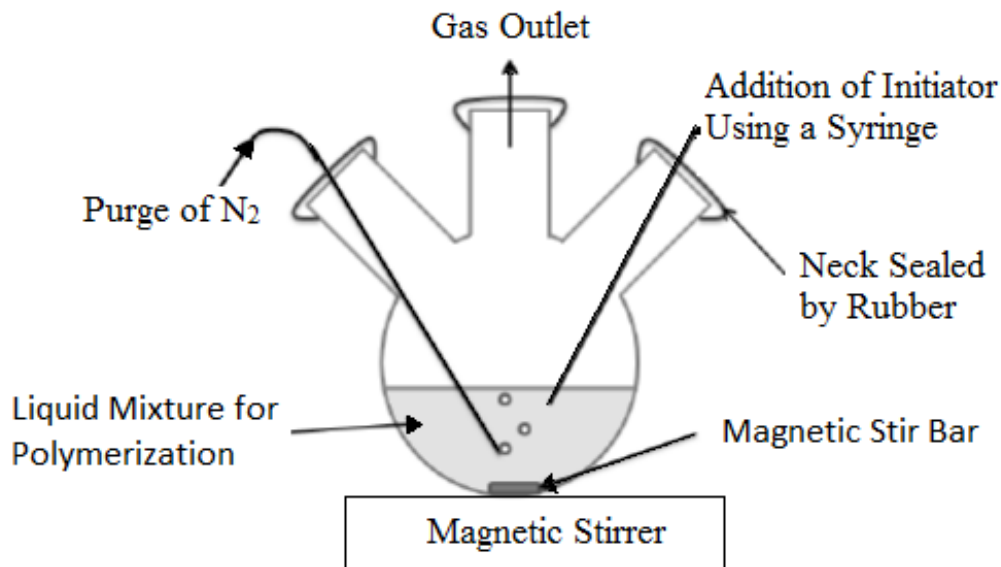


**Figure 3-3: Apparatus used for polymer synthesis [3]**

After 1 hour purging with  $N_2$  gas, 2.3 mL of ammonium persulfate solution (10 g/L) was added into the mixture at a rate of 1 mL/min to initiate the polymerization. The sparging needle was withdrawn from the liquid surface 10 min after the addition of the initiator chemical. The viscosity of the mixture was visually observed to increase during this period. The polymerization reaction was allowed to run for at least 2 hours at room temperature. Mixing and purging of  $N_2$  was then stopped and the reaction flask was sealed. The obtained polymer was a transparent gel, with a rubber-like texture. The resulting gel was left overnight to complete the polymerization reaction. The polymer was then stored in a cooler environment or purified immediately.

The polymer gel was removed from the reaction flask and dissolved in at least 500mL of Milli-Q water, mixed at 250rpm to break up the gel. A heated, pressurized filtration device was used for the purification of the CP05. The polymer was purified in batches by this device. The base plate of the container had a heating element that could be set at 65°C with an 8 cm Whatman 50 filter paper placed on top of it. The filter paper, sieve plate (to support the filter paper), and container were secured by gaskets to prevent leaks. 200mL of polymer solution was added to the container and heated to a temperature above the LCST of the CP05 polymer. The container was then sealed and pressurized to 35psi. The polymer underwent a coil-globule transition and gelled out of the solution. The remaining Milli-Q water, salts, and organic monomers were forced by the



pressure through the filter paper pores. The dense polymer gel was collected the top of the filter paper.

The polymer was transferred to a non-stick Teflon heating bowl. The pressurized filtration device was cleaned thoroughly with surfactants and solvents (not including the rubber gaskets). The purification process was repeated with new filter paper for the rest of the diluted polymer solution. A key point is that the solution should be heated above the polymer LCST before the device is pressurized. The polymer in the Teflon plate was dried in a vacuum oven overnight at 65°C, producing a stable translucent solid. The molecular weight of the polymer was determined by intrinsic viscosity measurements using an Ubbelohde viscometer with 5000ppm of CP05 dissolved in tetrahydrofuran.

#### **3.1.4 CP05 Polymer Solution Preparation**

Milli-Q water with resistivity of 18.2  $\Omega$ , prepared by an Elix 5 followed by a Millipore-UV plus water purification system (Millipore Inc., Canada) was used throughout the study. Reagent grade hydrochloric acid (Fisher Scientific) and potassium hydroxide (KOH, 85% pure, Flakes, Nitrogen flushed, Acros Organics) were used as pH modifiers. Potassium chloride (>99.0 wt% KCl, Fisher Scientific) was used as supporting electrolytes for the preparation of model tailings water.

A 1000 ppm polymer (CP05) stock solution was prepared by dissolving the required amount of polymer in deionized water at room temperature. The stock solution was agitated for 24 hrs to ensure complete relaxation and dissolution of the polymer. All solutions were prepared one day prior to their use in settling tests. Throughout the study, polymer concentrations are always expressed with reference to total suspension mass, unless otherwise stated.

### **3.2 Instruments and Procedures**

#### **3.2.1 Settling Column**

A two-part settling column was custom-designed and fabricated to ensure minimal disturbance of the settled bed for rheology measurement. The apparatus was manufactured by machine shop technicians of the Chemical Engineering Department of the University of Alberta. A 40 cm settling column of 5 cm inner diameter was separated into a lower section at 10 cm from the base and a 30 cm upper section. The two sections were joined by a water-tight flange that was o-ring

sealed. The entire column and flanges were made of transparent acrylic (see Figure 3-4). The column was purposely designed to remove the supernatant above the settled bed to enable further characterisation of the sediment (yield stress, dewatering) without transfer and handling errors. Pouring of the settled sediment from one container to another would destroy particle structure, rendering any further rheological characterisation meaningless. The cross-sectional diameter was specifically chosen to minimize any edge effects that may occur when measuring the shear yield stress using a vane geometry [57, 58]. With this apparatus it was possible to measure the rheological behaviour of the sediment bed in-situ.

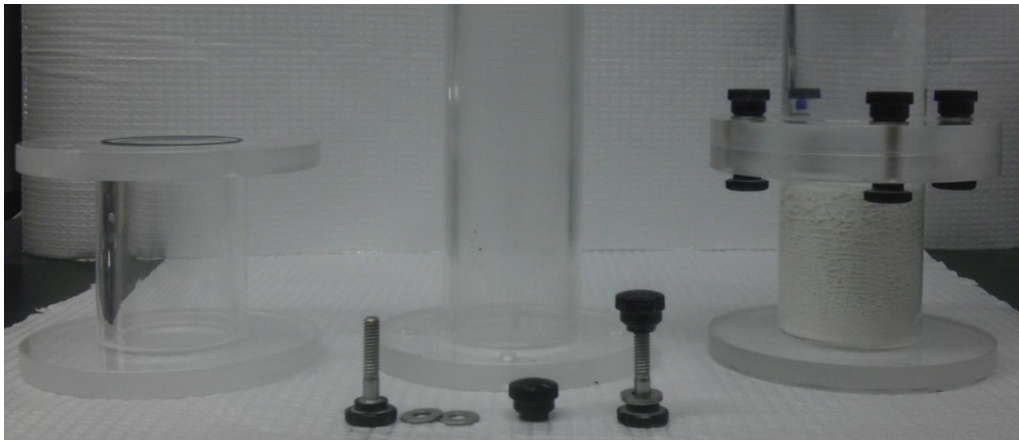


**Figure 3-4: Disassembled and assembled two-part settling column**

A second column was designed for hydraulic drainage measurements of the settled bed (see Figure 3-5). With the same column dimensions mentioned previously, the base plate was exchanged for a flange and gasket set that clamped a filter paper (6.5 cm diameter, Fisher Scientific 41) and metal grate. The filter paper pore size allowed the passage of entrained water within the sediment, a metal grate supported the weight of settled suspension. The base plate included a watertight plug that could be removed to start the drainage of the settled sediment.

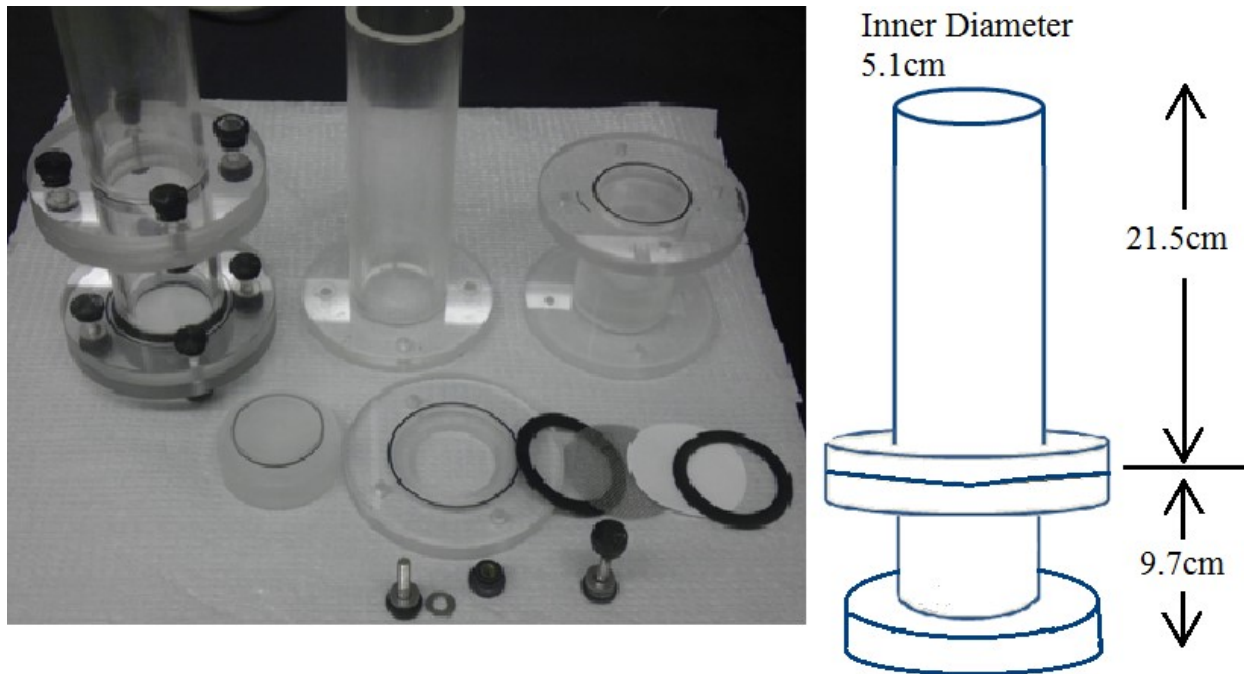


**Figure 3-5: Disassembled drainage column and dimensions drawing**

### **3.2.2 Suspension Agitation and Mixers**

Mechanical stirrers were used to mix suspensions during flocculant addition. A 250 mL beaker was used as a mixing container for many of the settling experiments, and a 1000 mL beaker was used for the combination of settling and yield stress/drainage experiments. The mixing was designed to achieve sufficient turbulent mixing conditions. Since these two experiments were performed in different containers with different ratios of vessel diameter to liquid, the rates for mass transfer and liquid motion will be dissimilar. Refer to Table 3-1 for vessel sizing and scaling ratios.

An overhead mechanical stirrer (IKA® Digital Stirrer RW20, Fisher Scientific) and an axial flow impeller (blade diameter of 3.8 cm, 45° pitched, and 4-bladed) were used to provide agitation for the settling experiments in the 250 mL beaker. A similar axial flow impeller (blade diameter of 5.0 cm, 45° pitched, and 4-bladed) was used in the larger volume tests with the 1000 mL vessel. A tailor-made 316L stainless steel baffle was inserted into the beaker to prevent solid body rotation and vortex motion. A picture of the mixing set-up is shown in Figure 3-6.

**Table 3-1: Mixing vessel sizing and geometric scale comparison**

Sample Size	100 mL	400 mL
Beaker Volume	250 mL	1000 mL
Beaker Diameter	6.7 cm	9.4 cm
Liquid Height	3.6cm	5.9 cm
Rotor Diameter	3.8 cm	5 cm
Baffle Width	0.6 cm	0.7 cm
Height / Diameter Ratio	0.54	0.63
Rotor / Diameter Ratio	0.56	0.53
Liquid Height / Rotor Ratio	0.95	1.18

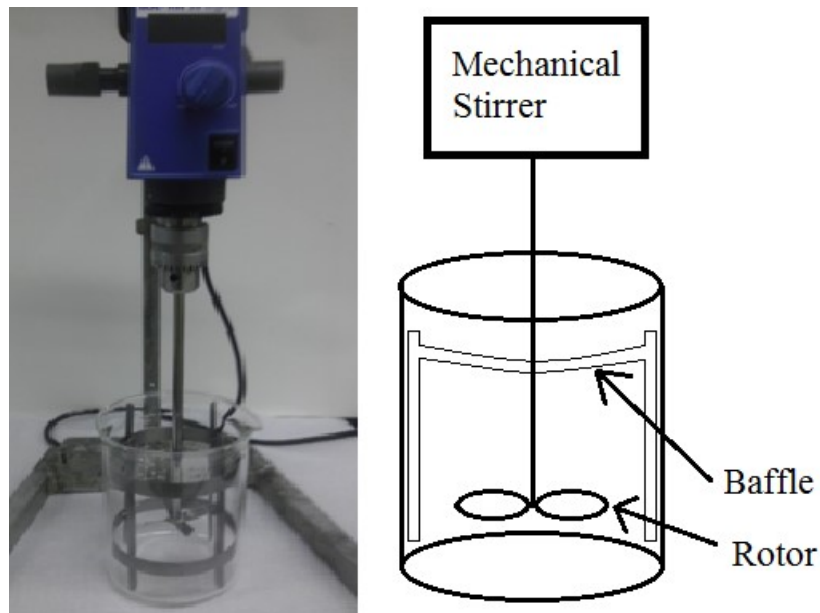


**Figure 3-6: Set-up for suspension agitation and flocculant addition**

### 3.2.3 Settling Tests and Procedures

All of the tests were conducted using the same model tailings, mixing conditions, and polymer stock solutions as summarized below. Error bars are calculated using by standard deviation. A polymer dosage of 100 ppm (with respect to the total mass of the clay suspension) was used for all settling, drainage, and rheological experiments. The different conditions and procedures used in the settling tests are described in this section.

- Model tailings suspension: 5 wt% of kaolinite clay in deionized water with 10 mM KCl
- Flocculants: A copolymer CP05 of 95 mol% (N-isopropylacrylamide) (NIPAM), and 5 mol% *N*-[3-(Dimethylamino)propyl]methacrylamide (DMAPMA), Hyperfloc® AF246 polymer (MW  $14.5 \times 10^6$  g/mol) purchased from HyChem Inc., USA

Temperature was varied from room temperature (21°C) to 50°C at increments of 5°C. The experiments at 50°C represented a typical temperature for waste tailings from oil sands extraction and were above the coil-globule transition point of the CP05 polymer [2].

pH was varied from 5.5 to 10.5. Dilute mixtures of KOH and HCl were used to control pH. The typical pH for tailings suspensions in the industry is pH 8.0 to 10.0. This pH range was found to be most ideal for tailings treatment and received the most attention in literature and industry.

The primary focus of this study was to explore the use of the switchable properties of the CP05 polymer as an effective flocculant and dewatering agent. The following procedures modify temperature and pH during and after flocculation to evaluate the utility of a temperature responsive polymer.

#### **Settling test procedure 1 – EMES (Elevated Temperature Mixing and Elevated Temperature Settling)**

A suspension of prepared model tailings (section 3.1.2) was transferred to a beaker and mixed with a mechanical stirrer at 500 rpm. The beakers were clasped and suspended in a heated water bath. Once the desired temperature was reached, the pH was measured and adjusted before polymer addition. While stirring the suspension at 350 rpm, a predetermined volume of polymer solution was added dropwise at an addition rate of 1 mL/s to the homogenized model tailings.

The targeted polymer dose for flocculation is 100 ppm. The mixing was reduced to 220 rpm for 5 min after polymer addition, while keeping the suspension at a constant temperature.

After mixing, the suspension was transferred to either a 100 mL graduated cylinder for settling tests, or to a 1 L custom-made 2-part settling column for rheology or hydraulic drainage tests. The suspension was transferred to a preheated settling column in a thermostatic water bath. The top of the settling column was sealed and the settling column inverted 5 times, after which the cylinder was positioned upright. The mud-line (solid-liquid interface) was recorded as a function of time. This procedure was performed at different temperatures between 21°C and 50°C.

For example, experiment code 40S40M indicates that both flocculation and settling of the kaolinite suspension are performed at 40°C. The **RMRS** procedure (Room-temperature mixing and Room temperature Settling) was the same as the EMES procedure, and every step was performed at room temperature.

### **Settling test procedure 2 – RMHS**

CP05 was mixed into the kaolinite suspension at room temperature following the same polymer addition and mixing procedure described above. Immediately following the polymer addition, mixing stopped and the beaker transferred to a heated water bath (>50°C). The stirring was then restarted and a thermometer was used to monitor the suspension temperature. Once the temperature exceeded 50°C, stirring stopped and the suspension was transferred to a preheated settling column. These conditions ensured the coil-globule transition of the CP05 polymer after flocculation and before particle settling.

The primary difference between these first two settling procedures, RMRS and RMHS, was that immediately following the addition of the CP05 flocculant the suspension temperature was raised above the LCST of the polymer in RMHS to initiate a coil-globule transition.

### **Settling test procedure 3 – pH Switch**

This procedure was similar in concept to procedure 2. The suspension pH is changed instead utilizing temperature to induce a polymer coil-globule transition. Prior to flocculation the clay suspension was slowly heated to 40°C and its pH changed to 8.5. The polymer solution was added to flocculate the suspension, with mixing being continued for 5 minutes after polymer

addition. During this mixing period the pH of the polymer-clay solution was adjusted to pH 12 by addition of a KOH solution.

#### **Settling test procedure 4 – Post-settling temperature switch (RMRS + Heat)**

The purpose of the switching test (Procedure 4) is to study the effect of temperature change on densification of the sediments of flocculated model tailings. The settling test was identical to the three procedures mentioned earlier. Following settling, the sediments were allowed to consolidate for 1 hr, and then the entire column was transferred to a thermostatic water bath, set to 55°C. The heated settling column was left at this temperature for 24 hrs. After cooling down to room temperature, rheological measurements were performed to evaluate the effect of densification on the sediment.

#### **3.2.4 Shear Yield Stress Measurement Test Procedure**

The settled sediment rheology was measured using a HAAKE Rotovisco VT550 rotational viscometer (Thermo Fisher Scientific, USA). An FL100 vane geometry was attached to the viscometer spindle and the rate of rotation controlled using the instrument software. The FL100 vane consists of six thin blades arranged at equidistant angles around a small cylindrical shaft. The diameter of the vane tool is 22 mm and the height is 16 mm. A schematic of the vane was previously shown in Figure 2-11.

Shear yield stress of the consolidated sediment (undisturbed for 24 hrs) was measured in the settling column. After consolidation the clear supernatant was removed from the settling column using a pipette. The water content of the sediment was calculated by mass balance. The shear yield stress of the sediment was measured using the vane method [57, 58]. A vane tool fitted to the Haake VT550 viscometer was inserted into the sediment to a pre-determined height (5 mm below the sediment interface) as indicated by the notch on the vane tool. With the vane inserted in the sediment, the vane geometry was slowly rotated by the viscometer at a constant rate of  $0.014 \text{ s}^{-1}$ , with the torque versus time profile recorded. The sediment underwent an initial linear elastic deformation reaching a maximum resistance to the vane's rotation before flowing like a fluid. From the maximum torque and the vane dimensions the yield stress can be calculated.

## **Gravity Drainage**

The settling tests for these experiments would be identical to any of the procedures mentioned previously in Section 3.2.3. Settling of the flocculated clay is performed in the drainage column shown in Figure 3-5. The sediment for drainage tests is handled in the same manner as the sediments tested for the yield stress. The settling column containing the sediment was held above an electronic balance using a ramrod and clamp. The plug underneath the sediment was pulled, and the entrained water in the paste drains through the filter clamped to the bottom of the settling column. A beaker was positioned on the tared balance to collect the drained liquid. The flow rate of fluid that passed through the filter is measured for 30 minutes. The plug of the vessel was replaced and the yield stress of the sediment was immediately measured using the viscometer.

### **3.2.5 Quartz Crystal Microbalance with Dissipation Monitoring (QCM-D)**

Quartz crystal microbalance with dissipation monitoring (QCM-D) (Q-Sense, Sweden) was used to measure the adsorption properties of the CP05 polymer in simulated process water onto a silica crystal sensor. In addition to adsorption rate experiments, the conformation of CP05 at increasing temperature (25°C to 50°C) was assessed by measuring both the frequency and dissipation response of the polymer adsorbed onto the sensor surface.

Silicon dioxide-coated sensors (model system for the silica T-basal plane of kaolinite) were purchased from Q-sense. The sensors are AT-cut with a diameter of 14 mm and a fundamental shear oscillation frequency of 5 MHz [68]. The measurement cell was mounted on a Peltier element, which provided accurate temperature control ( $\pm 0.02$  °C). For each QCM-D experiment, deionized water was pumped through the flow module using an IPC-N peristaltic pump (Ismatec, Switzerland).

The QCM-D sensor is a thin quartz disk sandwiched between a pair of electrodes. AC voltage applied to the two electrodes causes the crystal to oscillate at its acoustic resonance frequency. Upon removal of applied voltage, the crystal resonance decreases exponentially. By analysing the oscillation (the resonance frequency (F)) and its decay (energy dissipation factor (D)) it is possible to calculate the apparent adsorbed mass and conformational nature of the adsorbed film (rigidity, thickness). Measurement of resonant frequency change was highly accurate with a sensitivity of about  $0.5 \text{ ng/cm}^2$ , according to the manufacturer [68].



Dissipation (D) is defined as the loss of energy per oscillation period divided by the total energy stored in the system. Changes in the dissipation factor ( $\Delta D$ ) are primarily related to viscoelasticity (softness) of the adsorbed layer. The softness is related to structural changes of the film adhering on the sensor surface, and hence is one indicator of conformational changes of the adsorbed CP05.

### **QCM-D Test Procedures for Polymer Adsorption and Conformational Changes**

Prior to polymer adsorption measurement, the sensors were cleaned with 2 wt% SDS solution, rinsed with deionized water, dried with nitrogen and placed under an UV lamp for 20 minutes to remove any organic contaminants. The flow modules and sensor mounts were washed with 2% Hellmanex prior to each experiment, followed by thorough rinsing with deionized water and blow-drying with nitrogen.

The cleaned QCM-D silica sensor was mounted in the QCM-D flow chambers, and air was pumped at a flow rate of 0.15 mL/min for 5 min. Deionized water was then pumped at 0.15 mL/min through the flow module and over the sensor to measure the  $\Delta f$  of air displacement by water on the silica sensor and to establish a stable baseline. A  $\Delta f \approx -720$  Hz was considered a good indication of a clean sensor. The frequency gain was reset to zero as reference in preparation for polymer addition.

To simulate the adsorption of polymers on solid surfaces during the flocculation process, simulated ideal process water was pumped into the chamber until the adsorption of ions in process water on the sensor reached equilibrium plateau. Polymer solution, prepared by adding polymer stock solution at a specific dosage to Milli-Q water, was then introduced into the flow module at the same flow rate until a new constant signal was achieved. All measurements were conducted with the same background solution, which was 10mM KCl in Mill-Q water solution and pH 8.5 (the same as the polymer solutions) and at a constant flow rate of 0.15 mL/min.

The adsorption kinetics of the CP05 polymer was determined using a 10 ppm CP05 polymer solution. The sealed containers of background solution and polymer solution were heated in a water bath to the experiment temperature. The background solution was pumped continuously through the flow module of QCM-D at 0.15 mL/min until the temperature and sensor signal are at equilibrium. The polymer solution was then added until a stable signal was produced.

Also performed with the QCM-D were experiments that involved the step-ramp of QCM-D temperature in order to study the conformational change of the CP05 polymer. The polymer solution (500 ppm) was pumped onto the sensor at 20°C and pH 8.5 for several minutes. The flow of polymer solution was stopped and the Milli-Q water was pumped through the QCM-D until the frequency signal reached a constant value. The purpose of rinsing is to remove excess polymer that was not attached to the sensor, leaving behind a polymer layer firmly adsorbed to the silica surface. Pumping of fluid was stopped and the sensor module temperature was raised in increments of 5°C steps. Measurements were taken after the frequency signal reached a constant value or equilibrium after each temperature change. To differentiate the signal changes resulting from heating the water from those created by heating the adsorbed polymer, two parallel silica sensors (one silica sensor with adsorbed polymer and one without) were used for this heating experiment.

## **Chapter 4 : Effect of p[NIPAM-co-DMAPMA] Temperature Response on Settling, Rheology, and Dewatering of Kaolinite Suspensions**

Polymer flocculants are typically utilized in mineral processing to enhance solid-liquid separation. Effective flocculation is dependent on attractive interparticle forces and the ability of polymer molecules to form bridges across dispersed particles. These properties can be fine-tuned through experimental conditions such as temperature and pH. In this chapter, experimental conditions for tailings processing are optimized using a polymer, CP05, which exhibits a coil-globule transformation at a critical temperature.

### **4.1 Coil-Globule Transition Properties**

Temperature sensitive polymers display a lower critical solution temperature (LCST) above which the polymer chains shrink into hydrophobic globules [69]. This phenomenon, known as a coil-globule transition, occurs when the secondary amine functional groups of the NIPAM bond preferentially with each other than their interaction with the water. The addition of DMAPMA monomers provide the polymer with a cationic charge, making it a more effective flocculant of charged colloidal particles. The addition of the DMPAMA monomer adjusts the pNIPAM coil-globule transition temperatures. For example, a pure pNIPAM polymer solution has an LCST at 32°C, while the pH sensitive copolymer (CP05) has an LCST which is pH sensitive, see Figure 4-2. The presence of the protonated tertiary amine from the DMAPMA monomer interferes with this transition temperature. In acidic conditions the charge of these functional groups inhibits complete transition from the coil to globule state. Such transition is only possible in weakly basic conditions (pH 8.0 - 11.0).

A temperature responsive pNIPAM polymer dissolved in water will precipitate, making the solution turbid when heated above the LCST. The LCST for NIPAM can be estimated by measuring solution turbidity as a function of temperature. In this study, the solution turbidity was measured using a Turbidimeter (HF Scientific DRT-15CE Portable Turbidimeter, Fisher Scientific). The LCST of CP05 was defined as the midpoint of the transition zone, the steepest part of the turbidity-temperature curve. Figure 4-1 shows the change in solution turbidity as the solution temperature is increased from room temperature. Experimental conditions: 2000 ppm polymer solution prepared at pH between pH 8.0 and 10.5.

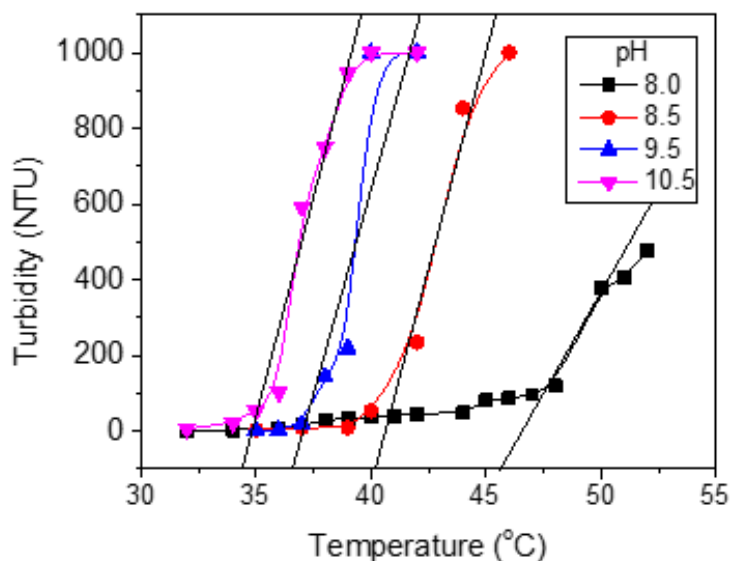


**Figure 4-1: Lower critical solutions temperatures (LCST) of CP05 at different pH measured by solution turbidity**

The polymer LCST is dependent on the degree of co-polymerization. For example, pure NIPAM has an LCST of 32°C and CP05 at pH 8.5 has an LCST of 41°C. The LCST is dependent on the polymer charge density provided by the DMAPMA co-monomer, which is pH dependent. As shown in Figure 4-1, the higher the pH, the lower the LCST of the CP05. Below pH 8.0, CP05 started to lose its temperature switching characteristics as the solubility of CP05 became dominated by highly protonated hydrophilic tertiary amide groups of the DMAPMA copolymer. It is evident that CP05 could not be utilized as a temperature responsive polymer in neutral or acidic suspensions.

The relationship between the LCST of the NIPAM CP05 polymer and its dependence on temperature and pH can be illustrated in a phase diagram. Figure 4-2 shows the distinct phases of the CP05 polymer solution. The fitted plot lines were for guidance and do not represent simulated data. The error bars are the range of temperatures where steep changes in solution turbidity were seen, representing a possible transition zone of polymer properties.

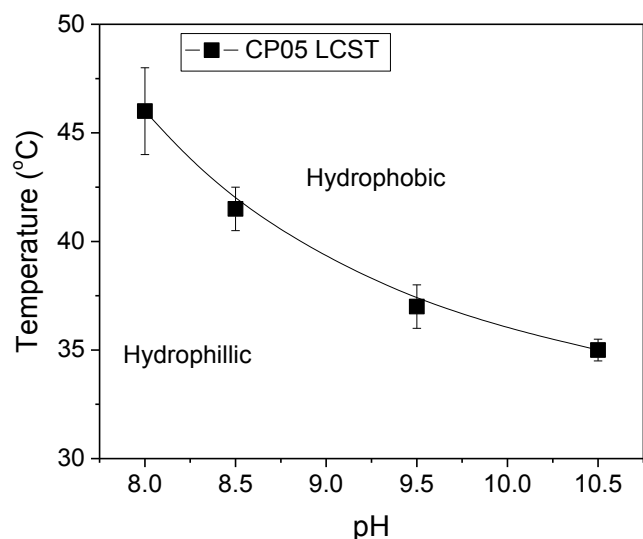


**Figure 4-2: Phase diagram of CP05 constructed using LCST, measured by turbidity at different pH**

The phase boundary marked the change in dominant forces of the polymer, between hydrophobic and hydrophilic functional groups, as observed by changes of the polymer solubility. The change in hydrophobicity of a NIPAM-DMAPMA temperature sensitive flocculant can be achieved using system conditions. A transition of the polymer's coil-globule state can be induced by changing the solution temperature from 25°C to 50°C at a constant pH 8.5. The change in hydrophobicity of the CP05 flocculant can also be promoted through changes in solution pH. The coil-globule transition of the CP05 polymer can also occur by adjusting the solution pH from 8.5 to 11.0 while maintaining the solution temperature at 40°C. The dual sensitivity (temperature and pH) of CP05 polymer could be beneficial to industries that have tailings streams with low concentrations of buffering agents.

#### **4.2 Effect of Settling Procedure**

The flocculation behavior of the CP05 polymer has been studied previously [3]. The CP05 synthesized by the author had a LCST of 38°C and an average molecular weight of 2.4 MD. The performance of CP05 was evaluated in terms of settling rate, clarity of the supernatant, and floc strength. Filtration rate and solids content of the filter cake were also used to measure the efficiency of the polymer aid in dewatering by filtration. Settling and filtration tests were carried out using 5 wt% kaolinite suspensions in deionized water at pH 8.5. The settling procedures used

by Chan were adapted for the present study. Figure 4-3 shows the influence of mixing and settling temperature on the initial settling rate of flocculated kaolinite suspensions [3].

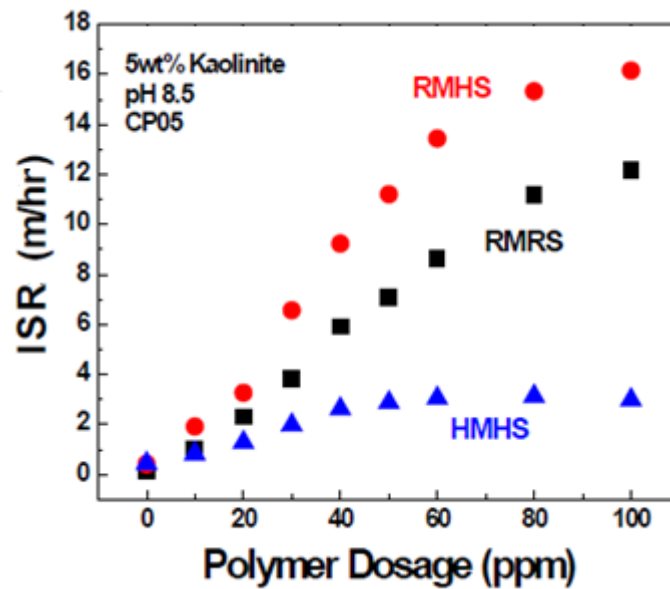


**Figure 4-3: Initial settling rate of 5 wt% kaolinite suspensions dosed with CP05 at increasing concentration from 0 to 100 ppm. The mixing and settling temperatures are indicated in the legend [3]**

CP05 was added to kaolinite suspensions at different temperatures to study the effect of the CP05 coil-globule transition on flocculation performance. Three settling conditions were considered: RMRS, RMHS, and HMHS, as outlined in Chapter 3. The HMHS refers to settling and mixing at 45°C, which was above the CP05 LCST. This procedure will be referred to as 45M45S for this study.

Two critical observations can be noted from Figure 4.3. Firstly, initial settling rates at pH 8.5 are dependent on polymer dosage in the range of 0-100 ppm. Over this concentration range there is no evidence of polymer overdosing that would have been detrimental to flocculation performance. Secondly, the temperature of mixing and settling had a significant effect on floc growth and bridging efficiency (as indicated by differences in the initial settling rate). The results in Figure 4-3 show that the initial settling rate for RMRS was greater than 45M45S. At 45°C (above the LCST) the polymer is transformed into a hydrophobic globule prior to flocculation, hence the flocculation efficiency of the system becomes limited by the polymer's ability to bridge particles.

The optimum performance achieved by RMHS was attributed to the effective CP05 polymer conformational transition between the flocculation and settling steps. During flocculation the CP05 polymer remained in the coil (opened) state, effectively bridging the particles to form large flocs. Increasing the temperature above the LCST promotes globule transition to form dense particle flocs that settle rapidly. This confirmed that CP05 attached strongly to the kaolinite surfaces and did not detach from the particles when the temperature was increased above LCST.

### 4.3 Application of Temperature Responsive Polymer

#### 4.3.1 Settling

Figure 4-4 shows the initial settling rates (ISR) of 5 wt% kaolinite suspensions prepared at different pHs between pH 5.5 and 10.5 and dosed with 100ppm CP05 polymer. Two temperature controlled protocols were considered: RMRS and RMHS.

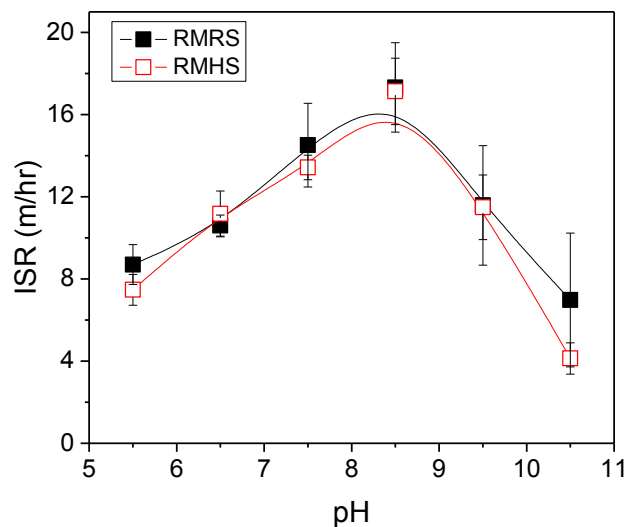


**Figure 4-4: Initial settling rate of 5 wt% kaolinite suspensions flocculated by the addition of CP05. Experimental variables: solution pH and temperature protocols. Settling column – 100 mL**

The two temperature protocols (RMHS and RMRS) did not exhibit any significant difference in settling performance. The most effective flocculation is at pH 7.5 – 8.5 and decreased when the solution was more acidic or alkaline. This data was performed with the same experimental set-up (100mL) as Margo Chan [3]. The CP05 polymer at room temperature produced fluffy flocs with

high water content. These flocs were squeezed like a sponge to produce a denser floc when the temperature was raised above the LCST (see Figure B-3). In theory, a denser floc should produce higher initial settling rates and result in more compact sediments [70]. An assumption of the model is that the number of particles in the floc and the mass of the floc are constant. During coil-globule transformation of the CP05 polymer, the floc structure is disturbed and may result in partial breakup of the polymer-clay floc and particle detachment. The LCST transformation could lead to a mass loss from the floc as the polymer contracts and realigns itself within the floc. There was evidence of particle detachment based on post-settling turbidity in Figure 4-7.

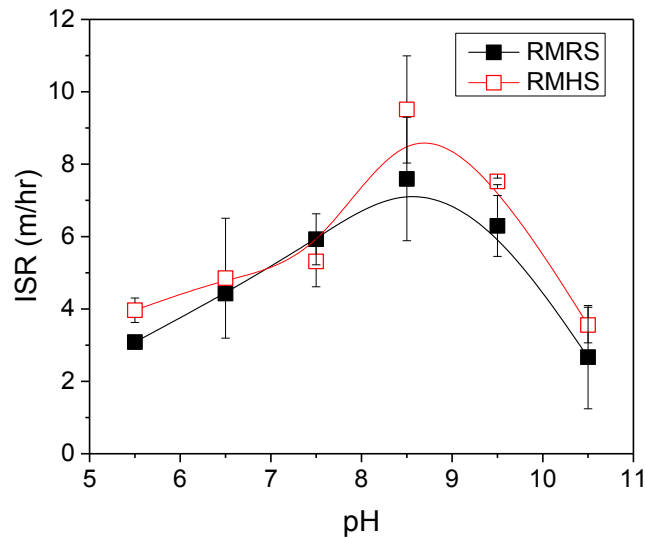


**Figure 4-5: Initial settling rate of 5 wt% kaolinite suspensions flocculated by the addition of CP05. Experimental variables: solution pH and temperature protocols. Settling column – 1 L**

Figure 4-5 shows the initial settling rates for flocculated kaolinite suspensions prepared in a large volume and settled in the 1L purpose built settling column (see, Figure 3-5). The dependence on the temperature protocol (RMHS and RMRS) is seen when the suspension pH is greater than 8.0. Similar to the work by Chan [3] an improvement in settling rate is observed for RMHS compared with RMRS. The influence of the coil-globule transition on the settling rates is clearly visible and the result is in agreement with theoretical models [70]. The temperature mediated coil-globule transition in the RMHS should make the flocs denser and faster settling.



Compared with the small volume samples (Figure 4-4), the large volume samples (Figure 4-5) exhibit a lower initial settling velocity. While the mixing speed is consistent in both preparation methods (see sections 3.2.2 and 3.2.3), the vessel and impeller dimensions are different. The less severe mixing conditions of the large flocculation set-up (intensity of turbulence and shear stress on the flocs) would have less influence on particle detachment and fracturing of the flocs.

The solution pH affects both the charge on the polymer and on the kaolinite particle, resulting in a narrow pH range for optimal flocculation conditions. To explain the pH dependent flocculation in Figures 4.4 and 4.5, the pH dependence of both polymer and clay properties should be determined first. The pKa of DMAPMA is pH 8.9; pKa indicates the pH where 50% of weak base groups on the co-polymer is protonated (cationic charge) [71]. With increasing solution alkalinity the DMAPMA becomes less protonated. Hence, CP05 loses its positive charge and the beneficial effect of electrostatic attraction to the negatively charged clay surfaces. Below pH 8.0 the coil-globule transition of the NIPAM is ineffective due to the increased protonation of the amine group. This is in good agreement with results in Figure 4-5 which shows no dependence on the temperature protocol at pH < 8.5. The optimal pH for the polymer to have both the switchable nature of the NIPAM and the charge density provided by DMAPMA is between pH 8.0 and 9.5. Figure 4-6 shows the zeta potential curves of silica and kaolinite particles at various solution pH.

In this experiment, kaolinite was mixed with a high dosage of CP05 polymer. The resulting sediments were drained, decanted, and diluted with a 10 mM KCl solution which acted as a background electrolyte. For each pH, zeta potential measurements are carried out at least 3 times, and the average value was reported. The resulting zeta potential of the polymer coated particles showed that the cationic CP05 polymer readily adsorbs onto the negatively charged kaolinite particle. The zeta potential changes for silica and kaolinite in the presence of CP05 correspond to the expected charge density behavior of CP05. As the suspension becomes more basic the CP05 coated particle charge density becomes negligible, corresponding to our knowledge of the protonation of DMAPMA [71]. The pH dependent behavior of the polymer, and not the charged particles, was dominant, providing evidence of complete polymer coating.

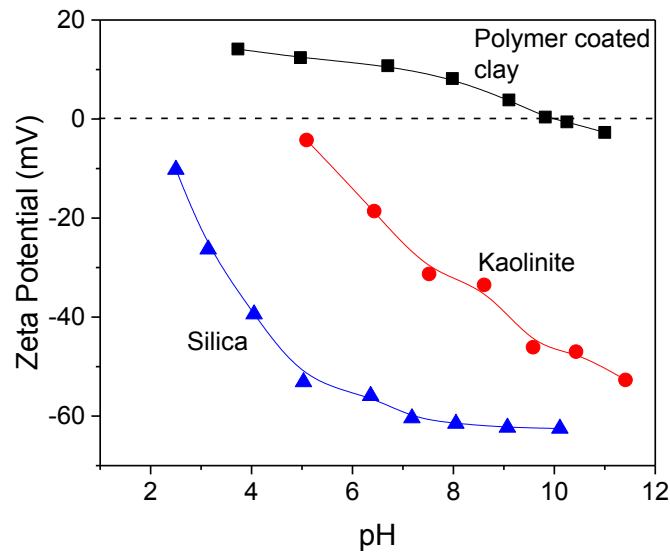


**Figure 4-6: Zeta potential of kaolinite and silica particles. Experimental variables: solution pH and CP05 addition**

The overall zeta potential for kaolinite is not fully descriptive since the particle is anisotropic [72]. As noted, kaolinite is composed of two-layers, a silica oxide basal plane and an alumina layer. The isomorphous substitution is believed to be the main cause of basal plane charges. The pH dependence of kaolinite zeta potential is attributed to breaking silica-oxide bonds and hydrolysis of broken bonds in acidic and alkaline environments. In the pH range of 5.0-7.0, kaolinite would exhibit a negatively charged silica basal face, and a positively charged alumina face, with positive edges [15]. Such anisotropy can promote edge-face interactions to form a “house of cards” arrangement when the clay particles aggregate. Beyond the iso-electric point of the alumina basal plane, both surfaces are negatively charged.

The dependence of polymer charge density and particle zeta potential is relevant to explain the settling behavior of CP05 (Figure 4-4). At high pH, diminishing polymer charge resulted in poor settling behavior. Under these conditions, the polymer had some affinity for adsorption on silica or clay based on hydrogen bonding. The flocs formed at high pH were the weakest due to the weak binding force and poor bridging mechanism of CP05 at these conditions. The resulting clay-polymer sediment had the highest solids content in the tested pH range due to the stacked arrangement of the particles (see Figure B-3 in Appendix B) [73]. High solids content did not

translate into high yield stress (see Figure 4-8), as the polymer was only weakly bonded and had a low degree of inter-particle bridging.

At experimental conditions of pH ~5.5, CP05 had its highest charge density, leading to a high degree of affinity with the negatively charged basal planes of the kaolinite. The CP05 was an effective flocculant at pH 5.5, as evidenced by the low turbidity of the supernatant immediately after settling (see Figure 4-7). The ‘house of cards’ arrangement of the kaolinite clay, as discussed in the literature review, resulted in looser aggregates by the introduced polymer, leading to a high water content sediment in acidic suspension conditions (see Figure B-3) [73]. Low suspension pH conditions were not optimal for floc growth and there are different mechanisms that can account for this. It is possible that the repulsion of the alumina basal plane and the CP05 reduced the surface area that the polymer can approach and adsorb.

#### 4.3.2 Supernatant Turbidity

The measurements of the supernatant clarity of the settled suspension provides evidence of floc behavior and stability of flocs with different pH and temperature protocols. The supernatant turbidity was measured after 2 min settling. Control experiments using Milli-Q water and 0.01 wt% kaolinite suspension at pH 8.5 resulted in turbidities of 0.05 and 149 NTU, respectively.

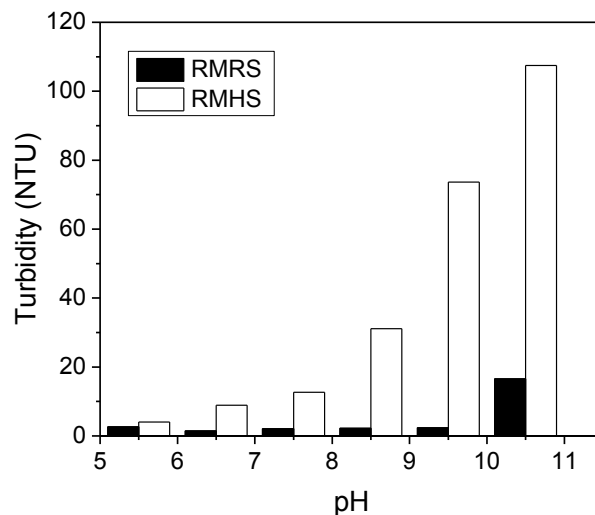


**Figure 4-7: Supernatant turbidity of 5 wt% kaolinite suspensions flocculated by the addition of CP05. Experimental variables: solution pH and temperature protocols. Settling column – 1 L**

In cases where  $\text{pH} < 8$ , RMRS and RMHS procedures resulted in a supernatant turbidity less than 50 NTU. The difference in supernatant clarity between RMRS and RMHS was significant. The turbidity of the supernatant was higher for the RMHS procedure. It appears that a portion of the kaolinite colloids detached from the aggregates upon increasing the suspension temperature and the contraction of the flocs. When the polymer undergoes a coil-globule transition, some of the weakly attached particles would be pushed off the polymer by spatial hindrance. The coil-globule transition of the polymer in the RMHS procedure pulled the flocs closer together while the charge of the colloids pushed back. The detached particles remain dispersed and cause the high supernatant turbidity shown in Figure 4-7.

The measured variation in supernatant clarity (over the pH range) was consistent with the variable protonation of DMAPMA. The turbidity was highest at alkaline conditions because of the reduction in the protonation of the CP05 polymer. At high pH conditions the charge density of the polymer is at its minimum. The negligible charge of the polymer makes the adsorbed bonds between CP05 and the kaolinite weaker, hindering its ability of bridging kaolinite particles during flocculation. As a result, the flocculation efficiency reduces, leading to more kaolinite particles remaining dispersed in the supernatant. This was more clearly observable in the RMHS procedure than in the RMRS procedure.

The trend in Figure 4.7 suggests one possible explanation for the similar results for the RMRS and RMRS initial settling rates presented earlier (see Figure 4.4). In the pH range where the coil-globule transition was possible (pH 8.5-10.5) there was a significant increase in supernatant turbidity resulting from the RMHS procedure. The transition caused an increase in floc breakage and the detachment of kaolinite particles. The densified flocs produced in the RMHS procedure should settle faster than the fluffy flocs produced in the RMRS. The assumption was that the flocs in these two cases had the same mass and number of particles [70]. Figure 4.7 provides evidence of a significant loss of particles and mass from the flocs produced by the RMHS procedure. This mass loss is driven by the detachment of particles and fracturing of the aggregate during the coil-globule transition. If the settling flocs of the RMHS had less mass and possessed a weaker driving force to settle than the flocs produced by RMRS procedures, this would account for the similar settling rates of the two temperature protocols in Figure 4-4.

Under most experimental conditions polymer adsorption is irreversible [33]. The electrostatic force of the charged CP05 and the kaolinite should prevent desorption of the polymer for all but the most alkaline conditions [56]. An exception is pure pNIPAM which has been examined for its switchable adsorption in many studies [74]. It was typically used in research as a pure form of pNIPAM, or in blend with a neutral co-polymer. Below the LCST the polymer had little electrostatic attraction to other colloids or surfaces they come into contact with. Above the LCST the polymer had favorable self-association conditions via hydrophobic force. Therefore, not only was the solubility of the polymer switchable the adsorption behavior pNIPAM is reversible as well. The CP05 copolymer of NIPAM and DMAPMA had a similar relationship of reversible adsorption only at conditions of high pH, when the DMAPMA had a low level of protonation.

### 4.3.3 Yield Stress

The effects of different procedures and stimuli on the rheology and bed structure of clay sediments flocculated using CP05 were studied. The results in Figure 4-8 show that the yield stress of flocculated clay sediments can be improved or degraded by the proper application of the temperature stimuli. The steps for each procedure were described in Chapter 3.3.5.

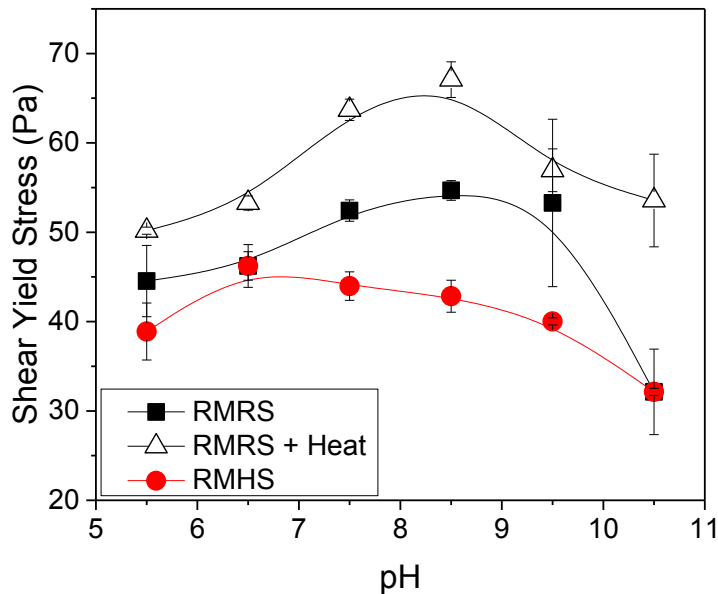


**Figure 4-8: Shear yield stress of settled kaolinite suspensions with 100 ppm CP05. Experimental variables: suspension pH and temperature protocol**

The suspension was allowed to consolidate overnight and sealed with parafilm to limit natural buffering with atmospheric carbon dioxide. Figure 4-8 shows the yield stress as a function of pH of kaolinite-polymer sediments resulting from flocculation. The yield stress is heavily influenced by pH, which in turn controls the relative charges of the CP05 polymer and kaolinite [60].

The variation of the yield stress as a function of pH for these three procedures was consistent with the flocculation behavior detailed earlier in this chapter. The 'RMRS + Heat' (see Procedure 4 in Section 3.2.3) led to the highest sediment yield stress, and RMHS, the lowest. The most efficient flocculation was in the pH range of 7.5-8.5, with decreasing floc strength and size in acidic and alkaline suspensions. The pHs between 7.5-8.5 were below the pKa of DMAPMA, meaning more than 50% monomer protonation and a strong cationic charge for CP05. Favorable polymer and clay electrostatic interactions resulted in a high degree of bridging that was beneficial to both flocculation kinetics and yield stress. The inter-particle forces that created larger flocs also formed a strong particle networks between the settled clay. The strength of the hydrogen and electrostatic bonding had a direct influence on the shear yield strength of the sediment.

The RMHS flocculation procedure appears to be detrimental to creating the sediment yield stress. In theory, the RMHS procedure creates densified flocs and higher solids content sediment, compared to the RMRS procedure. The dense flocs and the tangled (hydrophobic) state of the heated CP05 did not create a strong inter-particle network during sedimentation. The polymer is less effective at bridging and producing large inter-particle floc structures when using the RMHS settling procedure.

The secondary heating procedures (RMRS + Heat) attempted to avoid this issue by heating the flocculated sediment after settling was completed. It was assumed that the force of polymer transformation would result in further consolidation of the sediment bed by forcing water out of the flocs and sediment. This procedure (RMRS + Heat) took the large fluffy flocs and strong interparticle network produced by the RMRS flocculation procedure and heated the sediment above the LCST of CP05. There was a marked improvement in the solids content obtained from this procedure, and a corresponding enhancement of the shear yield stress [60]. The improvement was especially evident in the pH range of 8.0-10.5, over which the CP05 polymer had a sharp transition between hydrophilic and dehydrated states. There is evidence that

kaolinite-CP05 sediment undergoing a coil-globule transition led to particle detachment (Section 4.3.3), a similar effect to the RMHS procedure mentioned earlier in this chapter (see Figure 4-7).

In Figure 4-8, the peak yield stress was at pH 7.5-8.5 and the yield stress decreased when the suspension pH was either more acidic or basic. The solids content of the sediment was 15.5% to 18% when the conditions for flocculation were pH 8.5 and 10.5 respectively. There was no improvement in sediment yield stress to match this increase in solids content. Previous studies by Johnson assert that the shear yield stresses of kaolinite suspensions is dependent on the solids content [60]. Such dependence was not observed, most likely due to lower solids content of sediments. The particle association by polymer bridging dominates the resistance to sediment flow.

In summary, the optimal flocculation kinetics and maximum yield stress observed at pH 7.5-8.5 are the result of several factors. This was the pH range where kaolinite faces are both negatively charged for maximum surface area available to the cationic CP05 flocculant. The pH 7.5-8.5 range is also where the DMAPMA monomer in CP05 was protonated (highly cationic).

#### **4.3.4 Drainage of Sediments**

The dewatering characteristics of kaolinite have been studied extensively by Besra (2000) et al., who demonstrated that they are dependent on pH and zeta potential [75]. There are additional considerations including the particle size and distribution, sphericity of the particles, bed porosity, and water retaining capacities that result from the arrangements of the settled particles. These are of particular importance for kaolinite as the randomized “house of cards” particle arrangement traps large volumes of water and causes resistance in the sediment to dewatering. A polymer flocculant improved both the settling and dewatering capabilities of kaolinite suspensions. However, the resulting sediment trapped a great deal of water that must be removed for effective tailings management. The filtration characteristics have been assessed through the measurement of the filtration rate, which provided a qualitative comparison of the kaolinite cake’s resistance to drainage. The specific resistance of the filter cake to filtration cannot be directly calculated without a known pressure difference across the filter paper. The natural drainage of the sediment cakes was driven by gravitational force [75]. The comparison of liquid drainage rates provided information concerning floc structure and particle detachment resulting from the switching of the CP05 polymer.

The classic theory for filtration is that water drains through capillaries that snake through the settled cake. The largest capillaries drain first and increasingly larger pressure drops across the cake are required to drain the water from the smaller capillaries [75]. The high filtration rate was indicative of large floc size that resulted in large capillaries and pore space for easy drainage. The drainage rate can provide evidence of the presence of fine particles that are not part of the larger network of flocs. These fines result in blocked pores in the sediment cake and filter paper, which increase the resistance to filtration and decrease the drainage rates. The similar principle applies to dewatering by natural liquid drainage under gravity. Figures 4-9 and 4-10 compare the dewatering behavior of the settled kaolinite treated with 100 ppm using three of the previously discussed temperature stimuli procedures.

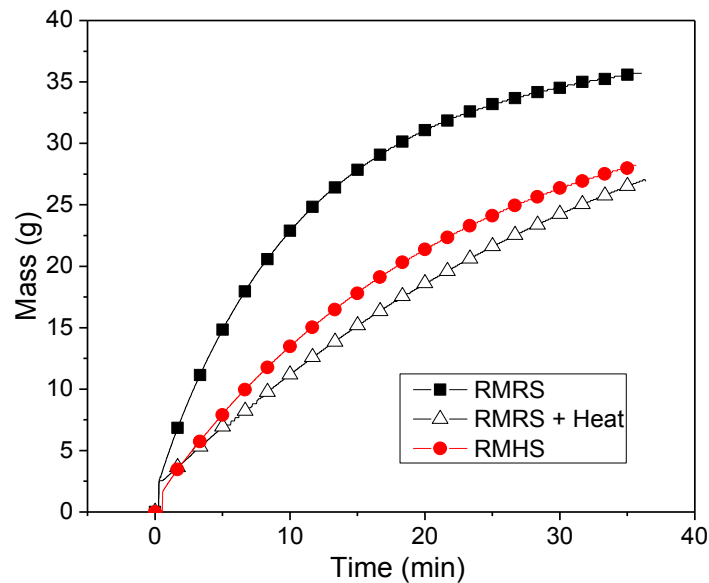


**Figure 4-9: Dewatering of settled kaolinite suspensions flocculated with 100 ppm CP05 at pH 8.5 over 35 minutes. Experimental variable: suspension heating procedures**

It can be observed from Figures 4-9 and 4-10 that the filtration characteristics for the sediments created by RMHS closely resembled those produced by secondary heating of a flocculated bed (RMRS + Heat). The extent and rate of settling is poor for the polymer-clay mixtures that have undergone at some point in increase in temperature above the CP05 LCST. The temperature transition detaches particles from the floc and blinded the filter paper, slowing the sediment



dewatering, as seen in the reduction in drainage rate of RMRS sediments to RMRS+Heat and simple RMHS settling procedures.

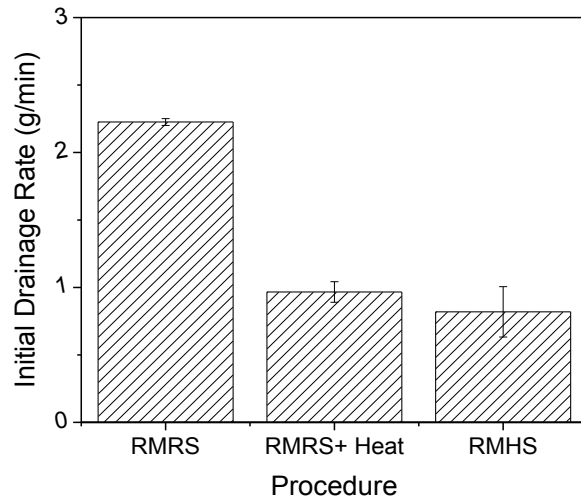


**Figure 4-10: Initial drainage rates of settled kaolinite suspensions flocculated with 100 ppm CP05 at pH 8.5. Experimental variable: suspension heating procedures**

The blinding of the filter paper occurred in both cases when the LCST of the CP05 was exceeded for the coil-globule transition, when polymer-clay flocs were either in suspension or in sediment (RMHS and RMRS + Heat). The RMRS offers the best performance for dewatering, giving the highest drainage rates and yield stresses of drained sediment.

Figure 4-11 compares the yield stress before and after the dewatering of the sediment. Once again the yield stress of sediments produced by RMHS and RMRS+Heat are similar. After dewatering, there was a 3 wt% difference between solids content of the RMRS sediment and the one formed by the ‘RMRS + Heat’ procedure. This difference in solids content resulted in a 33% increase in yield stress of the dewatered clay before liquid drainage (Figure 4-8), matching some literature expectations [60]. The goal of the ‘RMRS + Heat’ procedure was to consolidate the sediment and make it denser. The procedure was successful in this goal but had the additional effect that was detrimental to dewatering of the sediment. The RMRS had the fastest and most extensive dewatering, and lead to a denser paste and high shear yield stress compared to the other two procedures. Hence, the application of the coil-globule transition was not optimal for the long-term management of tailings.

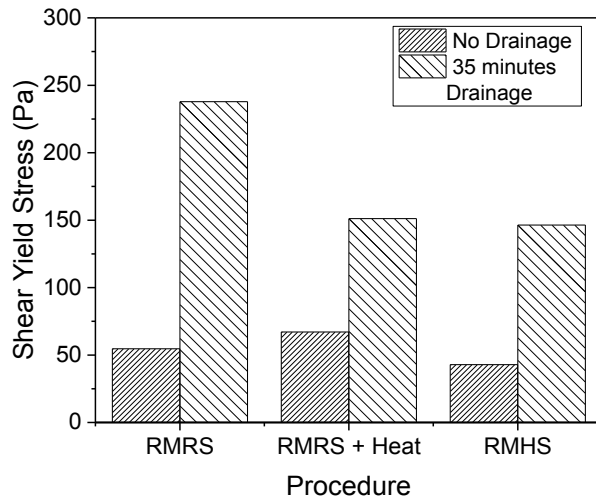


**Figure 4-11: Shear yield stress of dewatered settled kaolinite suspensions flocculated with 100 ppm CP05 at pH 8.5. Experimental variable: suspension heating procedures**

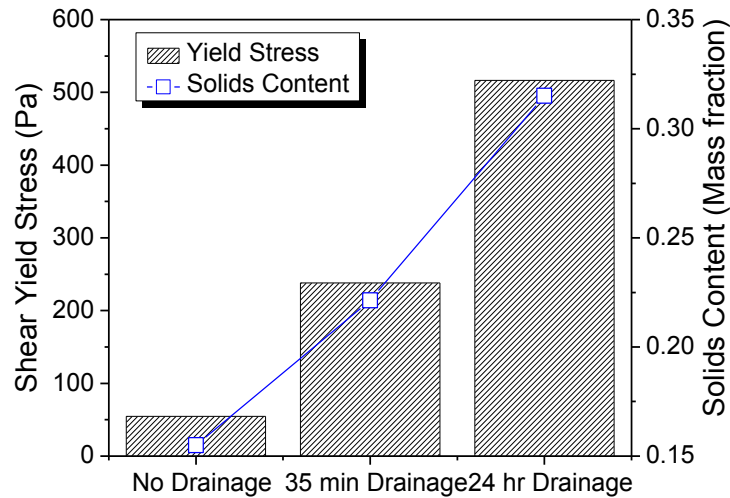


**Figure 4-12: Shear yield stress and solids content of kaolinite suspensions flocculated with 100 ppm CP05 at pH 8.5 using RMRS procedure, varying dewatering times**

To demonstrate the viability of the CP05 copolymer for tailings management, the dewatering of the clay sediment was extended over a 24 hour period (Figure 4-12). Over this period, the filter cake continued to slowly lose moisture through drainage and evaporation. The cake reached a

shear yield stress of 500 Pa and 33 wt% solids. The final solids content was calculated by mass balance calculations using the total mass of supernatant water which was removed during settling. The AER Directive 74 requires 5000 Pa one year after deposition of the treated fine tails [8].

#### 4.3.5 Raking and Yield Stress

It was demonstrated previously that multi-stage polymer addition and stirring processes can improve the dewatering of flocculated clay sediments. This approach was inspired by the research of Kingsly [76], with some modifications for testing of the sediment yield stress.

In Stage 1, 100 ppm CP05 flocculated the kaolinite suspension at a stirring speed of 350 rpm. This ensured even distribution of the flocculant, particle collision, and exposes the flocs to the same shear stress as in other experiments. The suspension settled in the 1-L settling column for 10 minutes. The supernatant was then decanted and weighed.

Stage 2 of the experiment involved the raking of the sediment in an effort to release water without fracturing the settled flocs. The sediment was mixed by hand at around 4 rpm using a steel sample spoon in a “Figure-8” pattern. The sediment was stirred for 3 minutes and then allowed to rest for 10 minutes. The released supernatant was removed and then the sediment was mixed for a second 3 minute period.

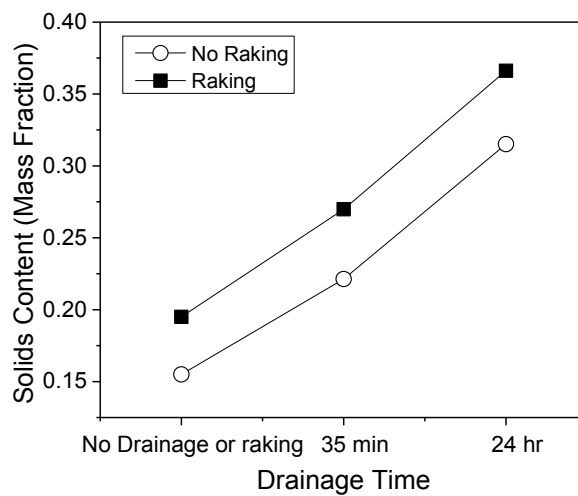


**Figure 4-13: Solids content of dewatered settled kaolinite suspensions flocculated with 100 ppm CP05 at pH 8.5 using RMRS procedure, illustrating the influence of raking samples**

Figure 4-13 shows a comparison of the dewatering capabilities of kaolinite-polymer sediment produced using the single stage polymer settling and a multi-stage settling-raking procedures. Raking resulted in the additional compression of the kaolinite bed and an improvement to the sediment solids content. The improved rheological characteristics were evident in the increase in yield stress of the raked, as sediment compared to the settled kaolinite, as shown in Figure 4-14. The raking of the sediment caused additional bed consolidation and water release without releasing fines that would blind the filter paper.

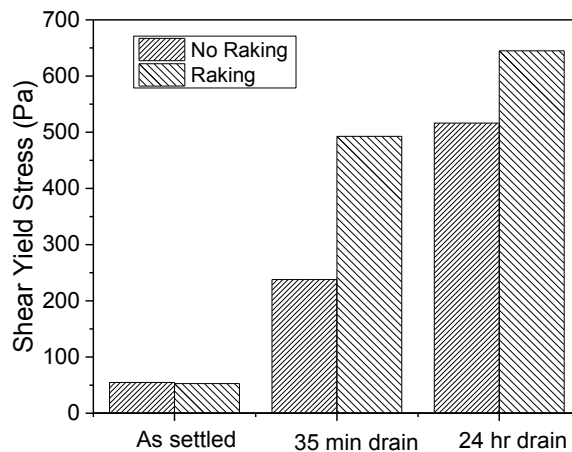


**Figure 4-14: Shear yield stress of dewatered settled kaolinite suspensions with 100 ppm CP05 at pH 8.5 using RMRS procedure, illustrating the influence of raking samples**

#### 4.4 Conclusions

The temperature mediated coil-globule transition (RMHS) resulted in a small improvement of the settling rates of the kaolinite suspensions. The driving force acting on the settling particles is increased by the densification of the kaolinite-polymer floc, but was decreased by a mass loss caused by the detachment of particles from the transforming floc, as shown by increased turbidity of the supernatant. The utilization of the RMHS had a negative effect on supernatant clarity and sediment properties. Performing the switch after settling (RMRS + Heat procedure) is beneficial to tailings management by decreasing sediment volume and increasing yield stress. However, this procedure had a negative effect of decreasing dewatering qualities of the sediment due to particle detachment. In the kaolinite-CP05 system there is an optimal pH range (8.0-9.5) for both suspension flocculation and rheological characteristics of the sediment.

## Chapter 5 : Studies of Isothermal Flocculation using CP05

The stimuli-sensitive flocculant CP05, was synthesized in-house, purified, dried, and stored in stable conditions. The NIPAM monomer responsible for the coil-globule transition, and the DMAPMA was responsible for the polymer's cationic charge. The synergy of these two monomers results in the pH sensitive LCST. In chapter 4 the flocculation performance was studied as a function of pH (fixed between pH 5.5 and 10.5) while applying temperature changes (21°C and 50°C) to the polymer-clay suspension at different stages in the flocculation and consolidation processes. Chapter 5 presents data at the optimal pH for flocculation (pH 8.5) and varies the operating temperature up to and beyond the LCST. The aim of this chapter is to explore the opportunity of using pH to exceed the LCST conditions of CP05 and benefits of operating at elevated flocculation temperatures near the CP05 LCST. QCM-D and FBRM were used to analyze the polymer properties and flocculation performance.

### 5.1 Kaolinite Flocculation

#### 5.1.1 Isothermal Settling

The initial settling rates of a 5 wt % kaolinite slurry demonstrating the dependence on solution temperature during flocculation (pH 8.5, 10 mM KCl solution) is shown in Figure 5-1.

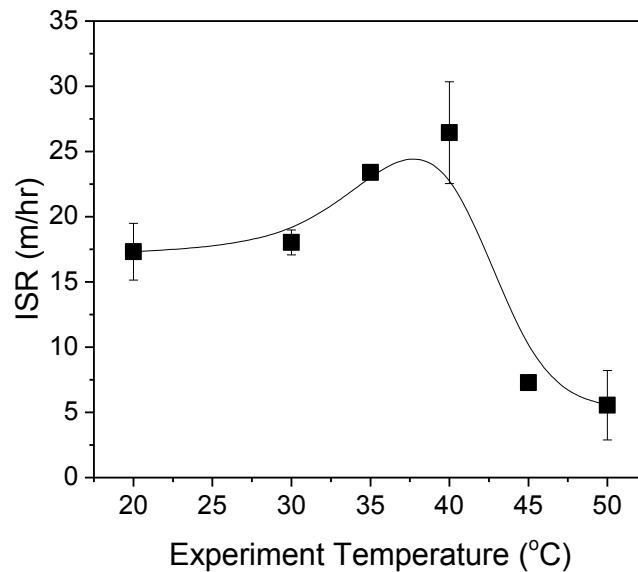


**Figure 5-1: Initial settling rates as a function of suspension temperature for 5 wt% kaolinite at pH 8.5, flocculated with 100 ppm CP05**

The experimental protocol was detailed earlier in section 3.2.3, known as EMES, where E refers to the elevated temperature, maintained for suspension mixing, flocculation, and settling. Figure 5-1 shows an incremental increase in the settling rate as the suspension temperature approaches the LCST temperature, 40°C at pH 8.5. Interestingly, there is a clear optimum in the initial settling rate at a solution temperature just below the LCST. Beyond the LCST for CP05 the settling rate decreased significantly, a result of the tangled (globule) polymer conformation. The results for procedures HMHS are given in Appendix B. Previous studies of flocculation have observed a similar phenomenon when flocculating colloidal particles with PEO and PAM based polymers and colloid [32, 69]. The possible reasons for enhanced settling performance just below the CP05 LCST is discussed in the following sections of this chapter.

## **5.2 Studies of p[NIPAM-co-DMAPMA] Adsorption using QCM-D**

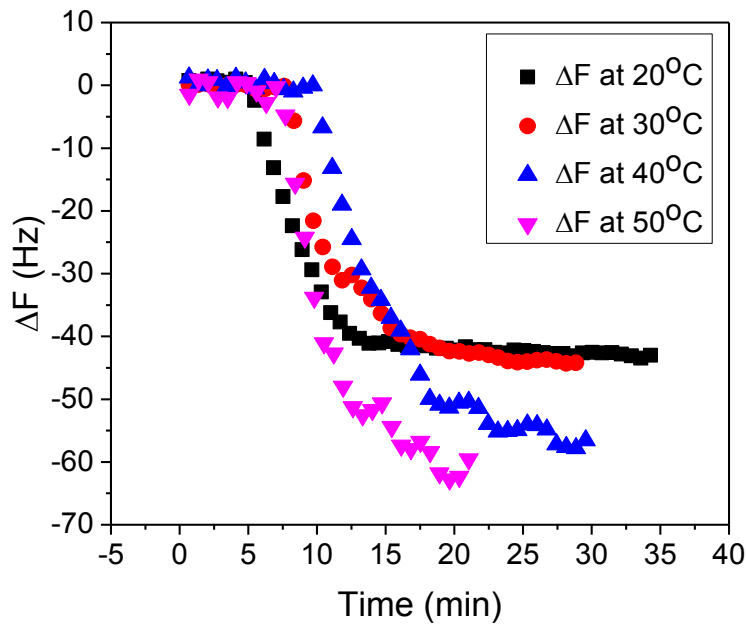
### **5.2.1 Polymer Adsorption Kinetics**

To better understand the enhanced settling performance at conditions close to the LCST a series of experiments were conducted using QCM-D and FBRM. Firstly, the rate of CP05 adsorption onto a silica sensor (representative of the silica basal plane) was studied by QCM-D. The CP05 solution (10 ppm) was heated to the desired experimental temperature prior to being pumped through the QCM-D. To ensure no temperature fluctuations, the baseline fluid and the QCM-D measurement cells were all heated and maintained at the desired experimental temperature. The CP05 solution was pumped into the QCM-D module at a constant flow rate which remained unchanged during the period of CP05 adsorption. As the CP05 adsorbs on the silica sensor the resonance frequency of the crystal is measured to decrease. Eventually adsorption becomes limited by the decreased surface area due to molecular crowding on the sensor surface (adsorption barrier-controlled regime).

The adsorption rate of CP05 onto kaolinite was approximated by the rate of frequency change (mass gain) on a silica sensor surface. Studies have shown that the trend in flocculation efficiency correlates inversely with the trend in adsorption rate [32, 33, 77]. In other words, slower adsorption rates result in improved flocculating performance. The slower adsorption allows the polymer to attach to particles in a stretched and untangled conformation, enabling more effective particle bridging which leads to improved settling rates. A similar negative

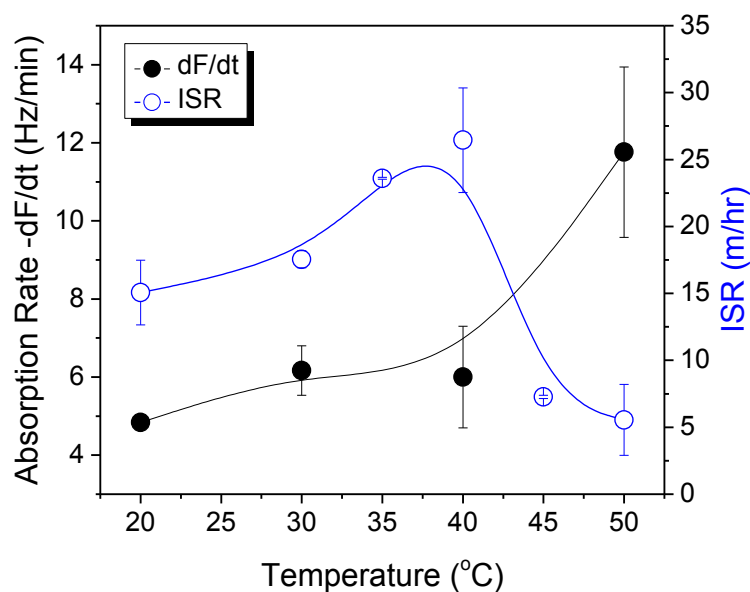
correlation also occurs at higher temperatures where settling and adsorption rates increase and decrease, respectively.

Figure 5-2 shows the kinetics of CP05 adsorption onto a silica QCM-D crystal sensor. Changes in the frequency ( $\Delta f$ ) are indicative of mass adsorption on the silica sensor. Therefore, the change in frequency as a function of time,  $(df/dt)$ , are comparable to the rates of CP05 adsorption.



**Figure 5-2: CP05 polymer adsorption on silica sensor surface as a function of temperature at pH 8.5 using 10 ppm CP05**

Figure 5-3 compares the relative CP05 adsorption rate and initial settling rate of flocculated kaolinite at equivalent solution temperatures. Unfortunately, there does not appear to be a clear correlation between the two parameters. The polymer adsorption did not increase in the 20-40°C temperature range, unlike the flocculation settling rates. The pH in all experiments was maintained at pH 8.5



**Figure 5-3: Polymer adsorption rate and suspension initial settling rate as a function of temperature. Flocculation performed with 5 wt% kaolinite at pH 8.5 with 100 ppm CP05. Polymer adsorption onto silica QCM-D sensor, using 10 ppm CP05 at pH 8.5**

Based on the Sauerbrey equation, the change in silica sensor frequency is linearly dependent on the mass deposited on the sensor surface [78]. Hence, the rate of frequency change is linearly dependent on polymer adsorption rate. As shown in Figure 5-3, the CP05 adsorption rate was highest at temperatures above the LCST where the CP05 polymer was in a collapsed coil dehydrated state. The enhanced rate of the CP05 adsorption at temperatures above the LCST could result from an increase in the molecule diffusion [77], or the hydrophobic state of the polymer leading to a higher efficiency of successful collisions between the polymer and the sensor surface. Regardless, the observed response of the CP05 partly agreed with the model proposed by McFarlane, i.e., the fastest adsorption corresponds to the poorest flocculation performance and slowest settling suspension [34]. This experimental result does not fully explain why the maximum in settling performance was measured at 40°C.

In addition to the adsorption rate, the overall signal change recorded by the QCM-D at different temperature can be compared, as shown in Figure 5-4.



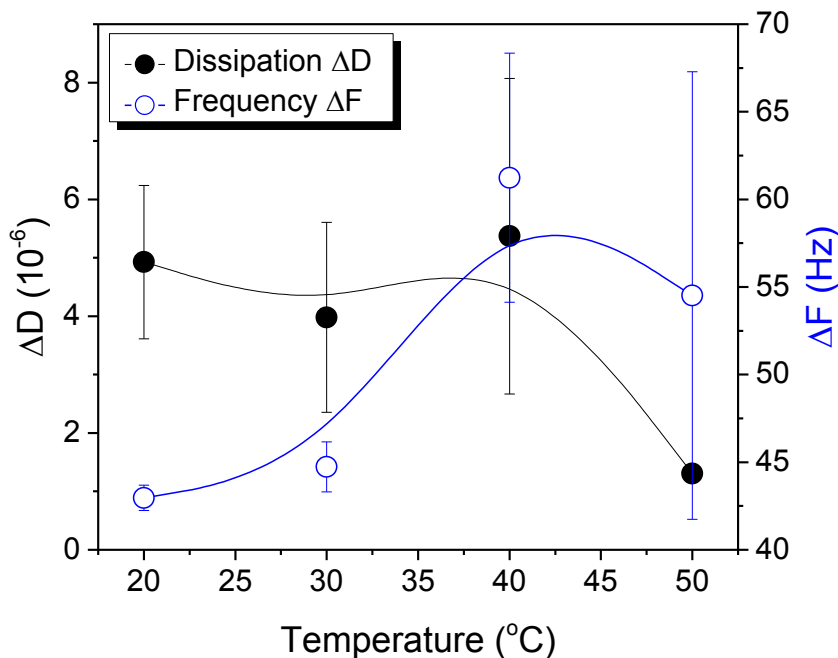


**Figure 5-4: CP05 polymer adsorption onto silica as a function of temperature. Frequency and dissipation responses of the QCM-D silica sensor using 10ppm CP05 at 8.5 pH**

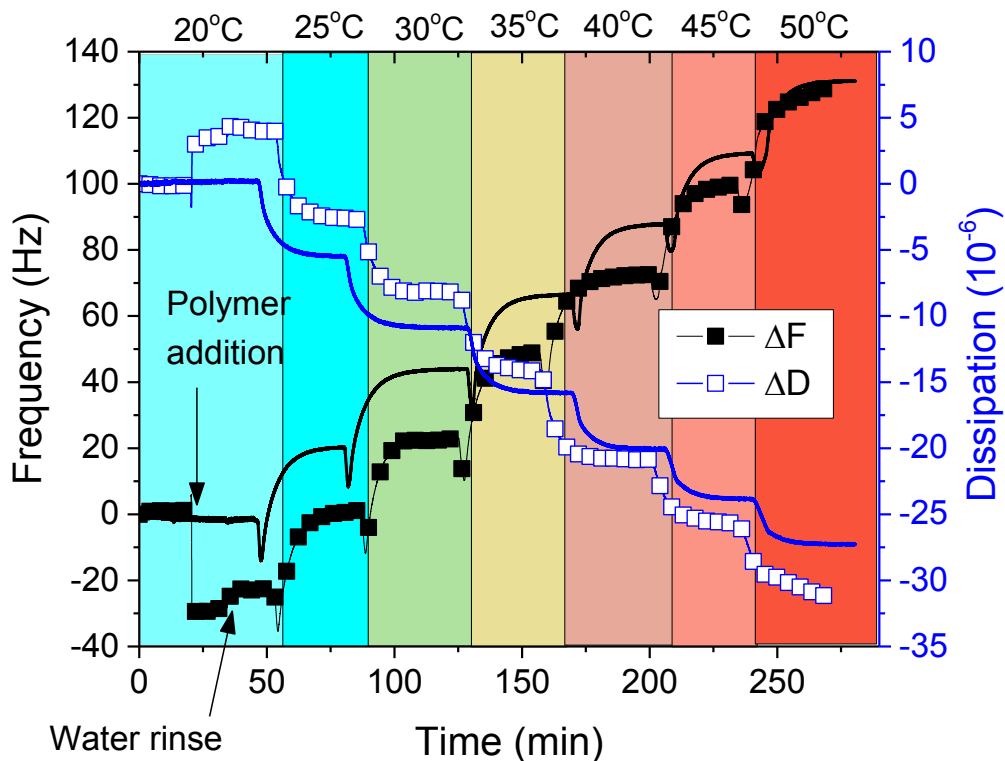
Adsorptions tests (Figure 5-4) indicate that  $\Delta f$  was at a maximum for the higher temperatures, at both 40 °C and 50 °C. This result was variable and inconsistent, but indicates there may be a higher uptake of adsorbed polymer at these conditions. Higher mass uptake above the CP05 LCST was expected for the dehydrated state of the polymer at 50 °C. At conditions above the CP05 LCST, the polymer quickly adsorbed onto the silica surface. Adsorbing as a thick layer was the most stable arrangement for the polymer due to hydrophobic interactions. The  $\Delta D$  of at 50 °C is near zero, indicating that the adsorbed coiled polymer does not change the rigidity or softness of the adsorbed polymer layer. The  $\Delta D$  in lower temperature experiments (20°C to 40°C) indicates that the adsorbed relaxed polymer does increase the softness (viscoelasticity) measured by the silica sensor. The experiments shown in Figure 5-4 is a comparison of polymer adsorption case, the next set of experiments will attempt to isolate the properties of the CP05 polymer that change with temperature.

### 5.2.2 Temperature Ramp QCM-D Experiment

QCM-D was used to study the polymer conformational property as a function of increasing solution temperature. Two sensors were recorded in parallel: one sensor was exposed to the

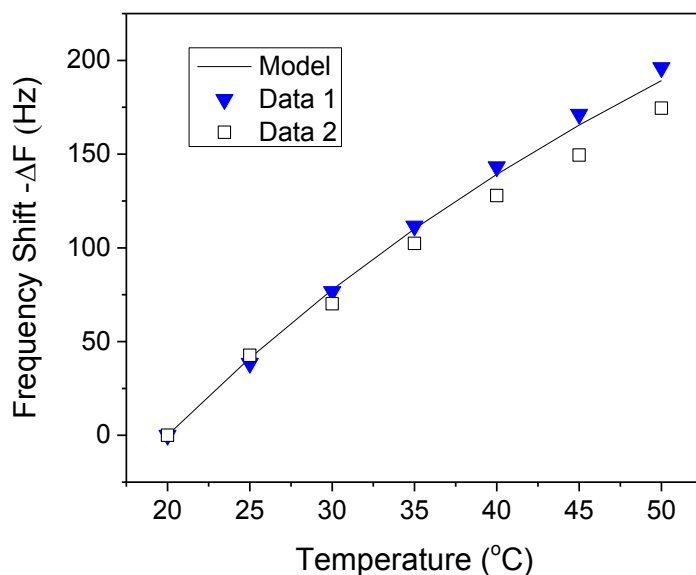
adsorbed polymer layer (adsorbed at 20°C) and the second sensor acted as a control to account for the influence of temperature on the water physical properties (density and viscosity).

Figure 5-5 shows both the frequency and dissipation response of the uncoated and polymer coated (CP05 adsorbed) silica sensors as the temperature was incrementally raised. For the polymer coated system CP05 at a concentration of 500ppm was first pumped into the QCM-D flow cell. Once the frequency and dissipation had reached a steady state the measurement cell was rinsed with Milli-Q water of pH 8.5 with the temperature and salt concentration (10 mM KCl) being identical to those in the polymer solution. After a period of time the rinse was stopped leaving a strongly adsorbed polymer layer on the sensor surface. The  $\Delta F$  and  $\Delta D$  signal recorded for the first sensor records the response of both the adsorbed polymer and the water solution to the changing temperature.



**Figure 5-5: Frequency and dissipation response of QCM-D sensors as a function of solution temperature. Symbols: Milli-Q water at pH 8.5 (solid line), CP05 polymer (square symbols). CP05 (500 ppm) first adsorbed at 20°C and subsequently washed with 10 mM KCl water at pH 8.5 to form a stable film.**

A second sensor containing only deionized water was run in parallel with the same temperature stimulus. The adsorbed water layer will cause measurable shifts in frequency and dissipation that are recorded by the QCM-D sensors as the temperature is incrementally increased. These shifts were caused by changes in water viscosity and density, and can be predicted using the Kanazawa Model [79]. A comparison between experimental data and models for water solution and a silica crystal is presented in Figure 5-6.



**Figure 5-6: Frequency shift of deionized water versus temperature ramp for silica QCM-D crystal. Solid line was the response predicted by Kanazawa model, symbols represent different experimental runs**

In both parallel sensors there is an adsorbed layer of water solution. The influence on the sensor resonance signal from the water medium should be consistent. The difference in crystal sensor frequency and dissipation responses to the temperature ramp for these two parallel sensors was considered to be the responses solely of the adsorbed CP05 polymer. The responses plotted in Figure 5-7 are differences in  $\Delta F$  and  $\Delta D$  recorded by the parallel sensors for each step in the temperature ramp.

Figure 5-7 compares the frequency and dissipation responses of adsorbed CP05 polymer. An increase in  $\Delta F$  would indicate a loss of mass from the polymer layer, as demonstrated by the coil-globule transition between 40 and 45°C. The mass loss was caused by the hydrophobic and

dehydrated polymer layer pushing water away from the silica sensor surface into the bulk phase and possibly the detachment of some of the adsorbed coiled polymer.

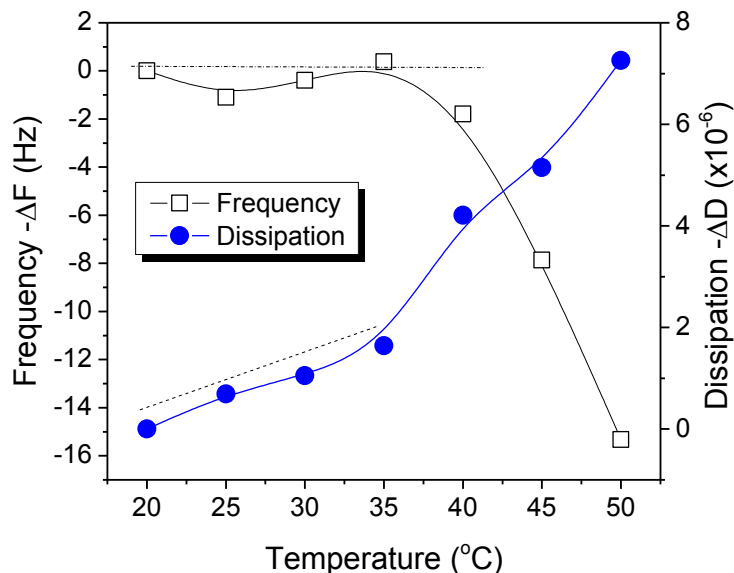


**Figure 5-7: Frequency and dissipation shifts caused by temperature ramp on QCM-D silica sensor, isolating the response of the adsorbed CP05 polymer layer**

A decrease in dissipation ( $\Delta D$ ) represented an increase in the rigidity of the adsorbed polymer layer [41]. There was a steady decrease in sensor dissipation, indicating that the polymer transition was not a simple step-change from a hydrophobic to a hydrophilic state at the LCST. The sensor dissipation attributed to the polymer layer was highest below the LCST of the polymer, when it was hydrated and extended out into the solution. The dissipation property of the adsorbed polymer appears to change more gradually and linearly as the conditions approach the LCST. The dissipation of the polymer may provide an explanation for increased flocculation efficiency.

At 20°C the CP05 is at its most elastic structure, and it would readily adsorb onto multiple kaolinite surfaces in this conformation during flocculation. Above the LCST the polymer is in a collapsed, rigid state and adsorbed more rapidly onto a surface. However, the length of the polymer was compromised and bridging between particles became difficult. The polymer in the 35-40°C temperature range was in transition between these two states. CP05 in the 35-40°C temperature range was still in a relaxed conformation for ideal flocculation, but significantly

more rigid and inflexible than the CP05 polymer at room temperature. CP05 at 35-40°C has similar conformational and electrostatic properties to CP05 at room temperature conditions, except for the property of polymer viscoelasticity. The settling results indicate that flocculation at 35-40°C led to a significant improvement to floc size and settling rate (see Figure 5-1). Flocculation efficiency may have been significantly improved by higher polymer rigidity. The next step is to isolate this property and study the influence of floc strength of polymer-kaolinite suspensions.

### **5.3 Polymer Elasticity and Floc Strength**

A method of tracking flocculation efficiency and floc size in real time for a particle suspension utilizes the FBRM (Focused Beam Reflectance Measurement) technology of Mettler Toledo. This technique measures average particle dimension and relative particle count, and is accurate for a large range of particle concentrations and suspension clarities. The basic measurement principle of FBRM is a light source focused on an extremely small area with a set of lenses, to create a focal point [80]. The lenses are rotated by a motor at a constant speed such that the focused beam scans a circular path at the interface between the probe window and the particle system. The particles and particle structures caught in the sweep of the focused beam will backscatter some of the projected light back to the probe [80].

These pulses of backscattered light are detected by the probe and translated into Chord Lengths based on the simple calculation of the scan speed (velocity) multiplied by the pulse width (time). A chord length is simply defined as the straight-line distance from one edge of a particle or particle structure to the other edge. Thousands of these chord lengths are measured per second, allowing for real time monitoring of both particle size and concentration.

The average particle size was presented in this research as weighted squared mean. This means that some data points contribute more than others to the final average instead of each data point contributing equally. The objective of using the weighted average value was to emphasize changes among the largest chord length, which had a lower probability of being measured. This calculation provides a better representation of the flocculation of the kaolinite particles.

Figure 5-8 compares the real-time data of mean floc size recorded by the FBRM for two different procedures, RMRS and 40M40S. In theory, a more rigid polymer should create stronger flocs

that are less prone to rupturing when exposed to the shear stress created by mixing the suspension [81]. The FBRM allows real-time tracking of floc growth and destruction.

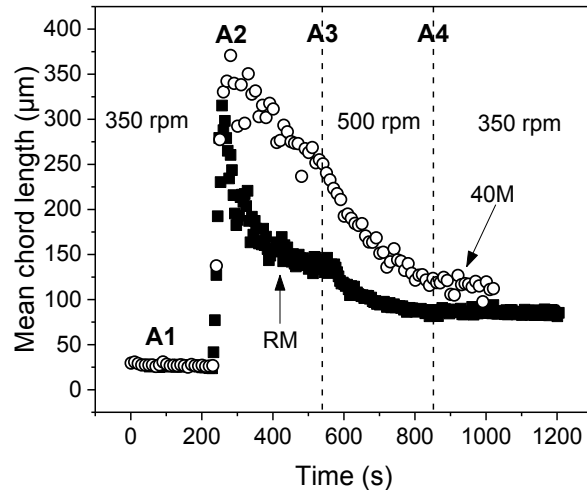


**Figure 5-8: Mean floc size of 5 wt% kaolinite suspensions flocculated with 100 ppm of CP05, comparison of room temperature and 40°C mixing and flocculation**

CP05 was used to induce flocculation of a kaolinite suspension at 350 rpm agitation speed, reaching a maximum floc size in a few seconds. Flocculation experiments were performed at both room temperature and 40°C. The maximum floc size attained for these two experiments immediately following the addition of the CP05 was similar (around 325-350µm). The suspension was mixed for 5 minutes at 350 rpm following flocculation, then 500 rpm for a further 5 minutes, and lastly mixing was reduced to 350 rpm. The flocs formed were inherently unstable and their size decreased throughout the mixing period of the suspension as a result of fracturing of the flocs and particle detachment. The flocculant was rapidly adsorbed onto the particles and formed bridges between them, leading to flocculation. As the flocs grew the probability of finding weak bonds in the aggregated structure increased, leading to fracturing of the floc from the shear stress of mixing.

The floc rupturing process can be examined quantitatively by relating floc strength to the rate of floc fracturing. Strength index equations are shown below with the values given in Figure 5-9. These equations capture the relative size changes of the floc when subjected to different levels of agitation [81].

Low Shear Floc Strength Index (%) =  $100 \times (A3 - A1) / (A2 - A1)$

High Shear Floc Strength Index (%) =  $100 \times (A4 - A1) / (A3 - A1)$

Where A1 refers to the initial mean floc size of the clay colloids, A2 refers to the maximum floc size during flocculation, A3 refers to the mean floc size after 5 minutes of agitation at 350 rpm, and A4 refers to the mean floc size after 5 minutes of mixing at 500 rpm.

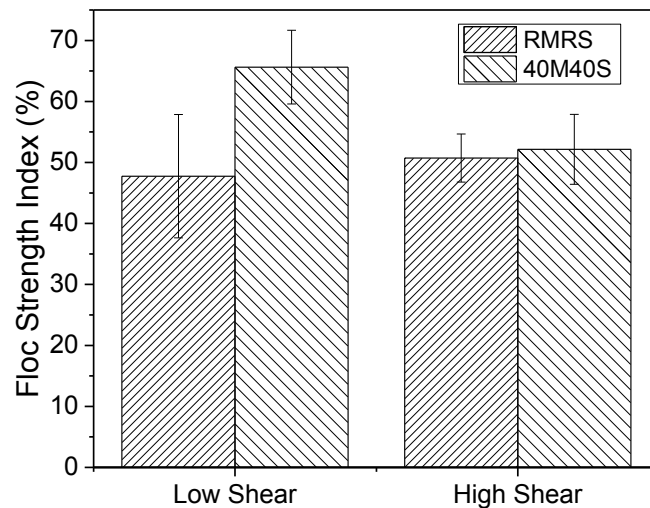


**Figure 5-9: Comparison of floc strength indexes of 5 wt% kaolinite suspensions flocculated with 100 ppm CP05, using different settling procedures**

Figure 5-9 compares the floc strength indices for flocculation at 40°C and room temperature. The ‘low shear’ index refers to the 5 minute period immediately after flocculation when the suspension was being agitated at 350 rpm. The ‘high shear’ index refers to the 5 minute period where the suspension was mixed at 500 rpm. If there was no fracturing of the flocs following flocculation, the flow shear index would be 100%. If the flocs were to rupture completely back to their original state as colloids, the calculated floc strength index would be 0%. The flocs produced and agitated at 40°C fractured to a lesser degree than the ones formed at room temperature, at the low shear conditions. The strength index was 66% and 47% for the flocculated suspensions at 40°C and room temperature, respectively. When the agitation rate was increased to 500 rpm, the extent of fracturing was almost equal according to the high shear floc strength index.

Increasing the flocculation temperature from 20 to 40°C had little effect on polymer charge, confirmation, particle charge, and had minimal effect on the density and viscosity of the aqueous solution. The viscoelasticity (stiffness of the polymer) was the only factor that changed significantly in this temperature range. The increased intra-particle interaction between the secondary amine groups of NIPAM monomers is responsible for the change in polymer rigidity. The rigid polymers at 40°C created flocs that were more resistant to the shear stress after flocculation. The final flocs settled in the experiment were larger at 40°C than at room temperatures when they were mixed at identical procedures. In summary, an increase in polymer viscoelastic properties creates larger, more shear resistant flocs at during flocculation at 40°C and is responsible for the faster flocculation rates, as shown in Figure 5-1, at this temperature.

#### **5.4 pH Switch and Polymer Response**

There is a possible variation in the settling procedure to induce a coil-globule transition in a flocculating kaolinite-CP05 suspension. It is feasible to induce a transition in the CP05 transition using a change in suspension pH at certain conditions. It was mentioned in the previous chapter that the DMAPMA copolymer interfered with the hydrophobic-to-hydrophilic transition of CP05. The extent to which the DMAPMA monomer interferes with the transition depended on its degree of protonation, and hence depends on the suspension pH. At  $\text{pH} < 8.0$  the high charge density prevented the transition altogether. At basic conditions ( $\text{pH} > 10$ ) the CP05 polymer was comparable to that of pure pNIPAM in performance. Such pH dependent transition provided an opportunity: over a precise elevated temperature range the coil-globule transition can be initiated solely by an increase in suspension alkalinity. Since  $\text{pH} 8.5$  and  $40^\circ\text{C}$  was found to be an optimal settling condition and is close to the LCST of the CP05 these were chosen as the initial conditions of flocculation. After the flocculant was added at this condition, the agitation was decreased to 220 rpm and the pH was rapidly increased using dilute potassium hydroxide (See Procedure 3).

Figures 5-10 and 5-11 show the results of the procedures for elevated temperature flocculation and pH induced coil-globule transition in relation to RMRS.



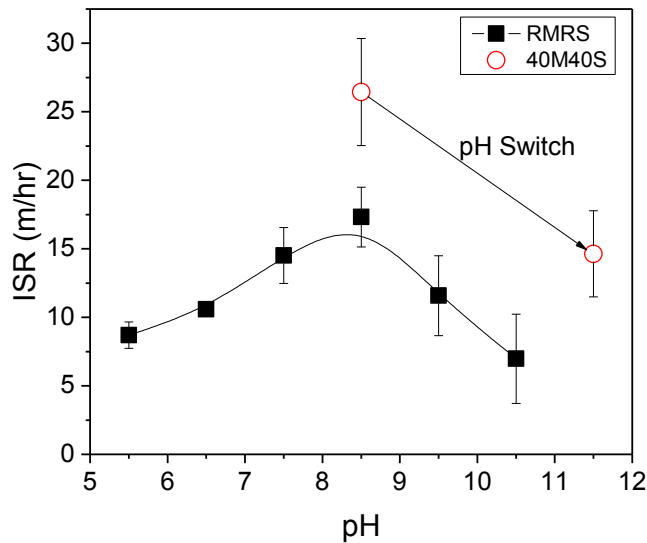


**Figure 5-10: Initial settling rate of 5 wt% kaolinite suspensions, demonstrating the application of coil-globule transition by pH Switch. Experimental variables: pH and temperature protocols. Settling column – 100 mL**

Compared to room temperature flocculation, settling at 40°C provided a significant improvement in the flocculation performance of kaolinite suspension. However, while settling near the LCST of CP05 (40M40S) may create slightly larger flocs, the results showed no improvement to the yield stress which was tested at room temperature conditions.

Switching the pH at these same conditions following polymer addition, as described in procedure 3, dramatically reduced settling rates. This behavior was not observed when a coil-globule transition was initiated by a temperature change (RMHS).

Since the charge density of the CP05 polymer was dependent on pH, switching to alkaline conditions would reduce the positive charge density of DMAPMA. Suspension pH has a strong influence on flocculation efficiency, but the change to pH in this procedure is after the particle flocculation. The RMRS procedure at pH 8.5 produces large fluffy flocs. When the polymer charge weakens the flocs would be more susceptible to fracture and particle detachment. Flocculation efficiency and sediment rheology were highly dependent on the magnitude of the polymer charge density. Weakening the charge of DMAPMA by a pH switch was detrimental to floc strength and yield stress [65].

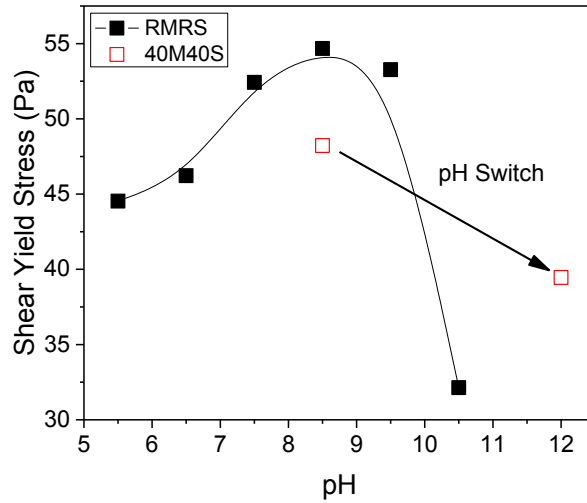


**Figure 5-11: Shear yield stress of flocculated kaolinite suspensions with 100 ppm CP05, demonstrating the application of coil-globule transition by pH Switch. Experimental variables: suspension pH and temperature protocol. Settling column – 1 L**

## 5.5 Sediment Dewatering and Filtration

Filtration rate and yield stress of the filter cake were used to measure the efficiency of polymer aids in dewatering by filtration.

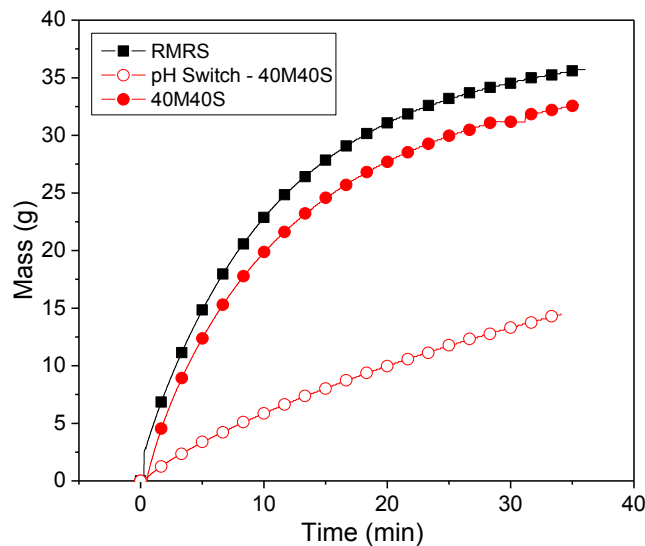


**Figure 5-12: Dewatering of settled kaolinite suspensions flocculated with 100 ppm CP05 at pH 8.5. Experimental variables: settling procedure. Settling column – 1 L**

The shear yield stress and cake drainage tests were performed at room temperature for all experiments. Figures 5.12 and 5.13 show the relative speed of dewatering for the flocculated fine clay sediments.

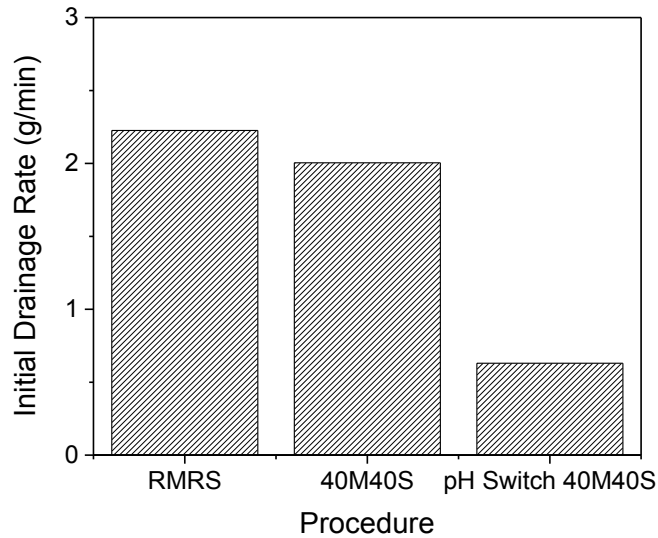


**Figure 5-13: Initial drainage rates of settled kaolinite suspensions flocculated with 100 ppm CP05 at pH 8.5. Experimental variables: settling procedure. Settling column – 1 L**

It can be observed from the results that flocculation and settling at 40°C (40M40S) produced similar sediments to those produced at room temperature. The most dissimilar one, with poor filtration, was the pH switch procedure at 40°C. The increase in pH results in a sediment of higher solids content sediment, but it the deprotonation of DMPAMA. The weak polymer charge density following pH switch resulted in weak flocs that fragment, creating a sediment of high water content and low strength, and hence low drainage rate. Previously, it was observed that increasing the temperature for the flocculation of the kaolinite suspension from 20°C to 40°C increased settling rates by twofold. This result was accomplished without compromising flocculation efficiency for dewatering characteristics, as shown in Figures 5-13 and 5-14.

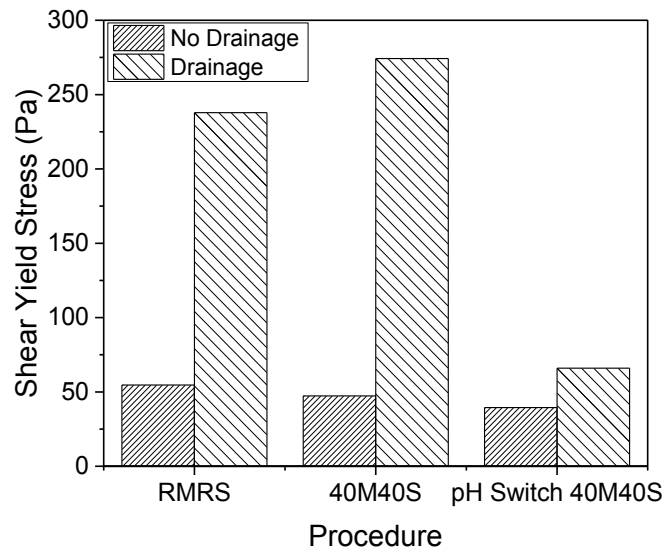


**Figure 5-14: Shear yield stress and solids content of dewatered kaolinite suspensions flocculated with 100 ppm CP05 at pH 8.5. Experimental variables: settling procedure. Settling column – 1 L**

#### 5.4 Conclusions

The aim of this chapter was to illustrate the use of pH to enact a coil-globule transition of the kaolinite-CP05 flocs. It was necessary to perform this experiment at temperature conditions close to the CP05 LCST. Therefore, flocculation, settling and mixing was performed at 40°C. The pH switch was found to be detrimental to aggregation because the increase in pH significantly decreased the polymer charge density, weakening the bridging bonds between particles and polymer. Performing the flocculation of kaolinite suspension at elevated temperatures (above room temperatures but below the LCST of CP05) was found to create significant improvements to the ISR and sediment drainage by increasing the average floc size. Studies of this phenomenon using QCM-D and FBRM established that this improvement is the result of increased stiffness of the CP05 polymer as conditions approached the LCST.

## Chapter 6 : Conclusions

This research investigated the temperature and pH responsive coil-globule transition of p[NIPAM co-DMAPMA] CP05 and its application for the improvement of flocculation efficiency, sediment rheological behaviour and dewatering. The co-polymer consisting of NIPAM and DMAPMA possessed both the coil-globule transition of NIPAM (when pH is above 8.0) and the cationic charge of DMAPMA. A novel settling column was designed to allow for the in-situ testing of the rheology and dewatering characteristics of flocculated fine sediments. With such settling columns, drainage rates and yield stress (before or after sediment dewatering) were measured on the sediment beds produced by the flocculation of kaolinite suspensions.

Compared with RMRS, the temperature mediated coil-globule transition (RMHS) had a negative effect on supernatant clarity and sediment rheology. Performing the switch after settling (RMRS + Heat) decreased sediment volume and increased yield stress, but had a negative effect on dewatering characteristics, i.e. yield stress following dewatering. The temperature of flocculation was found to have a profound influence on flocculation efficiency. Below the coil-globule transition temperature, increasing the temperature appeared to increase in rigidity and stiffness of the polymer strand, resulting in flocs of stronger shear resistance. This improvement in flocculation at elevated temperatures (40M40S) does not negatively influence the rheology and dewatering qualities.

From the batch settling tests, measurements of yield stress, and sediment drainage we can make the following conclusions:

There was a correlation between yield stress of sediments and initial settling rates, which depends on both the particle charge and polymer charge density for optimal bridging between the polymer and clay. The anisotropic nature of kaolinite clay creates optimal points for clay coagulation, and different optimal points for polymer flocculation.

The compressibility and switchability of the CP05 polymer provide an advantage over most polymers being used commercially for tailings flocculation. It brings flexibility to the tailings management process where a single responsive polymer can be optimized to perform multiple functions by fine tuning process conditions. In addition to changing polymer charge, conformation, and hydrophobicity, the stiffness of the polymer is also responsive and can be

optimized to the process needs. It was demonstrated that an adjustment to polymer stiffness during flocculation improves settling performance without sacrificing the properties of the fine particle sediment.

## **6.1 Future Work**

A primary characteristic for a commercial polymer is the molecular weight. A commercial polymer known as Zetag 8110 has an almost identical charge density to CP05, but is several times larger in terms of molecular weight [82]. High molecular weight polymers can lead to significant improvements to settling and rheological properties for model tailings treatment (see Appendix A). Modification to the CP05 synthesis process should be attempted with the goal of creating chain branching or drastically increasing the average molecular weight (ex. 2.5 Daltons for CP05 vs 18 Daltons for Zetag 8110) [82].

The procedure of RMRS with secondary heating (RMRS + Heat) cannot be easily adapted to industrial tails processing. The coil-globule transition requires additional heating of the tailings slurry to use the temperature response. An ideal polymer would undergo a coil to globule change when the suspension was cooled. With an ideal polymer the reheating of the fine tails is unnecessary and the compression of the flocs and the release of water occur when the suspension cools naturally. Currently being researched are responsive polymers whose switchable properties more closely match industrial practices of tailings management or have a different trigger such as pH and CO<sub>2</sub> content. These polymers should be tested on model kaolinite suspensions using the settling and rheology experiments described earlier in this thesis. The characteristics of initial settling rates, sediment dewatering are key parameters to identify the best performing responsive polymer flocculants.

There is an opportunity for CP05 to compete commercially in oil-sands tailings management against established industrial polymer flocculants. The bridging mechanism can be further improved with a secondary dose of a counter-charged polymer: an anionic polymer to match the cationic CP05 [54]. Preliminary work demonstrates the potential of a sequential dual polymer system in Appendix A. The synergy of the dual polymer system had a positive response on flocculation efficiency and dewatering that was disproportional to the small dose of anionic AF 246 added. The temperature responsive properties of CP05 were found to be still applicable in a dual polymer system. This concept should be pursued further on real tailings suspensions.

## References

1. *Canada's Energy Future: Energy Supply and Demand Projections to 2035 - Crude Oil and Bitumen Highlights*. 2013 August 15, 2013]; Available from: <http://www.nel-one.gc.ca/clf-nsi/rnrgynfmtn/nrgyrprt/nrgyfr/2011/fctsht1134crdl-eng.html>.
2. Xu, Z., *Fundamentals of Oilsands Extraction*. Course Pack 2011: University of Alberta.
3. Chan, M.C.W., *A Novel Flocculant for Enhanced Dewatering of Oil Sands Tailings*, MSc Thesis *Chemical Engineering* 2011, University of Alberta.
4. Kasperski, K.L., *A review of properties and treatment of oil sands tailings*. AOSTRA Journal of Research, 1992. **8**: p. 11-53.
5. (FTFC), F.T.F.C. *Advances in Oil Sands Tailings Research*. 1995. Edmonton.
6. Peachey, B., *Strategic Needs for Energy Related Water Use Technologies: Water and the EnergyINet*. 2005.
7. *Fact Sheet: Alberta's Oilsands Tailings Management*. 2011 [cited August 15, 2013; Available from: [http://www.oilsands.alberta.ca/FactSheets/Tailings\\_Management.pdf](http://www.oilsands.alberta.ca/FactSheets/Tailings_Management.pdf).
8. *Directive 074: Tailings Performance Criteria and Requirements for Oil Sands Mining Schemes*, 2009, Alberta Energy Regulator (AER): Calgary.
9. Matthews, J.G., Shaw, W.H., MacKinnon, M.D., Cuddy, R.G., *Development of Composite Tailings Technology at Syncrude*. International Journal of Surface Mining, Reclamation and Environment, 2002. **16**(1): p. 24-39.
10. MacKinnon, M.D., Sethi, A., *A comparison of physical and chemical properties of tailings ponds at the Syncrude and Suncor oil sands plants*, in *Our Petroleum Future*, 1993. AOSTRA.
11. Hunter, R.J., *Foundations of Colloid Science*. 2001, New York: Oxford University Press.
12. Ma, K., Pierre, A., *Clay Sediment-Structure Formation in Aqueous Kaolinite Suspensions*. Clay and Clay Materials, 1999. **47**(4): p. 522-526.
13. Van Olphen, H., *Introduction to clay colloid chemistry*. 1963.
14. Van Olphen, H., *An introduction to clay colloid chemistry, 1977*. National Academy of Sciences, Washington, DC, 1986.
15. Tombácz, E., Szekeres, M. *Surface charge heterogeneity of kaolinite in aqueous suspension in comparison with montmorillonite*. Applied Clay Science, 2006. **34**(1): p. 105-124.

16. Michaels, A.S., Bolger, J.C., *Settling rates and sediment volumes of flocculated kaolin suspensions*. Industrial Engineering Chemistry & Fundamentals, 1962. **1**: p. 24-33.
17. Masliyah, J., Bhattacharjee, S., *Electrokinetic and Colloid Transport Phenomena*, 2006. John Wiley & Sons Inc., Hoboken, New Jersey.
18. Stern, O., *The theory of the electric double layer*. Z. Electrochem, 1924. **30**: p. 508.
19. Derjaguin, B., Landau, L., *The theory of stability of highly charged lyophobic sols and coalescence of highly charged particles in electrolyte solutions*. Acta Physicochim. URSS, 1941. **14**: p. 633-52.
20. Verwey, E., Overbeek, J.G., *Theory of the stability of lyophobic colloids*. Journal of Colloid Science, 1955. **10**(2): p. 224-225.
21. Litzberger, C.G., Sumner, R.J. *Flow behaviour of kaolin clay slurries in Hydrotransport 16th International Conference*. 2004.
22. Hogg, R., *Flocculation and dewatering*. International Journal of Mineral Processing, 2000. **58**(1-4): p. 223-236.
23. MacKinnon, M., Boerger, H., *Description of Two Treatment Methods for Detoxifying Oil Sands Tailings Pond Water*. Water pollution research journal of Canada, 1986. **21**(4): p. 496-512.
24. Liu, J., Xu, Z., Masliyah, J., *Studies on Bitumen-Silica Interaction in Aqueous Solutions by Atomic Force Microscopy*. Langmuir, 2003. **19**(9): p. 3911-3920.
25. Ruehrwein, R., Ward, D., *Mechanism of clay aggregation by polyelectrolytes*. Soil science, 1952. **73**(6): p. 485-492.
26. Michaels, A., *Aggregation of suspensions by polyelectrolytes*. Industrial & Engineering Chemistry, 1954. **46**(7): p. 1485-1490.
27. Hogg, R., *Agglomeration models for process design and control*. Powder technology, 1992. **69**(1): p. 69-76.
28. Sharma, B., Dhuldhoya, N., Merchant, U., *Flocculants—an ecofriendly approach*. Journal of Polymers and the Environment, 2006. **14**(2): p. 195-202.
29. O'Shea, J.P., Qiao, G.G., Franks, G.V., *Solid-liquid separations with a temperature-responsive polymeric flocculant: effect of temperature and molecular weight on polymer adsorption and deposition*. J Colloid Interface Sci, 2010. **348**(1): p. 9-23.
30. Moss, N., Dymond, B., *Flocculation: theory and application*. Mine and Quarry Journal, May, 1978.



31. Franks, G.V., Zhou, Y., *Relationship between aggregate and sediment bed properties: Influence of inter-particle adhesion*. *Advanced Powder Technology*, 2010. **21**(4): p. 362-373.
32. Mporfu, P., Addai-Mensah, J., Ralston, J., *Temperature influence of nonionic polyethylene oxide and anionic polyacrylamide on flocculation and dewatering behavior of kaolinite dispersions*. *Journal of Colloid and Interface Science*, 2004. **271**(1): p. 145-156.
33. Hogg, R., *The role of polymer adsorption kinetics in flocculation*. *Colloids and Surfaces A: Physicochemical and Engineering Aspects*, 1999. **146**(1-3): p. 253-263.
34. McFarlane, A., Yeap, K.Y., Bremmell, K., Addai-Mensah, J., *The influence of flocculant adsorption kinetics on the dewaterability of kaolinite and smectite clay mineral dispersions*. *Colloids and Surfaces A: Physicochemical and Engineering Aspects*, 2008. **317**(1): p. 39-48.
35. Baillie, R.A., Malmberg, E.W., *Removal of clay from the water streams of the hot water process by flocculation*, 1969, Google Patents.
36. Xu, Y., Cymerman, G. *Flocculation of fine oil sand tailings* in *UBC-McGill International Symposium Metallurgical Society of CIM*. 1999.
37. Rao, S.R., *Flocculation and dewatering of Alberta oil sands tailings*. *International Journal of Mineral Processing*, 1980. **7**(3): p. 245-253.
38. Sworska, A., Laskowski, J.S., Cymerman, G., *Flocculation of the Syncrude fine tailings: Part I. Effect of pH, polymer dosage and Mg<sup>2+</sup> and Ca<sup>2+</sup> cations*. *International Journal of Mineral Processing*, 2000. **60**(2): p. 143-152.
39. Sworska, A., Laskowski, J.S., Cymerman, G., *Flocculation of the Syncrude fine tailings: Part II. Effect of hydrodynamic conditions*. *International Journal of Mineral Processing*, 2000. **60**(2): p. 153-161.
40. Xu, Y., Hamza, H., *Thickening and disposal of oil sand tailings*. *Mining Engineering*, 2003. **55**(11): p. 33-39.
41. Alagha, L., Wang, S., Yan, L., Xu, Z., Masliyah, J., *Probing Adsorption of Polyacrylamide-Based Polymers on Anisotropic Basal Planes of Kaolinite Using Quartz Crystal Microbalance*. *Langmuir*, 2013. **29**(12): p. 3989-3998.
42. Alamgir, A., Harbottle, D., Xu, Z., Masliyah, J., *Al-PAM assisted filtration system for abatement of mature fine tailings*. *Chemical Engineering Science*, 2012. **80**(0): p. 91-99.

43. Young, R.J.L., Lovell, P.A., *Introduction to Polymers*. 1991, New York: Chapman and Hall.
44. Heskins, M., Guillet, J.E., *Solution Properties of Poly(N-isopropylacrylamide)*. Journal of Macromolecular Science: Part A - Chemistry, 1968. **2**(8): p. 1441-1455.
45. Fujishige, S., Kubota, K., Ando, I., *Phase transition of aqueous solutions of poly(N-isopropylacrylamide) and poly(N-isopropylmethacrylamide)*. The Journal of Physical Chemistry, 1989. **93**(8): p. 3311-3313.
46. Guillet, J.E.H., Murray, D.G., *Polymeric Flocculants, Patent Number 4536294*, U.S. Patent, Editor 1985: United States of America.
47. Deng, Y., Pelton, R., *Synthesis and Solution Properties of Poly(N-isopropylacrylamide-co-diallyldimethylammonium chloride)*. Macromolecules, 1995. **28**(13): p. 4617-4621.
48. Franks, G.V., Li, H., O'Shea, J.P., Qiao, G.G., *Temperature responsive polymers as multiple function reagents in mineral processing*. Advanced Powder Technology, 2009. **20**(3): p. 273-279.
49. Li, H., Long, J., Xu, Z., Masliyah, J. *Flocculation of kaolinite clay suspensions using a temperature-sensitive polymer*. AIChE Journal, 2007. **53**(2): p. 479-488.
50. Li, H., O'Shea, J.-P., Franks, G.V., *Effect of molecular weight of poly(N-isopropyl acrylamide) temperature-sensitive flocculants on dewatering*. AIChE Journal, 2009. **55**(8): p. 2070-2080.
51. Burdukova, E., Haihong, L., Bradshaw, D.J., Franks, G.V., *Poly (N-isopropylacrylamide) (PNIPAM) as a flotation collector: Effect of temperature and molecular weight*. Minerals Engineering, 2010. **23**(11–13): p. 921-927.
52. Forbes, E., Bradshaw, D.J., Franks, G.V., *Temperature sensitive polymers as efficient and selective flotation collectors*. Minerals Engineering, 2011. **24**(8): p. 772-777.
53. Sakohara, S., Nishikawa, K., *Compaction of TiO<sub>2</sub> suspension utilizing hydrophilic/hydrophobic transition of cationic thermosensitive polymers*. Journal of Colloid and Interface Science, 2004. **278**(2): p. 304-309.
54. Sakohara, S., Hinago, R., Ueda, H., *Compaction of TiO<sub>2</sub> suspension by using dual ionic thermosensitive polymers*. Separation and Purification Technology, 2008. **63**(2): p. 319-323.
55. Sakohara, S., Ochiai, E., Kusaka, T., *Dewatering of activated sludge by thermosensitive polymers*. Separation and Purification Technology, 2007. **56**(3): p. 296-302.

56. O'Shea, J.P., Qiao, G.G., Franks, G.V., *Temperature responsive flocculation and solid–liquid separations with charged random copolymers of poly (< i> N</i>-isopropyl acrylamide)*. Journal of Colloid and Interface Science, 2011. **360**(1): p. 61-70.
57. Dzuy, N.Q., Boger, D.V., *Direct Yield Stress Measurement with the Vane Method*. Journal of Rheology, 1985. **29**(3): p. 335-347.
58. Dzuy, N.Q., Boger, D.V., *Yield Stress Measurement for Concentrated Suspensions*. Journal of Rheology, 1983. **27**(4): p. 321-349.
59. Rahman, M.H., *Yield Stresses of Mixtures with Bimodal Size Distributions*, in *Department of Chemical and Materials Engineering*. 2011, University of Alberta: Edmonton.
60. Johnson, S.B., Franks, G.V., Scales, P.J., Boger, D.V., Healy, T.W., *Surface chemistry–rheology relationships in concentrated mineral suspensions*. International Journal of Mineral Processing, 2000. **58**(1–4): p. 267-304.
61. Leong, Y.-K., Scales, P.J., Healy, T.W., *Effect of Particle Size on Colloidal Zirconia Rheology at the Isoelectric Point*. Journal of the American Ceramic Society, 1995. **78**(8): p. 2209-2212.
62. Zhou, Z.S., Michael, J.S., Scales, P.J., Boger, D. V. , *The yield stress of concentrated flocculated suspensions of size distributed particles*. Journal of Rheology, 1999. **43**(3).
63. Nasser, M.S. James, A.E., *Effect of polyacrylamide polymers on floc size and rheological behaviour of kaolinite suspensions*. Colloids and Surfaces A: Physicochemical and Engineering Aspects, 2007. **301**(1–3): p. 311-322.
64. Nasser, M.S. James, A.E., *The effect of polyacrylamide charge density and molecular weight on the flocculation and sedimentation behaviour of kaolinite suspensions*. Separation and Purification Technology, 2006. **52**(2): p. 241-252.
65. Zhou, Y., Yu, H., Wanless E.J., Jameson G.J., Franks G.V., *Influence of polymer charge on the shear yield stress of silica aggregated with adsorbed cationic polymers*. Journal of Colloid and Interface Science, 2009. **336**(2): p. 533-543.
66. Powrie, W., *Soil Mechanics – Concept & Applications* 2004, New York: Spon Press.
67. Kaya, A.O., Hakan, A., Yukselen, Y., *Settling Behavior and Zeta Potential of Kaolinite in Aqueous Media*. in *Proceedings of the International Offshore and Polar Engineering Conference*. 2003.

68. Johannsmann, D., *Viscoelastic, mechanical, and dielectric measurements on complex samples with the quartz crystal microbalance*. Physical Chemistry Chemical Physics, 2008. **10**(31): p. 4516-4534.
69. Deng, Y., Xiao, H., Pelton, R., *Temperature-Sensitive Flocculants Based on Poly (N-isopropylacrylamide-co-diallyldimethylammonium Chloride)*. Journal of Colloid and Interface Science, 1996. **179**(1): p. 188-193.
70. Masliyah, J., Czarnecki, J., Xu, Z., *Handbook on Theory and Practice of Bitumen Recovery from Athabasca Oil Sands*. Vol. 1. 2011: Kingsley Knowledge Publishing.
71. Creutz, S., Jérôme, R., *Effectiveness of block copolymers as stabilizers for aqueous titanium dioxide dispersions of a high solid content*. Progress in Organic Coatings, 2000. **40**(1): p. 21-29.
72. Yan, L., Englert, A.H., Xu, Z., Masliyah, J., *Determination of anisotropic surface characteristics of different phyllosilicates by direct force measurements*. Langmuir, 2011. **27**(21): p. 12996-13007.
73. Nasser, M., James, A., *The effect of electrolyte concentration and pH on the flocculation and rheological behaviour of kaolinite suspensions*. Journal of Engineering Science and Technology, 2009. **4**(4): p. 430-446.
74. Kawaguchi, H., Fujimoto, K., Mizuhara, Y., *Hydrogel microspheres III. Temperature-dependent adsorption of proteins on poly-N-isopropylacrylamide hydrogel microspheres*. Colloid and Polymer Science, 1992. **270**(1): p. 53-57.
75. Besra, L., Sengupta, D., Roy, S., *Particle characteristics and their influence on dewatering of kaolin, calcite and quartz suspensions*. International Journal of Mineral Processing, 2000. **59**(2): p. 89-112.
76. Ezeagwul, K.E., *Studies on Flocculation of Kaolin Suspensions and Mature Fine Tailings*, in *Department of Chemical and Materials Engineering 2008*, University of Alberta.
77. Besra, L., Sengupta, D., Roy, S., Ay, P., *Influence of polymer adsorption and conformation on flocculation and dewatering of kaolin suspension*. Separation and Purification Technology, 2004. **37**(3): p. 231-246.
78. Sauerbrey, G., *The use of quartz crystal oscillators for weighing thin layers and for microweighing applications* 1991.

79. Kanazawa, K.K., Gordon, J.G., *Frequency of a quartz microbalance in contact with liquid*. Analytical Chemistry, 1985. **57**(8): p. 1770-1771.
80. Heath, A.R., Fawell, P.D., Bahri, P.A., Swift, J.D., *Estimating average particle size by focused beam reflectance measurement (FBRM)*. Particle & Particle Systems Characterization, 2002. **19**(2): p. 84-95.
81. Negro, C., Sanchez, L.M., Fuente, E., Blanco, A., Tijero, J., *Polyacrylamide induced flocculation of a cement suspension*. Chemical Engineering Science, 2006. **61**(8): p. 2522-2532.
82. Inc, B.C. *Product Catalog Zetag 8110*. [cited 2014 May 10]; Available from: [http://worldaccount.basf.com/wa/NAFTA~en\\_US/Catalog/WaterSolutions/info/BASF/P RD/30478275](http://worldaccount.basf.com/wa/NAFTA~en_US/Catalog/WaterSolutions/info/BASF/P RD/30478275).
83. Fujishige, S., *Intrinsic viscosity-molecular weight relationships for poly (N-isopropylacrylamide) solutions*. polymer J, 1987. **19**: p. 297-300.

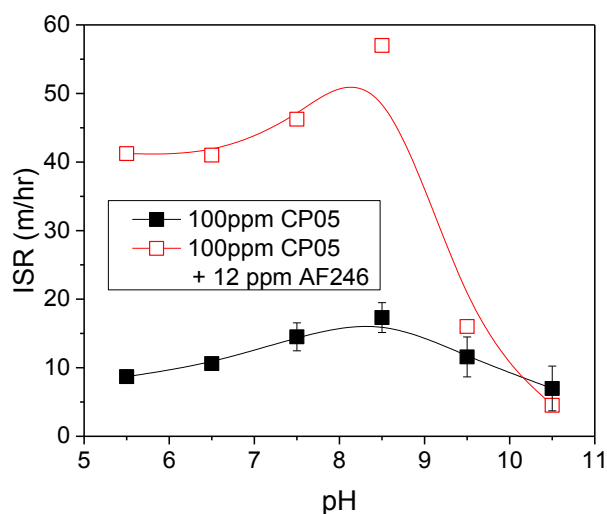
## **Appendix A : Dual Polymer Flocculation**

In this chapter, the effect of combinations of a cationic and temperature switchable copolymer CP05 (95 mol% NIPAM and 5% DMAPMA) and a high molecular weight anionic acrylamide based polymer known as HyChem AF 246 was investigated. It is widely known that the synergy of using a pair of oppositely charged polymers provides massive benefits to flocculation efficiency. These combinations are commonly seen in the pulp and paper industry and are slowly gaining interest for applications in mining tailings treatment. In addition to its industrial application the fundamentals of this process are fairly well understood, in terms of the influence of polymer molecular weight, charge density, and polymer conformation on the flocculation process. The aim of this particular study was to establish the benefits of using a dual polymer system for oil sands tailings treatment. The main goal was to firmly prove that using the temperature switchable properties of CP05 in a dual polymer system can result in a positive benefit to flocculation and dewatering.

### **A.1 Flocculation and Rheology of Dual Polymer Flocculation**

The procedures involving the preparation of kaolinite suspensions and the samples for setting and rheological tests are identical to the experimental procedures described in the previous two chapters. The key difference was the timing and application of the polymer dosages. This will be discussed over the course of the chapter.

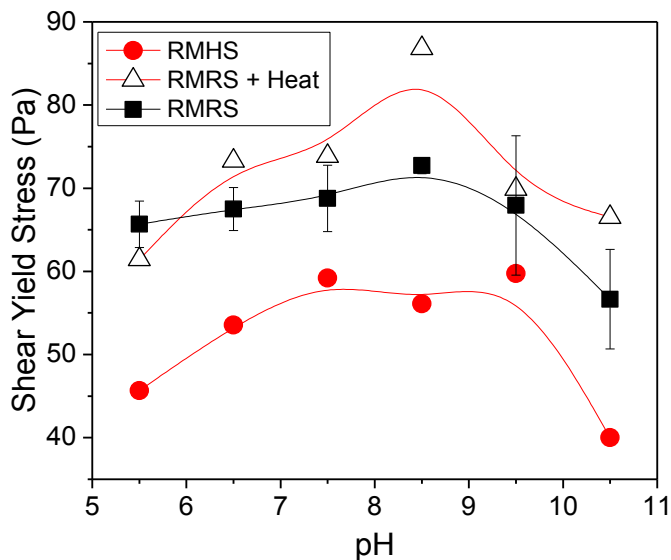
Figure A-1 shows a comparison of settling rates of kaolinite suspensions at different pH. It should be recalled that previous settling experiments were performed with 100ppm CP05 polymer additions. Thus, a 12% increase in polymer dosage with AF 246 increased flocculation settling speeds by 400% at pH 5.5 to 8.5. This sequential addition of the oppositely charged polymer, cationic CP05 and anionic AF 246, resulted in fourfold improvement of settling rates when the same polymer additives were introduced in a single polymer flocculation system. The settling rates for any suspension in this chapter are for the dual polymer system which involves the sequential dosing of the kaolinite suspension with 100ppm CP05 followed immediately by 12 ppm HyChem, unless otherwise stated.



**Figure A-1: Initial settling rate of 5 wt% kaolinite suspensions. Experimental variables: single and dual polymer settling systems, and solution pH. Settling column – 1 L**

The key to flocculation efficiency was the surface area that the charged polymer can quickly and preferentially adsorb onto. With respect to dual polymer flocculation performance at the pH range 5.5-7.0, the cationic polymer added first acted as charge neutralizers for the negatively charged silica basal planes in the kaolin. The anionic AF 246 added afterwards either adsorbed onto the positively charged alumina basal plane or the cationic CP05 already adsorbed onto the kaolinite surface. The AF246 was several factors larger than CP05 in terms of molecular weight, and acted as an effective bridge between flocs created by CP05. In essence, the AF 246 flocculates the flocs created by CP05 by bridging the sites of CP05 adsorption.

In the pH range 7.0 of 8.5 the same flocculation rate was witnessed as with the single polymer system with CP05 alone. The poor settling behavior found at pH > 9.0 resulted from the deprotonation of the DMAPMA copolymer. At this pH range the DMAPMA was above its pKa, and has only a feeble cationic charge. As a result, the efficiency of the dual polymer flocculation is lost. The flocculation appears to be most effective only when there is synergy between the two oppositely charged polymer chains. The AF246 still forms flocs through hydrogen bonding, but bonding capability and flocculation efficiency are greatly reduced.



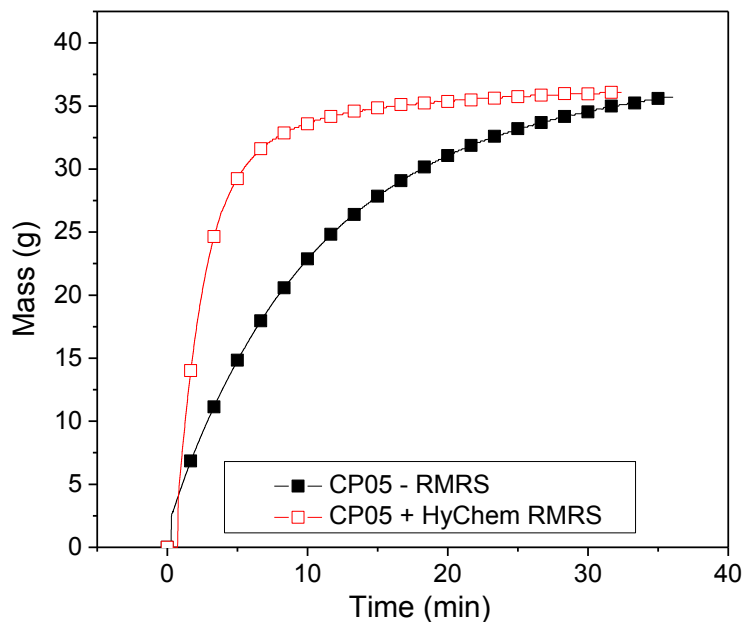
**Figure A-2: Shear yield stress of settled kaolinite suspensions flocculated with 100 ppm CP05 and 12 ppm AF246. Experimental variables: suspension heating procedures and solution pH. Settling column – 1 L**

Figure A-2 shows the same trends of the sediment yield stress for the dual polymer system as in the single polymer CP05-clay system. Similar to the previous experiments, the shear yield stress was fairly consistent for RMRS across the pH range, up to pH 9.5. The RMHS procedure resulted in sediments of the lowest shear yield stress. The coil-globule transition during flocculation reduces the ability of the polymer chain to act as a bridge across the particles and flocs. Without these bridges the clay-polymer network had less cohesion, and less force was needed to make the sediment flow. There were some benefits to the temperature sensitivity of the CP05 polymer. Heating and cooling the sediment across the LCST still produced additional consolidation and water release in this dual polymer system at pH > 8.0 using the “RMRS + Heat” procedure.

The highest drainage rates for any sediment produced in this research were for the dual polymer system. It was observed earlier that the addition of a small dose of second polymer of opposite (anionic) charge to the CP05 increased settling rates by fourfold. The shear yield stress and strength of the particle network were also improved more than proportionally to the small increase in polymer concentration. Figure A-3 shows a comparison of the dewatering behavior for single and dual polymer flocculation.



The large flocs formed by the sequential dual polymer addition were beneficial to sediment drainage. The total water removed by the comparable procedures in Figure A-3 was nearly identical. However the suspension treated with two polymers drains at a much faster rate. The resulting sediment volume and solids content were the same, but the structure of the flocs was the key difference. The second polymer added, anionic Hychem AF 246, acted as an anchor between the primary flocs created by the CP05. The resulting particle network was stronger and more shear resistant resulting in an improved shear yield stress. The high capillary sizes and hence the high filtration rate were indicative of large floc sizes.



**Figure A-3: Dewatering of flocculated kaolinite suspensions at pH 8.5. Experimental variables: single and dual polymer settling systems. Settling column – 1 L**

Figure A-4 compares the shear yield stress of sediments before and after drainage for single and dual polymer flocculation systems. These experiments were performed with the same mass of clay and the same suspensions pH for the same RMRS procedure. In contrast to the cases without drainage, yield stress of the sediments after drainage was greatly improved by the additional amount of HyChem polymer added. The synergy of the secondary flocculation from the oppositely charged AF 246 dramatically increased the strength and number of bonds in the settled clay.

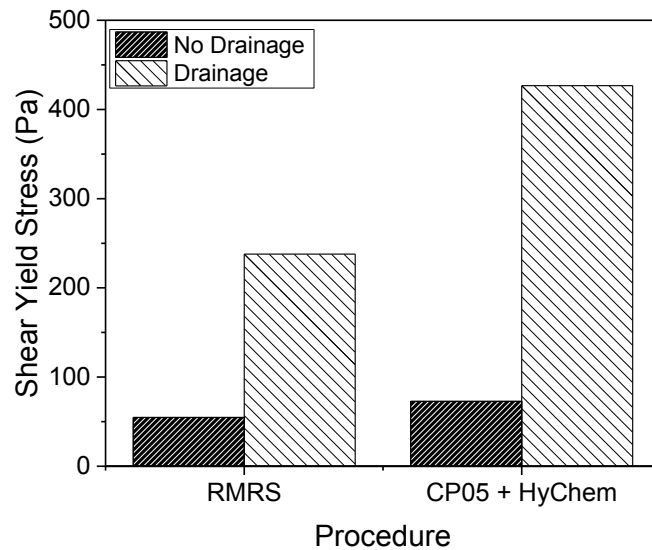
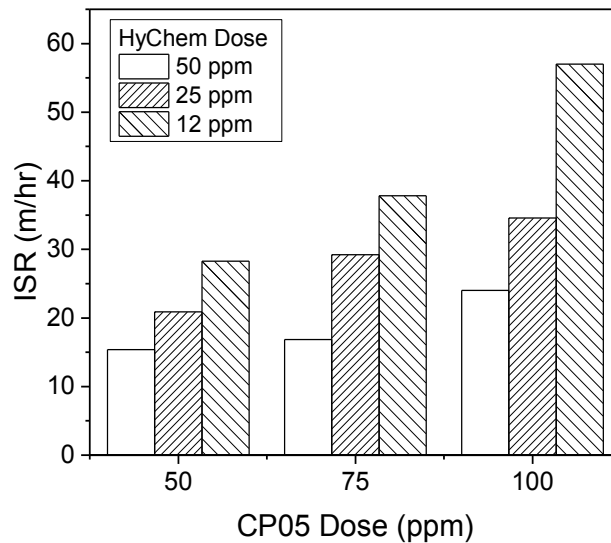


**Figure A-4: Shear yield stress of dewatered flocculated kaolinite suspensions at pH 8.5, comparison of dual and single polymer settling procedures**

### **A.2 Dual Polymer Flocculation Kinetics**

The flocculation and yield stress behavior were found to be dependent on the ratio of the two polymers. The experiments conducted with the polymer ratio of almost 10:1 by mass of CP05 to AF246 Hychem were found to be optimal for flocculation, as shown in Figure A-5. In all these experiments, the suspension was tested at the optimal pH of 8.5 and with room temperature flocculation and settling (RMRS) procedures.

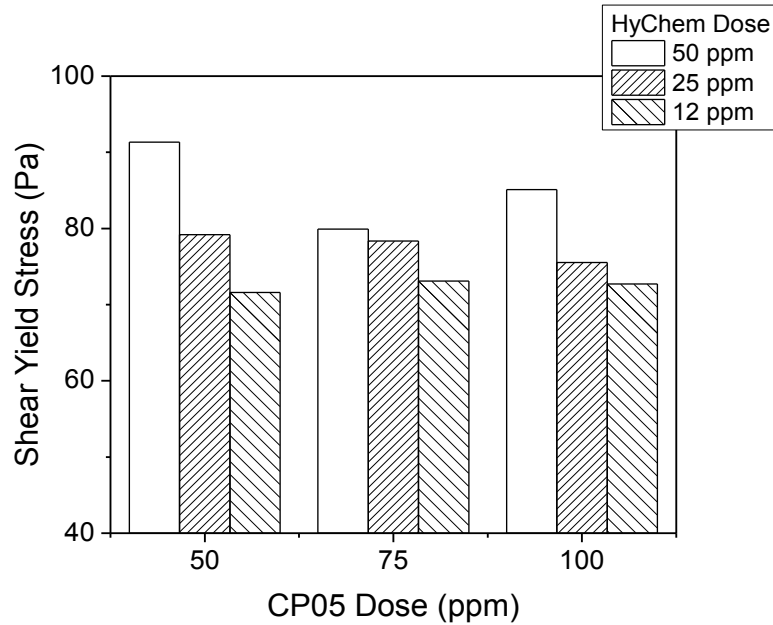
Figure A-5 reveals that the dual polymer flocculation was sensitive to overdosing from the AF246 anionic polymer. In this experiment the fastest settling is when the ratio of CP05 polymer to AF 246 is almost 10:1 (100ppm CP05 and 12 ppm AF 246). The slowest settling rates were observed when the polymer ratios were 1:1 (50 ppm CP05 and 50 ppm AF 246). An overdose case was where a polymer adsorption covers too much of the available particle surface area and begins to act as a dispersant rather than a flocculant in the system. The ideal flocculation case, only 50% of the surface area of a sphere should be covered by flocculant. When the flocculant acts as a bridge between particles, there needs to be exposed surface on all the particles to bond to. When too much AF 246 was added to the flocculation system all the patches of adsorbed CP05 necessary for secondary flocculation were covered, and the polymer chains were unable to act as a bridge between patches on multiple particles.



**Figure A-5: Initial settling rate of 5 wt% kaolinite suspensions at 8.5 pH, treated with varying dosages of CP05 cationic polymer and HyChem AF246 anionic polymer**

The optimal polymer ratio for the sediment rheology in a dual polymer system (Figure A-6) was different from what was optimal for flocculation rates, as shown in Figure A-5. The shear yield stress was dependent of the strength of the intramolecular bridging bonds between flocs and particles. AF 246 is a high molecular weight blend of anionic polymer chains. These large polymer chains have a disproportional influence on the shear yield stress. The higher the dose of the anionic AF246 the stronger the resulting shear yield stress as shown in Figure A-6.

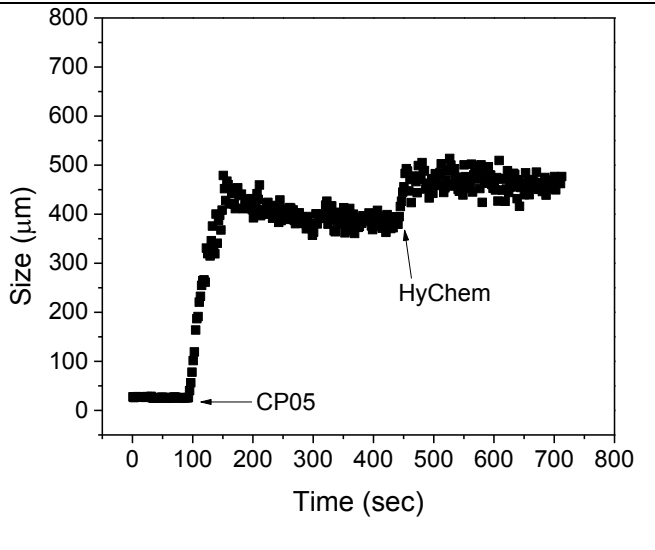
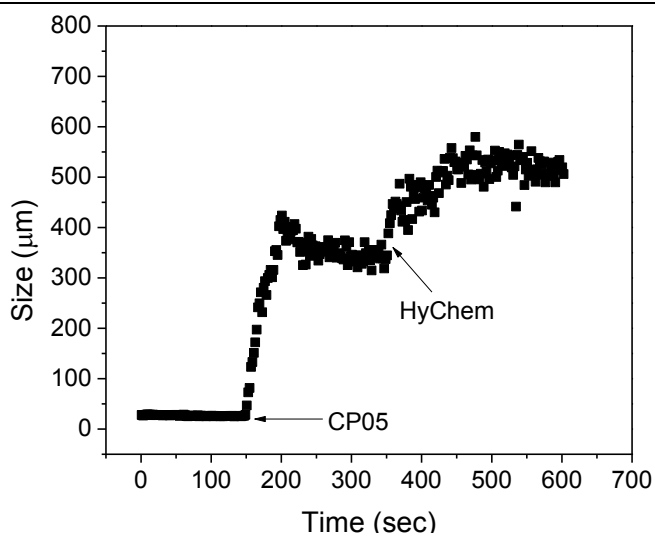
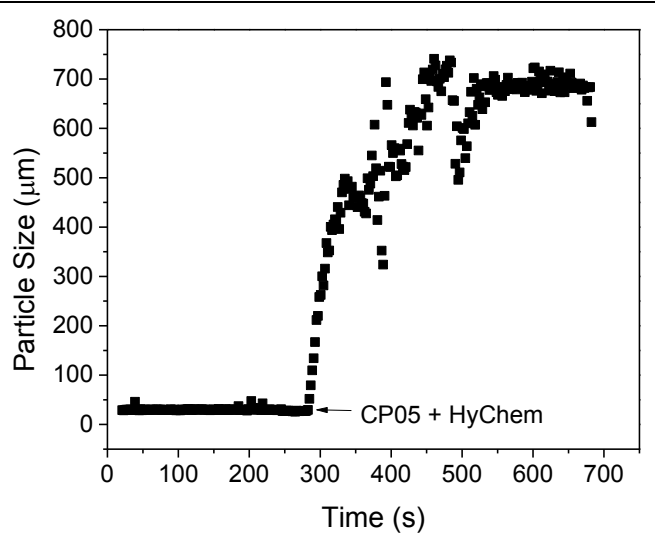
Previous research has found that sequential addition of two polymers was optimal for floc growth. This conclusion was derived by comparing the results obtained by the co-additions or sequential additions separated by varying time intervals. In sequential dual polymer systems, primary flocculation occurred within seconds of the CP05 polymer addition. The patches of adsorbed CP05 that act as a bridging site for secondary flocculation were time dependent.



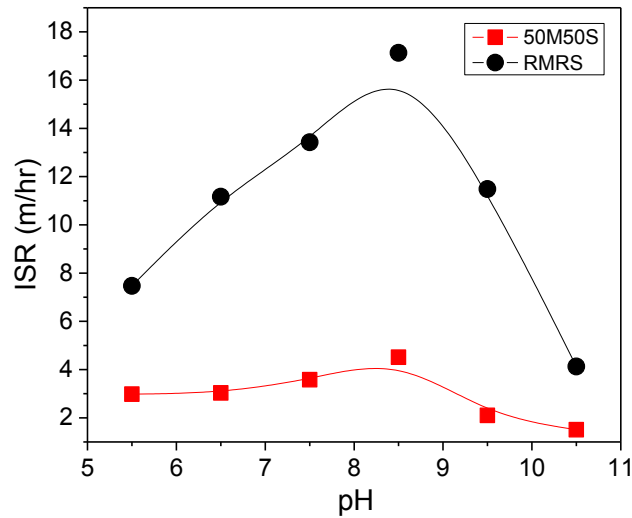
**Figure A-6: Shear yield stress of settled kaolinite suspensions at 8.5 pH, flocculated with varying dosages of CP05 cationic polymer and AF246 anionic polymer**

Table A-1 compares three cases of dual polymer flocculation, using the FBRM to track the change of mean particle size. The difference between each case was the time interval between the sequential doses of CP05 and AF 246 polymer added to the kaolinite suspension. The shorter the time interval is between the two polymer additions was the larger the flocs grow, drastically improving the settling rates.

**Table A-1: Mean floc size of 5 wt% kaolinite suspensions at pH 8.5 flocculated with 100 ppm of CP05 and 12 ppm AF 246**

<p>Time Interval Between Flocculant Doses:  5 minutes</p>	 <p>Graph showing Mean floc size (μm) vs Time (sec) for a 5-minute interval. The size starts at approximately 30 μm. At 100 seconds, CP05 is added, causing the size to jump to approximately 450 μm. At 450 seconds, HyChem is added, causing the size to jump to approximately 500 μm. The size remains relatively stable between 450 and 500 μm until 700 seconds.</p>
<p>2.5 Minutes</p>	 <p>Graph showing Mean floc size (μm) vs Time (sec) for a 2.5-minute interval. The size starts at approximately 30 μm. At 150 seconds, CP05 is added, causing the size to jump to approximately 400 μm. At 350 seconds, HyChem is added, causing the size to jump to approximately 550 μm. The size remains relatively stable between 500 and 600 μm until 700 seconds.</p>
<p>0.5 minutes</p>	 <p>Graph showing Mean floc size (μm) vs Time (sec) for a 0.5-minute interval. The size starts at approximately 30 μm. At 280 seconds, CP05 + HyChem is added, causing the size to jump to approximately 700 μm. The size remains relatively stable between 600 and 700 μm until 700 seconds.</p>

## Appendix B : Supplemental Data



**Figure B-1: Initial settling rate of 5 wt% kaolinite suspensions with 100 ppm CP05. Experimental variables: pH and settling procedures, RMRS and 50M50S (HMHS). Settling column – 1 L**

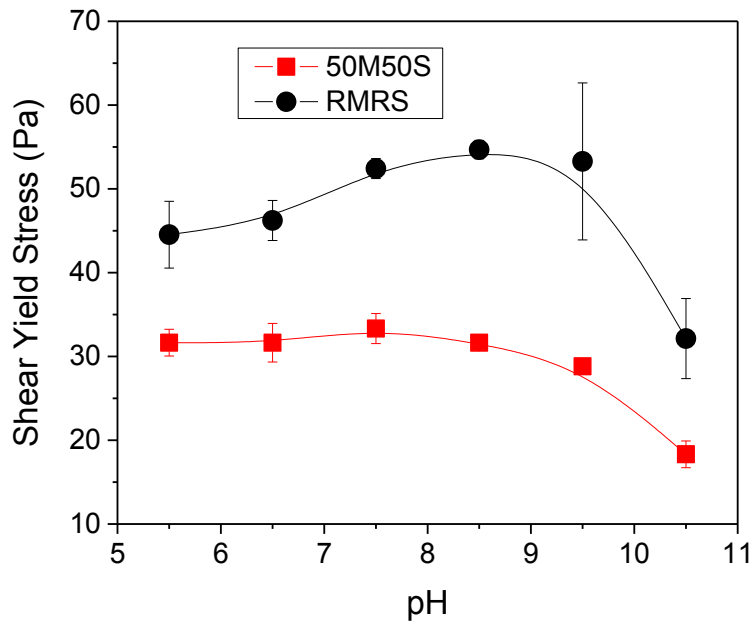


**Figure B-2: Yield stress of settled kaolinite suspensions with 100 ppm CP05. Experimental variables: pH and settling procedures, RMRS and 50M50S (HMHS). Settling column – 1 L**

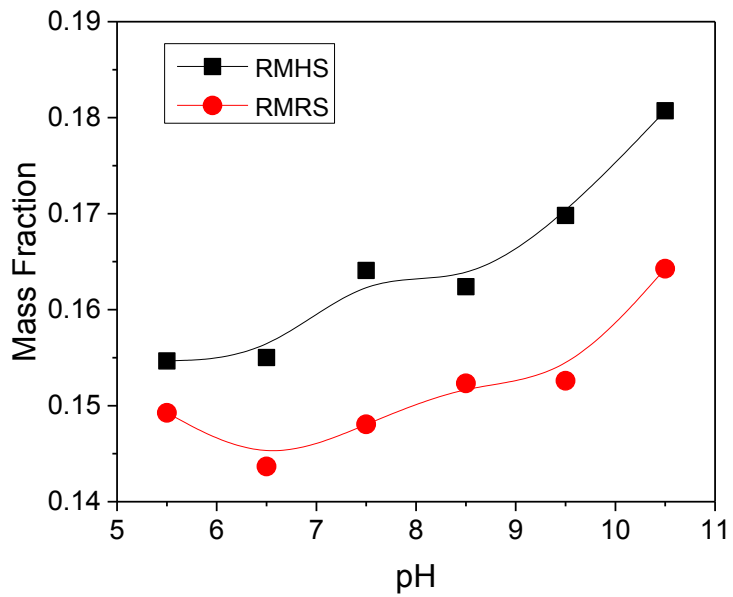


**Figure B-3: Solids content of settled kaolinite suspensions flocculated with 100 ppm CP05. Experimental variables: temperature protocols and solution pH. Settling column – 1 L**

## Appendix C : Polymer Molecular Weight Determination

According to Mark-Houwink equation,

$$[\eta] = KM_v^a \quad (C.1)$$

where K and a are characteristic constants for a given polymer solution at a specific temperature. In Eq. C.1,  $M_v$  is the viscosity-average molecular weight, and  $[\eta]$  is known as the intrinsic viscosity.

$$[\eta] = \lim_{c \rightarrow 0} \left( \frac{\eta_{sp}}{c} \right) = \lim_{c \rightarrow 0} \left( \frac{\eta - \eta_0}{\eta_0 c} \right) \quad \eta_{sp} = \frac{\eta - \eta_0}{\eta_0} \quad \eta_{red} = \frac{\eta_{sp}}{c} \quad \eta_I = \ln \left( \frac{\eta}{\eta_0} \right) \quad (C.2)$$

where c is the concentration of polymer solution,  $\eta_{sp}$  is the specific viscosity, and  $\eta_0$  is the initial viscosity and  $\eta_{red}$  is the reduced viscosity [43]. The intrinsic viscosity of polymer solution is the viscosity of solution without interacting polymer coils, i.e., an infinitely diluted solution. The specific viscosity,  $\eta_{sp}$  is related to the fluid viscosity increase due to all polymer solute molecules. The reduced viscosity,  $\eta_{red}$ , is the fluid viscosity increase per unit of polymer solute concentration, c. The intrinsic viscosity,  $\eta$ , is the limit of the reduced viscosity as the polymer solute concentration approaches zero. The intrinsic viscosity is also the limit of the inherent viscosity,  $\eta_I$ , as the solution polymer concentration approaches zero.

$$[\eta] = \lim_{c \rightarrow 0} \left( \frac{\eta_{red}}{c} \right) = \lim_{c \rightarrow 0} \frac{\ln \left( \frac{\eta}{\eta_0} \right)}{c} \quad (C.3)$$

A dual Huggins-Kraemer plot (Figure C-1) combines these two approaching limits in Eq. C.3 (inherent viscosity,  $\eta_I$  and reduced viscosity  $\eta_{red}$ ) to evaluate  $[\eta]$  of the polymer [43]. By extrapolating both data sets to zero concentration (infinite dilution), the y-intercepts of both lines should fall on the same point, and this point is known as the intrinsic viscosity of the polymer.



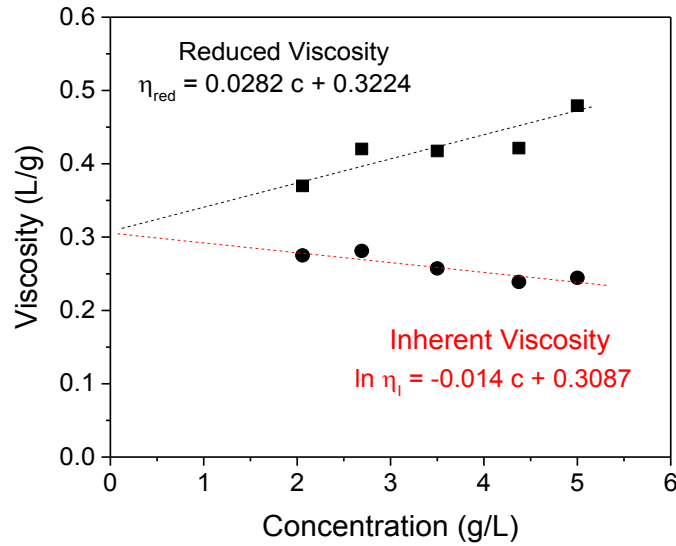


**Figure C-1: Dual Huggins-Kraemer plot for CP05**

At each concentration, both reduced viscosity and inherent viscosity were determined from the measured viscosity of polymer solutions using an Ubbelohde viscometer and plotted against the concentration of polymer solution. These viscosities are modelled by the Huggins and the Kramer equation, respectively.

$$\frac{\eta_{sp}}{c} = k'[\eta]^2 c + [\eta] \quad (C.4)$$

$$\frac{\left(\frac{\eta}{\eta_0}\right)}{c} = k''[\eta]^2 c + [\eta] \quad (C.5)$$

The cationic polymer (CP), p[NIPAM-co- DMAPMA], was dissolved in tetrahydrofuran (THF) at 27°C and the viscosity was measured using polymer solutions of five different concentrations. Intrinsic viscosity of CP was calculated by taking the average of the y-intercepts of both lines. By assuming narrow molecular weight distribution, the viscosity-average molecular weight,  $M_v$  is approximately equal to the number-average molecular weight,  $M_n$ .  $M_n$  of CP was estimated using the molecular weight relation of p(NIPAM) and the intrinsic viscosity from the dual Huggins-Kraemer plot [83].

$$[\eta] = 9.59 \times 10^{-3} M_n^{0.65} \quad (C.6)$$